bioRxiv preprint doi: https://doi.org/10.1101/435669; this version posted October 11, 2018. The copyright holder for this preprint (which was not certified by peer review) is the author/funder, who has granted bioRxiv a license to display the preprint in perpetuity. It is made available under aCC-BY-NC-ND 4.0 International license.

Adaptive walks on high-dimensional fitness landscapes and seascapes with distance-dependent statistics

Atish Agarwala
Department of Physics, Stanford University

Daniel S. Fisher
Department of Applied Physics, Stanford University

October 10, 2018

Abstract

The dynamics of evolution is intimately shaped by *epistasis* — interactions between genetic elements which cause the fitness-effect of combinations of mutations to be non-additive. Analyzing evolutionary dynamics involving large numbers of epistatic mutations is difficult. A key step is developing models that enable study of the effects of past evolution on future evolution. In this work, we introduce a broad class of high-dimensional random fitness landscapes for which the correlations between fitnesses of genomes are a general function of genetic distance. The Gaussian character allows for tractable computational and analytic understanding. We study the properties of these landscapes and the simplest evolutionary process, random adaptive (uphill) walks. We find that conventional measures of "ruggedness" do not much affect these. Instead, the long-distance statistics of epistasis cause properties to be highly conditioned on past evolution, determining the statistics of the local landscape (the distribution of fitness-effects of available mutations and combinations of these), as well as the global geometry of evolutionary trajectories. We also show that greedier walks tend to get stuck sooner at local fitness maxima. We then model the effects of slowly changing environments. These fitness "seascapes" cause a statistical steady state with highly intermittent evolutionary dynamics: populations undergo bursts of rapid adaptation, interspersed with periods where adaptive mutations are rare and the population must wait for new directions to be opened-up by changes in the environment. Finally, we introduce a computational framework for studying more complex evolutionary dynamics and on broader classes of high-dimensional landscapes and seascapes.

bioRxiv preprint doi: https://doi.org/10.1101/435669; this version posted October 11, 2018. The copyright holder for this preprint (which was not certified by peer review) is the author/funder, who has granted bioRxiv a license to display the preprint in perpetuity. It is made available under aCC-BY-NC-ND 4.0 International license.

1 Introduction

Evolution, even in the short term for "simple" asexual microbial populations with "simple" selective pressures, is a complex, non-linear dynamical process. One of the many sources of complexity is *epistasis* – the interactions among combinations of mutations. Most simply, pairs of mutations can have no benefit individually but benefits together, positive effects alone but deleterious ones together, and, once many mutations are involved, a plethora of other behaviors. These epistatic effects lead to correlations and anti-correlations in co-occurrence of mutations, which can have a dramatic effect on evolutionary trajectories. In trying to model epistasis, an important observation is that, generally, whether a mutation is beneficial or deleterious, and by how much, will depend on the both the environment and the genomic background, and hence the evolutionary history: any mutation that is unconditionally beneficial would have already occurred and fixed. Thus the details of epistasis will depend greatly on the context and one should hope for primarily statistical understanding.

At a basic level, we lack a theoretical understanding of the interplay between evolution and epistasis. There is a great deal of population genetic theory in cases where mutations are independent, and their contribution to the (log) fitness is additive [11, 14]. But, except in simple cases involving small numbers of mutations, little is understood generally about evolutionary dynamics in the presence of epistatic interactions. Many studies have focused on the statistical properties of epistasis by constructing and attempting to understand models of *fitness landscapes* – functions from genotype to fitness in a fixed environment. These are often conceptualized like physical landscapes with peaks and valleys [9], and theorists have endeavored to understand how properties of these landscapes constrain or enable evolution [36, 37, 39]. Some approaches have focused on quantitative "local" properties, such as using extreme value statistics to understand behaviors near fitness peaks [38], Others have focused on quantifying the geometry of fitness landscapes, including distributions of local maxima and numbers of uphill paths between points [10, 24, 50]. There is often an emphasis placed on defining and quantifying measures of "ruggedness", with the intuition that evolution is more constrained in rugged landscapes by limiting the number of routes along which the fitness can continue to increase, leading to getting stuck at local maxima [9]. But ruggedness is not well defined in general, and, as we shall see, local measures of it can be misleading. Moreover, there is an intrinsic problem with focusing primarily on fitness landscapes themselves. The interplay between epistasis and evolution is essential; one cannot try to separately understand them as the properties of the landscape in the vicinity of the current genome are highly conditioned by the past evolution whether in a fixed or changing environment. The properties of epistatic fitness landscapes *conditioned* on past evolution will generally be very different than the properties of "typical" points or regions on such landscapes. Even if epistasis is some sense "weak", over long times individuals will accumulate a large number of mutations

bioRxiv preprint doi: https://doi.org/10.1101/435669; this version posted October 11, 2018. The copyright holder for this preprint (which was not certified by peer review) is the author/funder, who has granted bioRxiv a license to display the preprint in perpetuity. It is made available under aCC-BY-NC-ND 4.0 International license.

[1] and thus conditioning on history will eventually become important.

A major conceptual difficulty is that fitness landscapes are very high dimensional: there are many potentially beneficial mutations and combinations of them. Yet intuition about landscapes and evolution in them is usually based on low-dimensional analogies. A large body of work in theoretical physics and probability theory has shown that geometry and dynamics in high-dimensional spaces, such as uphill paths on complex landscapes, can be very different than in their low dimensional analogues [6, 7].

Various experiments have provided some information about epistasis in natural systems. Extensive work has been done on fitness effects of combinations of pairs of knockouts in various microbes, in particular *S. cerevisiae* and *E. coli* [13, 22, 48]. However most knockouts are deleterious, and pairs of them at least as much so. But evolution is largely driven by beneficial mutations, thus it is not clear how much is learned from such experiments about statistical properties of epistasis that would affect evolutionary dynamics. High throughput studies of repeatedly mated yeast populations [4] have provided potentially valuable information, but even with some good combinations of genetic differences being produced, it is not clear what are useful measures of the features of epistasis that affect evolution. Furthermore, these measurements have thus far combined genomes that differ by large numbers of mutations, thus they are not directly relevant for the simpler problem of asexual evolution, our focus here, for which the landscape is explored locally with distant genomes having to be reached step by step.

In some relatively simple systems, a variety of *empirical fitness landscapes* — functions from genotype to measured fitness — have been analyzed and the consequences for evolution investigated theoretically. However, by their nature, these are restricted to exploring combinations of genomic changes on only a modest number of sites - typically in a single protein or RNA sequence [3, 24, 30, 50, 52]. While these studies can yield insights about specific evolutionary scenarios, such as antibiotic resistance caused by multiple mutations in a small number of proteins under strong, focused selective pressure, drawing general conclusions from these, especially about much higher dimensional landscapes, is certainly problematic.

Some experiments have explored the interplay between epistasis and evolutionary dynamics by laboratory microbial evolution [42, 50, 53]. Much has been learned about the fitness effects of individual beneficial mutations, [25, 29, 49], but thus far only limited amounts about epistatic interactions between the mutations found, beyond a general tendency towards "diminishing returns" epistasis: the net effect of beneficial combinations of mutations being less than the sum of their individual effects. However, this is not true of all combinations and it may well be that such anomalous combinations are particularly important for driving further evolution [23].

bioRxiv preprint doi: https://doi.org/10.1101/435669; this version posted October 11, 2018. The copyright holder for this preprint (which was not certified by peer review) is the author/funder, who has granted bioRxiv a license to display the preprint in perpetuity. It is made available under aCC-BY-NC-ND 4.0 International license.

All experimental studies face a spectrum of intrinsic challenges. One is the combinatorial explosion of possible genotypes, which is exponential in the number of sites being studied. This combinatorial explosion is associated with another key feature of epistasis: at large genetic distances, higher order interactions are important. When many genotypes are involved it is not enough to consider only pairwise interactions: correlations involving many sites on the genome become important. Indeed, "expanding" around a particular genome — the ancestor — in additive, pairwise, triplet interactions, and so on, is problematic. This is at best a way to parametrize the fitness landscape in the vicinity of a particular genome which is not essentially special: such an expansion could be already substantially different around another genome not far away.

Another layer of complexity comes from the dynamic nature of environments in which organisms find — and have found — themselves. The landscapes are really "seascapes", and typically change on timescales relevant for even short term evolutionary dynamics [2, 19, 20]. These changes can be driven by external physical and chemical factors, as well as changes in direct interactions between organisms or feedback on the environment by evolving organisms that populate it. As the net effects of mutations can be a delicate balance between positive and negative effects, even small changes in environment can change which mutations are beneficial and more generally the possible routes to adaptation via multiple successive mutations. Recent experiments have provided hints at how strong the effects of environmental changes caused by evolution are even in nominally "simple" conditions. This is seen for the first mutations that occur in yeast in low glucose [31] as well as from cumulative effects from many mutations in Lenski's long-term *E. coli* evolutions [18]. On long timescales in natural populations, dynamical changes in the environment, whether produced by abiotic changes or by the evolving populations themselves, are surely major drivers of adaptation.

With large numbers of sites involved in evolution, all one can hope for, generally, is to understand statistical properties of landscapes (and seascapes). New, more general theoretical approaches are vitally needed, both to develop intuition, and to guide future experiments and choose what statistical properties would be most instructive to measure. It is imperative that theorists build and study models that include caricatures of these key features: high-dimensional landscapes with some general statistical forms of epistasis, and, in the same framework, gradual time dependence of the landscape (about which one can hope more general can be said than about large sudden changes in the environment). Models should have no "special genomes" — such as "wild-type" — a priori, and instead one should carry out evolution from as random point and then try to understand the effects of epistasis and further evolution conditioned on past evolution. Some recent work has endeavored to analyze evolutionary dynamics on some classes of landscapes with simple models of epistasis, [36, 37, 40, 41]; however these analyses are computationally limited from exploring more

bioRxiv preprint doi: https://doi.org/10.1101/435669; this version posted October 11, 2018. The copyright holder for this preprint (which was not certified by peer review) is the author/funder, who has granted bioRxiv a license to display the preprint in perpetuity. It is made available under aCC-BY-NC-ND 4.0 International license.

general, or more high-dimensional landscapes.

In this work, we will develop understanding of the feedback between evolution and epistasis in a particular rich class of toy models. Motivated by the basic observation that effects of genetic changes are sums of many positive and negative contributions, we study (as have others) *random* fitness landscapes whose properties are characterized statistically. We develop a theoretical framework to understand a class of random fitness landscapes with *distance-dependent statistics* - where the correlations between the fitnesses of genomes are some function of the genetic distances between them. Our model class is flexible, with desirable biologically inspired features, and encompasses — while illuminating the problems with — many of the most commonly studied models of epistasis. By working in the tree-like limit of genotype space where there are many possible mutations but reversions are rare (as in the infinite-sites approximation) we develop a computational and analytical scheme which can be used to analyze simple evolutionary dynamics on arbitrarily high dimensional landscapes, as well as giving insights into key geometric properties of the landscapes.

Our analysis shows that evolution drives populations to highly atypical places on the fitness landscape — atypical far beyond just having anomalously high fitness. The patterns of epistasis in the neighborhood of the current genome, depends on the whole evolutionary trajectory of the population, which itself depends on long-genomic-distance (arbitrarily high order) patterns of epistasis. This is in part due to the high dimensionality of the fitness landscape, which allows rare events — although ones that evolution finds readily — to dominate the dynamics. Additionally, we show that epistasis tends to reduce variance in evolutionary trajectories allowing for paths that are genotypically different to be phenotypically (as far as fitness trajectories) similar. We then analyze slowly time-dependent landscapes and show that the atypical nature of trajectories and local landscapes conditioned on past evolution, persists when the fitness landscape has simple — and we expect more general — time dependence.

We conclude with potential directions for future theoretical studies and potentially informative experiments, particularly in light of our findings that intermediate-term evolution even with simple models of effectively-random epistasis are set by *long-distance*, *global* statistical properties of the landscape, rather than *short-distance*, *local* information such as measures of "ruggedness".

bioRxiv preprint doi: https://doi.org/10.1101/435669; this version posted October 11, 2018. The copyright holder for this preprint (which was not certified by peer review) is the author/funder, who has granted bioRxiv a license to display the preprint in perpetuity. It is made available under aCC-BY-NC-ND 4.0 International license.

2 Fitness landscapes with distant-dependent correlations

2.1 Random fitness landscapes

We begin with some general qualitative and quantitative aspects of fitness landscapes and epistasis. The main quantity of interest is the fitness function $F(g)$, which maps genotypes, g, to fitness values. The genome is most simply modeled by strings of 0's and 1's of length L – points on a hypercube. (However almost all the results discussed generalize easily to the case where all four base pairs are considered at each site.) A common convention is that all zeros corresponds to some ancestral/reference genotype, with 1's then representing mutations; we will not use that convention here as we will not want to assign special characteristics to any ancestor. Distances between genomes, defined as the number of sites at which they differ, will be a fundamental property in our models: of course, for these, the labeling of the reference genome is arbitrary.

The fitness function, $F(g)$, is often called the *fitness landscape*. Evolution tends to drive the population "up" the landscape to higher and higher fitness. A basic idea is that these upward trajectories are impeded by "ruggedness" with local maxima and other features that make some paths easier to traverse than others. In this work, we will study *random fitness landscapes*: ensembles of some classes of random functions over genotype space. The use of a random model is motivated by the fact that "fitness" is a very complex quantity. The net effect of any mutation or combination of mutations in a relatively well-adapted organism will be the sum of beneficial and deleterious effects, all conditioned on the evolutionary history and dependent on the particular environment. The hope is that a caricature of the landscape as a random function will capture some of the essence of the complex interplay between epistasis and evolution. Most previous theoretical work on fitness landscapes falls into two categories, focusing either on particular classes of random landscape models [15, 16, 26, 36, 52], or on models of specific simple situations like mutations in a single protein [50] or aspects of the fitness of particular viruses [32].

We would like to study broad classes of models that have certain key properties motivated by the desire to caricature biologically plausible/relevant features, and, secondarily, by nice analytical properties:

1. **Good scaling properties for large genomes:** We want to have well-characterized behavior in the limit of large genome sizes, but total distances between genomes much less than L, in particular avoiding pathologies related to the combinatorics of large genomes that are drawbacks of some oft-studied forms of epistasis.

bioRxiv preprint doi: https://doi.org/10.1101/435669; this version posted October 11, 2018. The copyright holder for this preprint (which was not certified by peer review) is the author/funder, who has granted bioRxiv a license to display the preprint in perpetuity. It is made available under aCC-BY-NC-ND 4.0 International license.

2. **Evolutionary-conditioned statistics:** We wish to understand evolution conditioned on past evolution and thus regions of the landscape that the population is led to by evolution. We would like such historical conditioning to be derived from the model as opposed to put in by hand. In particular, we will want to be careful not to assign any exceptional significance to a "reference" or "ancestral" genotype.

3. **Flexibility:** We want a modeling framework that encompasses models with a large variety of qualitative and quantitative structure in order to broadly understand the effects of epistasis, including the effects of both small numbers of mutations and genomes that are much further apart: i.e., both short-distance and long-distance structure.

4. **Tractable dynamics:** We need to be able to develop theoretical and computational means to explore evolutionary dynamics for long times and large genome sizes, with methods that scale well with genome length. This requires being able to efficiently generate and store pertinent information about the landscape.

We can satisfy the first three criteria by defining fitness landscapes using *distance-dependent correlation functions*. We thus choose F from an ensemble of random functions whose statistics depend only on the genetic distances between genotypes. A fundamental property of the ensemble is the correlation function between genomes as a function of the distance between them. We define the correlation function of fitness differences as

$$C(|g - g'|) \equiv \mathrm{E}[(F(g) - F(g'))^2] \tag{1}$$

for any pair of genomes g and g'. This average is taken over the ensemble of random models. This definition of the correlation function differs from standard ones: here C represents the relationship between the genetic distance $|g - g'|$ between two genomes and their distance in fitness space $F(g) - F(g')$. The choice to quantify the model in terms of fitness differences is in fact natural as relative fitness drives evolution. The correlations between any pair of fitness differences can be expressed in terms of $C(\ell)$:

$$E[(F(g_2)-F(g_1))(F(g_4)-F(g_3))] = \frac{1}{2}[C(|g_3-g_2|)-C(|g_3-g_1|)+C(|g_4-g_1|)-C(|g_4-g_2|)]. \tag{2}$$

With statistical properties defined in terms of genetic and fitness differences, no genome is special with respect to the ensemble as a whole. This is in contrast to defining models in terms of the distribution of fitness effects (DFE) of potential single mutations around a particular genome. For a general random landscape, the DFE depends on the evolutionary history: in particular, with increasing fitness the supply and magnitude of potential adaptive mutations both decrease. This statistical phenomenon is called diminishing-returns epistasis,

bioRxiv preprint doi: https://doi.org/10.1101/435669; this version posted October 11, 2018. The copyright holder for this preprint (which was not certified by peer review) is the author/funder, who has granted bioRxiv a license to display the preprint in perpetuity. It is made available under aCC-BY-NC-ND 4.0 International license.

and there are many models which are *defined* by this structure [15, 16, 52]. In contrast, we would like to understand the emergence of effects like diminishing-returns epistasis in a more general framework, by studying how well-adapted genomes are special due to the effects of past evolution. Our models allows us to specify global features of the epistasis, then let the entire history of the evolutionary dynamics determine the current DFE and epistasis among combinations of mutations around the current genome. This approach lets us generate and study evolution-conditioned regions of the fitness landscape, rather than putting in the structure of the "special" nature of a well-adapted genome in by hand.

While we will primarily be interested in fitness differences, in some landscapes, the absolute fitness is well-defined and is hence an (unmeasurable) characteristic of the initial genome. The absolute fitnesses scale as $C(L)^{1/2}$. If $C(L) = O(1)$ for large L then the absolute fitnesses are well defined in the infinite L limit on which we will primarily focus; if instead $C(L)$ scales as some increasing function of L, the absolute fitnesses are undefined. However, fitness differences (and therefore evolutionary dynamics) are always well defined in the large L limit.

To get numerically tractable models with large genomes, and even more so to enable general analysis of the evolutionary dynamics and effects of conditioning on past evolution, we must make major simplifications. We will thus (for the most part) assume that $F(g)$ is a Gaussian random function, and therefore the choice of C uniquely defines our models. The choice of Gaussian-random landscapes is certainly not biologically motivated, but it will enable us to begin to address general questions and develop computational and analytical tools. Understanding evolution on non-Gaussian landscapes is a major challenge: in the Discussion, we make some remarks about how some analyses might begin.

To understand the relationship between formulations in terms of epistatic interactions and the correlation function $C(\ell)$ of Gaussian random landscapes, it is instructive to first consider the two simplest models. First, is the *additive model* for which the effects of each mutation are statistically independent so that the fitness can just be represented as the sum of terms for each site with no epistasis. This corresponds to the choice $C(\ell) \propto \ell$. At the other extreme is the *independent fitnesses model* for which the fitness $F(g)$ of any genotype is independent of the fitness of all other genotypes. This corresponds to the choice $C(\ell) = 0$ for $\ell = 0$ and $C(\ell)$ equal to some positive constant for $\ell > 0$. The independent fitnesses model can be considered a "maximally epistatic" model.

In general, $C(\ell)$ parametrizes the correlation between the effects of the first mutation and ℓth mutation from a generic genotype. As mutations correspond to fitness differences, this correlation is given by the discrete second derivative $\frac{1}{2}\left[C(\ell+1) - 2C(\ell) + C(\ell-1)\right]$ (see Appendix A.1 for a derivation). In the additive model, the second derivative vanishes cor-

bioRxiv preprint doi: https://doi.org/10.1101/435669; this version posted October 11, 2018. The copyright holder for this preprint (which was not certified by peer review) is the author/funder, who has granted bioRxiv a license to display the preprint in perpetuity. It is made available under aCC-BY-NC-ND 4.0 International license.

responding to no correlation between effects of mutations (no epistasis); in the independent fitnesses model, the effects of one mutation and the next, and more generally, the effects of all others are highly anticorrelated.

Another simple model is called Rough Mount Fuji (RMF) model; the fitness function is a linear combination of an additive and an independent model [36]. The RMF model interpolates between the additive and independent model, but as we will see, in the large L limit in terms of evolutionary dynamics, it will usually behave like the additive model.

Another class of models that also interpolates between additive and independent limits has correlations between fitnesses that fall-off exponentially with distance:

$$C(\ell) \propto 1 - e^{-\ell/\xi} \tag{3}$$

for some correlation length ξ. The effects of mutations are then anticorrelated over the length-scale ξ, with correlations $\propto -\frac{1}{\xi^2}e^{-\ell/\xi}$. For $\xi \to 0$ this becomes the independent-fitnesses model, while for $\xi \to \infty$ (and rescaling to keep the fitness-differences of order unity), it becomes the additive model. More generally, for evolution on scales $\ell \ll \xi$, the landscape is approximately additive while for $\ell \gg \xi$ fitnesses are approximately independent. We will show that the *NK* model [26], composed of many blocks of interacting sites (defined in the next section), becomes an exponentially correlated Gaussian model in the limit of a large number of blocks.

A particularly interesting class of models we will analyze are those with *power law correlations*:

$$C(\ell) \propto |\ell|^{\alpha} \tag{4}$$

with $0 < \alpha < 1$. Note that $\alpha = 0$ corresponds to independent fitnesses, and $\alpha = 1$ corresponds to the additive model.

Figure 1 shows examples of linear cuts through landscapes for a variety of α. For intermediate α, C is unbounded as in the additive case, but the effects of consecutive (and subsequent) mutations are still anti-correlated. Large fitness differences exist on the landscape and are potentially evolutionarily accessible, but the anti-correlations are felt at long range. We will see that this structure can lead to evolutionary dynamics for which the effects of the diminishing-returns epistasis are weak enough to allow avoidance of local maxima for long periods of time, but eventually slow down the rate of fitness gain.

2.2 Amplitude spectra and relationship to other models

A common way to characterize epistasis is to break down the fitness into sums of contributions from k-wise interactions, with a measure of the overall contribution from the of k-wise

bioRxiv preprint doi: https://doi.org/10.1101/435669; this version posted October 11, 2018. The copyright holder for this preprint (which was not certified by peer review) is the author/funder, who has granted bioRxiv a license to display the preprint in perpetuity. It is made available under aCC-BY-NC-ND 4.0 International license.

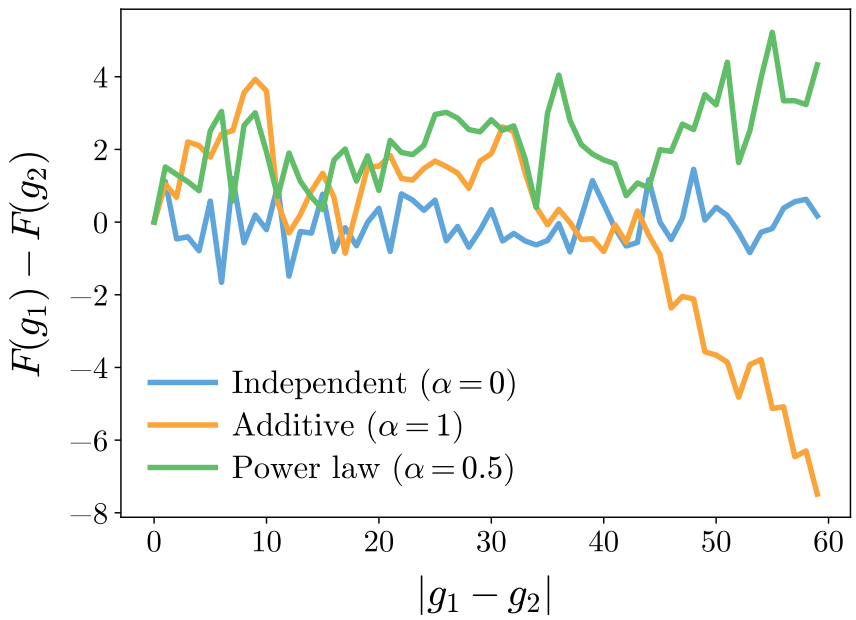

Figure 1: Examples of power-law-correlated fitness landscapes characterized by correlations $C(g_1 - g_2) = |g_1 - g_2|^\alpha$ with $\alpha = 0, 0.5, 1$. Shown are typical fitnesses along a random path on the landscape as a function of genomic distance: the number of mutations.

interactions parametrized by the *amplitude spectrum*, A_k [35]. We now show how to convert from the amplitude spectrum to an equivalent Gaussian model with distance-dependent correlations, and derive the amplitude spectra of some of the models previously defined.

The amplitude spectrum characterizes epistasis by measuring the square magnitude of interactions at each order. It can conveniently be written in terms of the discrete Fourier transform over the hypercube:

$$f_{\mathbf{k}} = \frac{1}{2^L} \sum_g e^{i\pi \mathbf{k}\cdot g} F(g) \tag{5}$$

with $\mathbf{k}$ a vector with k ones and $L - k$ zeros. $\mathbf{k}$ represents a particular set of sites on the genome. In the distance-dependent model, the symmetry under permutation of the sites in the genome implies that the statistical properties of $f_{\mathbf{k}}$ should only depend on the number of interacting sites k. Their distribution is fully characterized by the amplitude spectrum A_k defined by

$$A_k \equiv \langle f_{\mathbf{k}}^2 \rangle \ . \tag{6}$$

As each Fourier coefficient only depends on k sites of the genome, A_k is exactly the mean-square kth order global epistasis; A_0 the variance in average fitness (when this is finite), A_1

bioRxiv preprint doi: https://doi.org/10.1101/435669; this version posted October 11, 2018. The copyright holder for this preprint (which was not certified by peer review) is the author/funder, who has granted bioRxiv a license to display the preprint in perpetuity. It is made available under aCC-BY-NC-ND 4.0 International license.

the variance of the single-site (additive) terms in the fitness, A_2 the mean-square magnitude of pairwise epistatic interactions, and so on up to order L. The Fourier coefficients $f_{\mathbf{k}}$ completely define the covariance matrix, and there is a one-to-one correspondence between the A_k and the distance-dependent correlation $C(\ell)$. For Gaussian landscapes, this amounts to a complete definition of the model. (Note that we define the epistasis without reference to any particular genome, in contrast to expanding in orders of epistasis about some "ancestral" background as $F(g) = F(0) + \sum_i a_i\sigma_i + \sum_{i,j} b_{ij}\sigma_i\sigma_j + \sum_{i,j,k} c_{ijk}\sigma_i\sigma_j\sigma_k \ldots$, where $\sigma_i = 1$ if site i is mutated and 0 otherwise. This correctly captures the magnitude of global epistasis.)

In the limit of large genomes, there are problems with the scaling of A_k. We would like to study behavior that, in the limit of large L, is independent of L as long as the distances between genomes are much less than L. For example, if the fitness was a sum of single-site terms and pairwise epistatic terms, then one has to decide how the only non-zero coefficients, A_1, and A_2, depend on L. If these do not scale with L, then the effect of a single mutation would be pathological: the additive piece would contribute $O(1)$ while the pairwise terms would contribute $O(\sqrt{L})$.

From this example, we can also see the issues with having only a fixed number of non-zero A_k as $L \to \infty$. This remains true even if we rescale terms by factors of L. For example, with pairwise epistasis, the second order terms could be scaled down such that $A_2 = \frac{1}{L}\tilde{A}_2$ with $\tilde{A}_2 = O(1)$, so their total magnitude matches the magnitude of the first order terms — as in the conventional Sherrington-Kirkpatrick spin-glass model [45]. However, for changes of $\ell \ll L$ sites, the fraction of second order terms where both sites change is $\frac{\ell}{L} \ll 1$. Therefore over distance scales $\ll L$, this model is effectively additive, with $A_1' = A_1 + \tilde{A}_2$.

Another problem occurs if all orders of epistasis are comparably large: i.e., all A_k of the same order. The number of terms ($\mathbf{k}$'s) of order k is $\binom{L}{k}$. If the A_k are all non-zero and don't scale with L, then the middle terms with $|k - L/2| = O(\sqrt{L})$ dominate for large L. We will see that this gives the independent fitnesses model.

By construction, our distance-dependent correlated landscapes avoid these large L pathologies since $C(\ell)$ is independent of L. To relate these models to the amplitude spectra and make the large L limit well-behaved one needs to define a *rescaled amplitude spectrum*. A convenient choice is to pull out the binomial factor for the number of terms of each order and define

$$\rho_A(z) = L\binom{L}{Lz}A_{Lz} \tag{7}$$

for $z \in [0, 1]$, with Lz rounded to the nearest integer (which does not matter for large L). The $\rho_A(z)$ parameterize the magnitude of the *total* epistasis at order zL. The A_k (and therefore $\rho_A(z)$) can be computed directly from $C(\ell)$. Similarly, one can use $\rho_A(z)$ to compute $C(\ell)$:

bioRxiv preprint doi: https://doi.org/10.1101/435669; this version posted October 11, 2018. The copyright holder for this preprint (which was not certified by peer review) is the author/funder, who has granted bioRxiv a license to display the preprint in perpetuity. It is made available under aCC-BY-NC-ND 4.0 International license.

in Appendix A.3 we show that in the limit of large L

$$C(\ell) \approx 2 \int_0^1 (1 - (1-2z)^\ell) \rho_A(z) dz \tag{8}$$

Models with a well defined ρ_A in the limit of large L thus correspond to well-behaved distance-dependent correlation functions $C(\ell)$.

Most previously studied models correspond to simple forms of $\rho_A(z)$. The additive model has $\rho_A(z) = \delta(z)$ (with the limit needing to be taken carefully) while the independent model is $\rho_A(z) = \delta(z - 1/2)$ since all Fourier modes in it have equal weight. More generally, terms at different orders of epistasis contribute features of different length-scales to C with, just as for Fourier transforms, small z — thus small k — corresponding to large length-scale features. If a single $z < \frac{1}{2}$ dominates, $C(\ell)$ falls off exponentially with correlation length $\xi = -\log(1-2z)^{-1}$. Terms with $z > \frac{1}{2}$ cause oscillations in correlations and make the landscape more "rugged"; in the extreme limit, pure $z = 1$ corresponds to the parity function where every step leads to a change in sign of the fitness. The Random-Mount-Fuji (RMF) model is a sum of additive and independent parts and thus corresponds simply to the sum of delta functions in ρ_A at $z = 0$ and $z = 1/2$.

In a certain limit, Kauffman's NK model [26] of random landscapes is equivalent to a simple distance dependent model. The NK model splits the contribution to the fitness function into N (potentially overlapping) blocks B, each of K interacting sites. For each block of interactions there is an independent fitness model on the K sites in the block: which assigns an iid random value, $f_B(g_B)$, to each of the 2^K configurations of the sub-genome g_B, of that block. The total fitness is then $F(g) = \sum_B f_B(g_B)$. If the N blocks are chosen at random, and L and N are large, a central-limit-theorem-like argument shows that F limits to a Gaussian random function. More precisely, one can show that for $N \gg \binom{L}{K}$, when all blocks are represented many times, all the moments of F converge to that of a a jointly Gaussian random function with $A_k = \frac{1}{L}\binom{K}{k}\binom{L}{k}^{-1}$. The rescaled amplitude spectrum of the NK model is thus simply $\rho_A(z) \approx \delta(z - K/L)$. This corresponds to a distance-dependent correlation with

$$C(\ell) \propto (1 - e^{-\ell/\xi}) \tag{9}$$

where $\xi = -\log\left(1 - \frac{2K}{L}\right)^{-1}$.

Typically the NK model is studied in a different limit where N is $O(L)$, so only a small subset of all possible blocks are represented [26, 35, 37]. However the analysis of the Gaussian distance-dependent model should still be useful. As long as the within-block fitnesses are not broadly distributed, the fitness difference between two genomes at a genetic distance ℓ is approximately Gaussian if $N \gg \frac{L}{K\ell}$, corresponding to many blocks having at least one mutation. For $\frac{K}{L}$ small (long correlation length), this corresponds to roughly $\ell \gg \frac{\xi}{N}$.

bioRxiv preprint doi: https://doi.org/10.1101/435669; this version posted October 11, 2018. The copyright holder for this preprint (which was not certified by peer review) is the author/funder, who has granted bioRxiv a license to display the preprint in perpetuity. It is made available under aCC-BY-NC-ND 4.0 International license.

This suggests that the approximation of the NK model as a distance dependent correlation function may hold over a variety of scales, from $x \ll \xi$, for which each block has at most one mutation and the landscape is approximately additive, to $x \gg \xi$, for which most blocks have a mutation and the landscape is approximately independent.

The power law model $C(\ell) \propto \ell^{\alpha}$ has weight at all z but the crucial large ℓ behavior is controlled by small z. For large ℓ, the integrand in Equation 8 is dominated by z of $O(\ell^{-1})$; the integrand thus scales as $z\ell\rho_A(z)$ which implies $\rho_A(z) \propto z^{-1-\alpha}$ for small z (see detailed calculation in Appendix A.2). Note that with this scaling, the typical magnitudes of the k-th order terms for small k are of order $L^{(\alpha-k)/2}$ and their net contributions to a F are of order $L^{\alpha/2}$ for each k.

The amplitude spectrum can be used to define distance-dependent models more generally. By defining non-Gaussian but independent Fourier components whose second moments match $\rho_A(z)$, we can generate ensembles of functions which have second order statistics defined by $C(x)$ but different higher order statistics. We will discuss this approach further in Section 7.3 when we consider time-dependent landscapes. Until then we will restrict consideration to Gaussian-random landscapes and hence need work only with the correlation function $C(\ell)$; this greatly simplifies computations and understanding.

2.3 Local properties of landscapes

Many previous studies focus on "static" properties of landscapes, that is statistics near genomes not conditioned on prior evolution. One of the most commonly studied static properties is the distribution of local maxima [36, 37]. This metric is often taken as a measure of "ruggedness", with the aim of getting intuition for how the geometry of a landscape might shape evolution. However the notion of ruggedness is rather ambiguous, and, more generally, the dynamical consequences of such local properties of the geometry are very different in high dimensional spaces than intuition built on low dimensional ones might suggest.

In particular, local static properties depend entirely on short-range correlations and are completely insensitive to longer-range ones. Specifically, in Appendix C.1 we show that the probability of a genome being a local maximum in a Gaussian random landscape is given asymptotically by

$$P_{loc-max} \sim L^{-(1-r)/r} \tag{10}$$

with r the correlation coefficient of the fitnesses of the neighbors of a chosen point, which can be computed to be $r = 1 - \frac{1}{2}\frac{C(2)}{C(1)}$. This probability of being a local maximum is exponentially sensitive to local correlations. For the additive model, $r = 0$ and there is one maximum, for the independent model, $r = \frac{1}{2}$ so $P_{loc-max} = \frac{1}{L}$, and for the parity model $r = 1$ and

bioRxiv preprint doi: https://doi.org/10.1101/435669; this version posted October 11, 2018. The copyright holder for this preprint (which was not certified by peer review) is the author/funder, who has granted bioRxiv a license to display the preprint in perpetuity. It is made available under aCC-BY-NC-ND 4.0 International license.

$P_{loc-max} = \frac{1}{2}$.

But $P_{loc-max}$ is independent of the structure of long-range correlations; we will show that it is the long-range structure that drives evolution and determines how far uphill it can proceed before reaching a local maximum. Indeed, the RMF model, *NK* model, and power-law models can each be tuned to have similar numbers of local maxima, but have much different global structure. An RMF model with the additive piece being a fraction p of the fitness has $r = 1 - p$. An *NK* model with random blocks has $r = \frac{1}{2}\frac{K}{L}$. A power law model with exponent α has $r = 1 - 2^{\alpha-1}$. Therefore the *NK* model can have any r from 0 to $\frac{1}{2}$, and the other two models any value from 0 to 1. Given any two classes of models, we can always find pairs of models with the same local maxima structure, as these only depend on the parameters p, $\frac{K}{L}$ and α respectively. As we will see, the long-term evolutionary dynamics for these three models will be quite different, regardless of the value of r.

An interesting static property that depends on long range structure is the maximum fitness difference, $f_{\max(\text{ball})}(\ell)$, between a random point and all points in a ball of radius ℓ around that point. We are interested in large ℓ, but $\ell \ll L$. For the RMF model, $f_{\max(\text{ball})}(\ell) \sim p\ell\sqrt{\log(L)}$ since the maximum is achieved by mutating the ℓ sites with the largest additive fitness gains, with an uncertainty of only $\pm\sqrt{\ell}$ from the independently random piece. For the *NK* model, for $N = 1$ we have approximately K^ℓ independent fitnesses (as there are only K sites for which changes lead to fitness differences). This gives us $f_{\max(\text{ball})}(\ell) \sim \sqrt{\ell \log(K)}$ from the maximum of i.i.d. samples from a Gaussian.

For more general correlations, computing $f_{\max(\text{ball})}(\ell)$ is more complicated; nonetheless, we can proceed in a general way by realizing that most of the genomes in the ball are at the surface (that is at distance ℓ from the center). We can then approximate $f_{\max(\text{ball})}(\ell)$ as the maximum value of these L^ℓ identically distributed Gaussian random variables with mean 0, variance $C(\ell)$, and covariance $C(\ell) - \frac{1}{2}C(2\ell)$ as the points on the surface are typically distance 2ℓ apart. We thus have, generally,

$$f_{\max(\text{ball})}(\ell) \approx \sqrt{\frac{1}{2}C(2\ell)}\sqrt{\log(L^\ell)} \pm \sqrt{C(\ell) - \frac{1}{2}C(2\ell)} \tag{11}$$

The second, stochastic, term is due to the fluctuations of the average difference at genetic distance ℓ, while the dominant first term is due to the maximization over all such differences. For the particular case of power-law-correlated landscape, we have, asymptotically

$$f_{\max(\text{ball})}(\ell) \sim 2^{1-\alpha}\ell^{(1+\alpha)/2}\sqrt{\log(L)} \tag{12}$$

A crude estimate of the maximum fitness on the whole hypercube is given by $f_{\max(\text{ball})}(L)$; we expect this to be correct up to polylogs. Therefore the maximum absolute fitness $F^* \sim L^{(1+\alpha)/2}$ for power law landscapes - see Appendix C.2 for another heuristic derivation.

bioRxiv preprint doi: https://doi.org/10.1101/435669; this version posted October 11, 2018. The copyright holder for this preprint (which was not certified by peer review) is the author/funder, who has granted bioRxiv a license to display the preprint in perpetuity. It is made available under aCC-BY-NC-ND 4.0 International license.

We see that the behavior of $f_{\max(\text{ball})}(\ell)$ scales quite differently for the various models — with ℓ and sometimes even in L. The additive piece of the RMF model has the largest differences; the NK model and other short-range correlated models have the smallest differences as at long-distances they are like independent models. If evolutionary trajectories are able to travel significant distances, then long range features of the landscape, such as the maximum in a ball, are bound to matter. This discussion should make clear that very local structure, such as number of local maxima, gives very incomplete — indeed misleading — information.

3 Adaptive walks

"Static" properties of landscapes that focus on behavior near to typical points are misleading: one must take into account conditioning on prior evolution. To do this, we focus on understanding the properties of *random adaptive walks*. An adaptive walk corresponds to evolution in the strong selection weak mutation (SSWM) regime —adaptive mutations are rare, and when they establish they arise to fixation before the next adaptive mutation occurs. By studying the step-by-step dynamics of adaptive walks, particularly over a large number of steps, we will be able to understand directly the feedback between epistasis and evolution. We can then study the properties of genomes and the statistics of available mutations and epistasis among these, conditioned on the evolutionary history. This gives a far better and richer picture of the evolution on rugged landscapes than making qualitative arguments based on local geometric properties.

Specifically, we analyze a clonal population which follows some trajectory $g(x)$ in genotype space, where x indexes the number of mutational steps from the ancestor. At each step, the population randomly samples the space of all possible mutations. For each sampling, the mutation is either rapidly purged, or rapidly fixes. The probability of fixation is some non-decreasing function of the fitness difference $s_{g\to g'}$ between the current population genotype g and the mutant g'. Thus the probability of a transition going from g to g' can be written as

$$P(g \to g') = \phi(s_{g\to g'})/Z \tag{13}$$

where ϕ, the *fixation function*, is the probability of fixation given a mutation, and Z is a normalization factor. The dynamics of each step depends only on the local fitness landscape a single mutation away. If ϕ allows downhill steps. the dynamics will go on indefinitely. We will focus on uphill random walks which must eventually terminate at some local maximum.

There are various choices for ϕ that have been studied.

- **Random:** the next step is chosen uniformly at random from all uphill directions.

bioRxiv preprint doi: https://doi.org/10.1101/435669; this version posted October 11, 2018. The copyright holder for this preprint (which was not certified by peer review) is the author/funder, who has granted bioRxiv a license to display the preprint in perpetuity. It is made available under aCC-BY-NC-ND 4.0 International license.

- **Greedy:** The best possible step is chosen.
- **Reluctant:** Atypically small uphill steps are chosen — the extreme limit being to chose the smallest.
- **Natural:** The choice is weighted by some function of the fitness difference to reflect the chances of that mutation fixing. The appropriate choice for moderate sized populations in the strong-selection weak-mutation regime is $\phi \propto s$. In large populations, there can be much stronger weighting to large s [51].

For the bulk of this paper we will focus, for simplicity, on the *random step* model (i.e with $\phi(s)$ the step function): all adaptive mutations have the same probability of fixation, and deleterious mutations are always purged. Later we will briefly consider natural weighting — which results in only small changes in the behavior for modest size populations — and reluctant walks.

3.1 Adaptive walks on landscapes generated "on the fly"

The simplest way to study adaptive dynamics numerically would be to first draw a particular example of the landscape from the ensemble, and then perform adaptive walks on it. However this would be computationally expensive: for landscapes with non-trivial correlation structure as it would require 2^L random variables. Also, with only numerical work, drawing more general conclusions beyond the particular models studied would be fraught with difficulties.

There have been several numerical recent studies analyzing adaptive walks in the simpler *NK* and RMF models [36, 37, 40, 41]. These works have primarily focused on the lengths of adaptive walks before a local maximum is reached. Based on numerics, these claim to find a phase transition in the length of adaptive walks walks as parameters are varied [36, 37, 41]. (We will show analytically that this is a crossover effect for large, finite L in Section 6, and compute the crossover scale.) However, the numerical approaches used do not scale well to other parameter regimes, or to other models. The *NK* model, which has complex epistasis, has been simulated only with small blocks ($K = 8$) for which walks of length $\sim 10^3$ have been studied [36, 37]. The RMF models with large L are simple enough to run longer (up to walks of length 10^6) [41]. This is because the additive part of the RMF model only has L free parameters, and for the independent fitnesses part, only XL random parameters need to be drawn to simulate a walk of length X: these can be drawn as the walk progresses.

Distance-dependent landscapes allow us to do something similar for general patterns of epistasis. The Gaussian correlations make computing the local landscape around a single

bioRxiv preprint doi: https://doi.org/10.1101/435669; this version posted October 11, 2018. The copyright holder for this preprint (which was not certified by peer review) is the author/funder, who has granted bioRxiv a license to display the preprint in perpetuity. It is made available under aCC-BY-NC-ND 4.0 International license.

evolutionary trajectory a tractable task, both analytically and computationally. The current distribution of fitness effects can be computed as a conditional distribution based on the parts of the landscape already explored. This enables simulations of dynamics for large L, and has the big advantage of making explicit the role of past evolution on the currently accessible fitness landscape. We develop the dynamical approach in the remainder of this section and explore its consequences in Section 4.

The first key observation is that the stochasticity can be divided into two sources. First, the fitnesses of genotypes adjacent to the current genotype g need to be generated. This is equivalent to drawing the current distribution of possible single-mutation fitness effects (DFE). The transition probabilities $P(g \to g')$ can then be computed, and the next step chosen from the resulting distribution. This process is then repeated. Separating the stochasticity in this way ensures that the dynamical step and the DFE step remain statistically independent. The Gaussian distant-dependent correlation structure will mean that the conditional DFE only depends on $C(\ell)$ and the already-explored parts of the landscape.

The second simplification is that in the high-dimensional limit, a walk on a hypercube looks like a path on a tree (Figure 2a), with single mutational steps correspond to edges. The tree-like structure comes from the fact that the same site is not likely to be mutated twice, which is generally true if L is much larger than the total number, X, of mutations accumulated during the evolution. (More precisely we need $X^2 \ll L$, but as the number of sites mutated twice is small as long as $X \ll L$, we do not expect substantial errors from the tree approximation.) With the statistical symmetry of the landscape in the tree approximation, we can choose to label the genomes, g, by the number of mutational steps taken, x, with the distance $|g(x) - g(x')| = |x - x'|$. We will henceforth label the genomes and other quantities by the step number x.

A key property for the adaptive walk is the set of potential *single-step fitness gains* away from the genome at step x: $\{s_i(x)\}$, with i labeling the mutated site. The probability distribution of these, the DFE for the possible next steps, has empirical mean

$$\mu(x) = \frac{1}{L} \sum_i s_i(x) \tag{14}$$

the *average available fitness gain*. Both the potential fitness gains and their empirical mean, $\mu(x)$, are covariate Gaussian. The value of $\mu(x)$ is typically negative during evolution, indicating that beneficial mutations are less common than deleterious ones. Note that we will refer to empirical means within a landscape, such as $\mu(x)$ around a particular genome, as "averages", while means over the ensemble of landscapes we will refer to as "expectations". (In statistical mechanics terminology, expectations over the random landscape would be called "quenched averages".)

bioRxiv preprint doi: https://doi.org/10.1101/435669; this version posted October 11, 2018. The copyright holder for this preprint (which was not certified by peer review) is the author/funder, who has granted bioRxiv a license to display the preprint in perpetuity. It is made available under aCC-BY-NC-ND 4.0 International license.

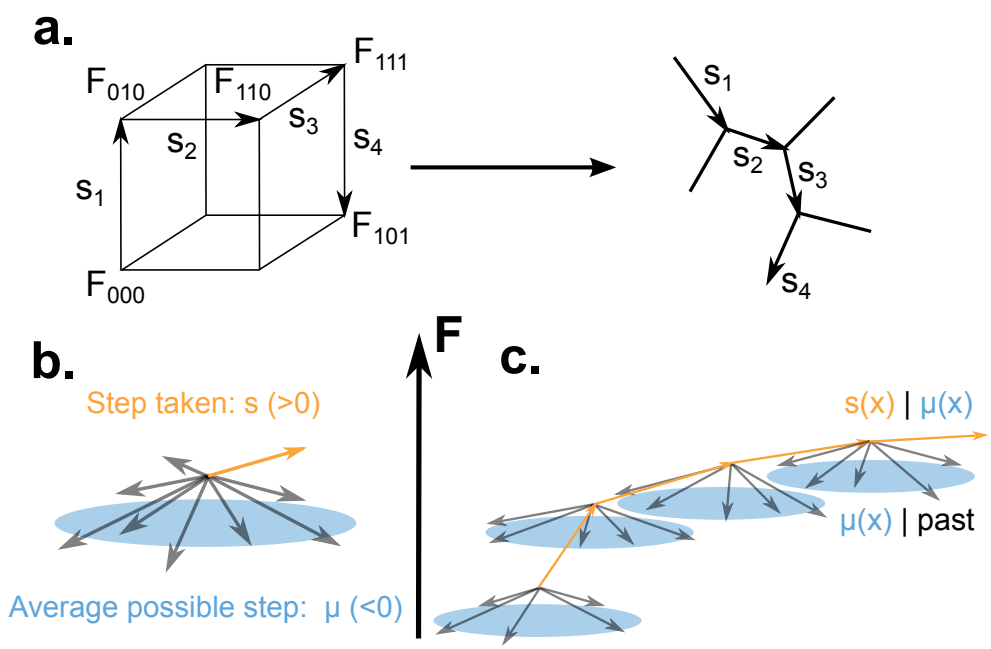

Figure 2: Schematic of adaptive walks on the hypercube. (a) In the high dimensional limit, a single site is mutated at most once, which causes the fitness landscape to look like a tree, with genotypes as nodes, and edges corresponding to fitness differences. (b) At any point, the distribution of single-step fitness gains, s, is parametrized by its mean μ (blue plane), which is typically negative, while individuals gains have some variance around μ (grey arrows). A particular uphill step (orange) is chosen randomly from the possible uphill steps, and taken. (c) Adaptive walks with the right statistics can be found by computing μ and then taking a random uphill step s from the distribution with mean μ; μ depends linearly on previously observed μ and the previous uphill steps s, plus a Gaussian random part. Evolution tends to cause uphill steps to become rarer and rarer by driving typical μ to be more and more negative, although the stochastic variations can sometimes make it less negative after a step.

In the limit of large L, the single-step fitnesses conditioned on the average possible gain, $\{s_i(x)|\mu(x)\}$, are asymptotically independent. They are Gaussian with mean $\mu(x)$ and variance

$$\sigma^2 \equiv \mathrm{Var}[s_i(x)|\mu(x)] \approx \mathrm{Var}[s_i(x) - \mu(x)] = \frac{1}{2}C(2) \tag{15}$$

Therefore, knowing $\mu(x)$ completely determines the DFE around current genome — it is a Gaussian with a known mean and variance (Figure 2b).

The value of $\mu(x)$, conditioned on previously observed fitnesses is itself a Gaussian random variable whose statistics can be computed using standard methods which we will review here. Suppose we have a jointly Gaussian collection of vector valued random variables $\mathbf{Z}$ and $\mathbf{W}$,

bioRxiv preprint doi: https://doi.org/10.1101/435669; this version posted October 11, 2018. The copyright holder for this preprint (which was not certified by peer review) is the author/funder, who has granted bioRxiv a license to display the preprint in perpetuity. It is made available under aCC-BY-NC-ND 4.0 International license.

with covariance matrix

$$\mathbf{\Sigma} = \begin{pmatrix} \mathbf{\Sigma}_{ZZ} & \mathbf{\Sigma}_{ZW} \\ \mathbf{\Sigma}_{WZ} & \mathbf{\Sigma}_{WW} \end{pmatrix} = \begin{pmatrix} \mathrm{cov}(\mathbf{Z},\mathbf{Z}) & \mathrm{cov}(\mathbf{Z},\mathbf{W}) \\ \mathrm{cov}(\mathbf{W},\mathbf{Z}) & \mathrm{cov}(\mathbf{W},\mathbf{W}) \end{pmatrix} \tag{16}$$

The conditional expectation $\mathrm{E}[\mathbf{Z}|\mathbf{W}]$ is a linear function of the values of $\mathbf{W}$. It can be computed as $\mathbf{K}_Z\mathbf{W}$, where the linear *response kernel* $\mathbf{K}_Z$ is defined by

$$\mathbf{K}_Z = \mathbf{\Sigma}_{ZW}\mathbf{\Sigma}_{WW}^{-1} \tag{17}$$

The conditional covariance can be written as

$$\mathbf{\Sigma}_{Z|W} = \mathbf{\Sigma}_{ZZ} - \mathbf{K}_Z\mathbf{\Sigma}_{WZ} \tag{18}$$

In our case, the $\mathbf{Z}$ is merely $\mu(x)$, and the $\mathbf{W}$ is the set of all $\mu(y)$ and $s(y)$ for $y < x$, where $s(y)$ are the fitness gains of the single steps actually taken during the evolution (dropping the site i as we are in the tree-like limit). Therefore, we can write the conditional expectation as

$$\mathrm{E}[\mu(x)|\mathbf{W}] = \sum_{y=0}^{x-1} K(x,y)\mu(y) + J(x,y)s(y) \tag{19}$$

For ease of later computation we write the response kernels $K(x,y)$ and $J(x,y)$ separately. The variance can be computed as:

$$V_\eta(x) \equiv \mathrm{Var}[\mu(x)|\mathbf{W}] = \mathrm{Var}[\mu(x)] - \sum_{y=0}^{x-1} K(x,y)\mathrm{E}[\mu(x)\mu(y)] + J(x,y)\mathrm{E}[\mu(x)s(y)] \tag{20}$$

In other words, we can write:

$$\mu(x) = \sum_{y=0}^{x-1} K(x,y)\mu(y) + J(x,y)s(y) + \eta(x) \tag{21}$$

where $\eta(x)$, the random part of the average available gain, is Gaussian distributed with variance $V_\eta(x)$.

We again emphasize that this randomness is over the ensemble, conditioned on the structure $\mathbf{W}$; $\eta(x)$ represents the uncertainty over the distribution of functions, not the stochasticity of the dynamics. Also note that the statistics of $\mu(x)$ depend only on fitness differences and not the absolute values $F(x)$; therefore they are well defined independent of L as desired.

The structure outlined above, implies that in the large L limit, we can simulate the dynamics by computing the statistics of the DFE, choosing a beneficial mutation, and repeating (Figure 2c). More precisely, we use the following dynamical procedure:

bioRxiv preprint doi: https://doi.org/10.1101/435669; this version posted October 11, 2018. The copyright holder for this preprint (which was not certified by peer review) is the author/funder, who has granted bioRxiv a license to display the preprint in perpetuity. It is made available under aCC-BY-NC-ND 4.0 International license.

1. Generate the conditional expectation of $\mu(x)$ given the previously observed $\{\mu(y)\}$ and $\{s(y)\}$ and the kernels, $J(x, y)$ and $K(x, y)$.
2. Choose a value of $\mu(x)$ drawn from Gaussian distribution with its conditional expectation and known variance, $V_\eta(x)$.
3. Generate a step $s(x)$ from the fixation function ϕ applied to a Gaussian with mean $\mu(x)$ and fixed variance, σ^2.
4. Repeat.

The joint Gaussianity makes computation highly efficient, as the distribution of $\mu(x)$, and hence the distribution of the $s(x)$, can be computed using simple linear algebra. Computing the response kernel at step x, requires a $2x \times 2x$ matrix inversion. This can be performed iteratively from the covariances competed at the previous step with cost $O(x^2)$. Computing $\mu(x)$ using the response kernels costs only $O(x)$. The total computation time for x from 0 to some X thus grows as X^3.

For all the simulated dynamics in this work, we chose, for simplicity, to approximate the response kernel at all steps by the kernels $\mu(X, y)$ and $s(X, y)$ at the final step X. Likewise, we used $V_\eta(X)$ to approximate $V_\eta(x)$ throughout the walk. This gives us the same computational complexity as the iterative inversion method. Numerical results show that $V_\eta(x)$ saturates quickly to the long time value $V_\eta(\infty)$ (as expected) and the analytical results in Section 3.2 suggest that the key parts of the response functions converge as well. This approximation gives largest errors at the start of the walk, but, as we will see in Section 3.3, the long-term dynamics depends only weakly on early times.

The response kernels depend only on the geometry of the path. If the walk geometry is known in advance (as it is for a population in the strong selection weak mutation regime on which we focus), the response kernels can be computed once and then used for multiple simulations on independent but statistically identical landscapes. Therefore T simulations of length X can be achieved in $O(X^3 + TX^2)$ time in the large L limit. The generation of the landscape "on the fly" has removed any dependence of the computational complexity on the dimension of the genotype space.

The form of Equation 21 assumes a walk along a single path, with the geometry of a straight line. However, the framework extends to trajectories with more complicated topologies as well. In particular, there is a computationally straightforward extension to the case of multiply branching paths on a single landscape. The response functions are computed via Equation 17 to obtain $\mu(x)$ at the end of any branch, and the potential single-step fitness gains $s_i(x)$ are independent when conditioned on $\mu(x)$.

bioRxiv preprint doi: https://doi.org/10.1101/435669; this version posted October 11, 2018. The copyright holder for this preprint (which was not certified by peer review) is the author/funder, who has granted bioRxiv a license to display the preprint in perpetuity. It is made available under aCC-BY-NC-ND 4.0 International license.

3.2 Single-path response kernels

In addition to enabling efficient computation, the response functions can be used to gain a qualitative and quantitative understanding of how the dynamics of adaptive walks depend on the past. We will take advantage of this structure to analytically approximate the statistics of fitness trajectories for a variety of landscapes, and obtain exact results for some simple cases.

The response kernels encode exactly the effect that the past evolution has on evolution in the near future. Because this depends on the *trajectories* of $\mu(x)$ and $s(x)$, and not simply their most recent or average values, the detailed dynamics of evolution determines the current DFE. The Gaussian nature of the landscape means that the present depends linearly on the past; however the evolutionary dynamics causes non-linear feedback via the selection of the uphill step from the DFE. This interplay between past and present is what gives rise to the complexities of evolutionary dynamics even in these Gaussian-distributed landscapes.

As we shall show explicitly, the response of $\mu(x)$ to $s(y)$ for $y < x$ (via the kernel $J(x, y)$), tends to be negative; the current possible steps are anticorrelated with previous ones taken. This negative feedback makes it harder and harder to find uphill steps as the evolution continues. The response of $\mu(x)$ to $\mu(y)$ (via the kernel $K(x, y)$) is somewhat subtle, but its net effect is to make $\mu(x)$ correlated with earlier $\mu(y)$.

3.2.1 Exponentially-correlated landscapes

We begin by analyzing the case of exponential correlations:

$$C(\ell) = \frac{1}{b}(1 - e^{-\ell/\xi}) \tag{22}$$

where $b = (1 - e^{-1/\xi})$ normalizes the family so that random single mutants have identical statistics ($C(1) = 1$) for any ξ.

For this model, the response structure is easy to compute in terms of the absolute fitness values $F(x)$. A direct calculation (detailed in Appendix B.3) shows that we have

$$\mathrm{E}[\mu(x)|\text{ past}] = -bF(x) \tag{23}$$

The dynamics is "memoryless" (Markovian) with regards to the fitnesses — only the last observed fitness matters. This relationship is in fact exact; that is, we can write

$$\mu(x) = -bF(x) \tag{24}$$

bioRxiv preprint doi: https://doi.org/10.1101/435669; this version posted October 11, 2018. The copyright holder for this preprint (which was not certified by peer review) is the author/funder, who has granted bioRxiv a license to display the preprint in perpetuity. It is made available under aCC-BY-NC-ND 4.0 International license.

without the conditional expectations. This is a very special property of the exponential landscape (and indeed, completely characterizes it for $b \in [0,1]$). The relationship is most clear in the independent limit where $b = 1$. Here, in the large L limit, $\mu(x) \equiv \mathrm{E}_{x+1}[F(x+1)|F(x)] - F(x) = -F(x) + O(L^{-1/2})$ where E_{x+1} is the empirical average, taken over all single steps away from x, is zero due to independence of fitness at other sites.

Equation 25, along with the definition of the step taken, $s(x) = F(x+1) - F(x)$, implies that the joint covariance matrix of the $\mu(x)$ and $s(x)$ is singular. The response function is degenerate to degree x. We can take advantage of the freedom of choice to make the response kernels take simple forms; two possible choices are

$$\mathrm{E}[\mu(x)|\text{ past}] = -b\sum_{y=0}^{x-1} s(y) + \mu(0) \tag{25}$$

or

$$\mathrm{E}[\mu(x)|\text{ past}] = -bs(x-1) + \mu(x-1) \tag{26}$$

The negative correlation with the previous fitness will drive the typical $\mu(x)$ to be more and more negative during evolution. Since the variance of $\mu(x)$ is constant, this leads to the typical DFE having fewer and fewer beneficial mutations, slowing down the rate of fitness gain, as expected. In Section 3.3, we will compute the dynamics for exponential correlations explicitly.

The variance σ^2 of the conditional $s(x)$ is given by

$$\sigma^2 = \frac{1}{2}C(2) = \frac{1}{2}(1 + e^{-1/\xi}) \tag{27}$$

which ranges from $\frac{1}{2}$ (independent model) to 1 (additive model) for increasing ξ.

3.2.2 Power-law-correlated landscapes and integral approximation

To understand the behavior of long walks — in which we are primarily interested — it is instructive to approximate the discrete response equation by the integral equation:

$$\mu(x) \approx \int_0^x dy\,[K(x,y)\mu(y) + J(x,y)s(y)] + \eta(x) \tag{28}$$

where we abuse notation and use J and K for the continuous analogues of the discrete response functions. Now $\eta(x)$ is the random part of $\mu(x)$, a Gaussian random variable with autocorrelation

$$\mathrm{E}[\eta(x)\eta(y)] = V_\eta \delta(x-y) \tag{29}$$

bioRxiv preprint doi: https://doi.org/10.1101/435669; this version posted October 11, 2018. The copyright holder for this preprint (which was not certified by peer review) is the author/funder, who has granted bioRxiv a license to display the preprint in perpetuity. It is made available under aCC-BY-NC-ND 4.0 International license.

As we are interested in the long-walk behavior, we use the asymptotic value, $V_\eta \equiv \lim_{x\to\infty} V_\eta(x)$, at which the conditional variance saturates.

In general, the kernels will depend on both x and y. But for $x - y \ll x$, we anticipate that they will approximately be functions of just the distance, $x - y$. In this limit, the integrals become convolutions and Fourier transforms can be used. For the case of power law correlations, Wiener-Hopf analysis (Appendix B) can be used in this $x - y \ll x$ regime, to obtain $J(x, y) \approx -c_J(x - y)^{-(1-\nu)}$ and $K(x, y) \approx \delta(x - y) + c_K\mathcal{P}(x - y)^{-(1+\nu)}$ with the exponent $\nu = (1 - \alpha)/2$ and $\mathcal{P}$ denoting the principal part (so that integrals over K have no contribution from the divergence at $x - y \to 0$). Here c_J and c_K are positive coefficients that can be written in terms of Beta functions and combinations of V_η and σ^2.

Armed with their scalings forms, and the structure of the singular integral equations that have to be solved, one can guess and check the exact kernels (valid when x, y and $x - y$ are all large):

$$J(x, y) \approx -c_J \,\mathrm{sign}(x - y) \left(\frac{y}{x}\right)^{\nu} \frac{1}{(x - y)^{1-\nu}} \tag{30}$$

and

$$K(x, y) \approx \delta(x - y) + c_K \,\mathrm{sign}(x - y) \left(\frac{x}{y}\right)^{\nu} \mathcal{P}\left(\frac{1}{(x - y)^{1+\nu}}\right). \tag{31}$$

The responses are of opposite signs, and the J drops off less sharply than the K. However, the sign of K is misleading due to the principal part. If the convolution with the past is done by parts, then we get

$$\int_0^x dy K(x, y)\mu(y) = \mu(x) - \frac{c_q}{x^\nu}\mu(x) - \int_0^x dy Q(x, y)\frac{d\mu}{dy} \tag{32}$$

with positive coefficient c_q and the kernel of $\frac{d\mu}{dy}$ defined by

$$Q(x, y) \equiv \int_0^y dz[K(x, z) - \delta(x - z)] \tag{33}$$

This form of the response shows that $\mu(x)$ is anticorrelated with both $s(y)$ and $\frac{d\mu}{dy}$ of the past.

From the form of the response kernel, we can already see a qualitative difference between the power-law and exponential cases; the conditional probabilities in general depend on the whole fitness-trajectory of the past evolution, not just the most recent fitness. This dependence on the long-ago past is crucial for shaping the long-term dynamics of random adaptive walks.

bioRxiv preprint doi: https://doi.org/10.1101/435669; this version posted October 11, 2018. The copyright holder for this preprint (which was not certified by peer review) is the author/funder, who has granted bioRxiv a license to display the preprint in perpetuity. It is made available under aCC-BY-NC-ND 4.0 International license.

3.3 Typical fitness-trajectories of adaptive walks

Given an analytical form for the long-distance response kernel, we can obtain analytical understanding of the typical fitness trajectories of random adaptive walks. The response kernels give an integral equation for the conditional expectation (across adaptive walks over the whole ensemble of landscapes) of $\mu(x)$ in terms of past $\mu(y)$ and $s(y)$, and then the value of $\mu(x)$ determines the distribution of $s(x)$. Since $\mathrm{E}[\mu(x)|\text{past}]$ is linear in past values, we can use the response kernels to get a self-consistent set of equations for the expectation over all adaptive walks on all landscapes $\mathrm{E}_{walks}[\mu(x)]$ and $\mathrm{E}_{walks}[s(x)]$.

We define the *fitness gain* of a trajectory as a function of the number of steps, x, along it as

$$f(x) \equiv F(x) - F(0). \tag{34}$$

Due to the distance-dependent correlation structure, $f(x)$ should, for walks with $x \ll L$, be independent of L. We start with simple examples where the answers are known from simple methods, and work up to the more complicated cases.

3.3.1 Simple landscapes

The simplest situation is the additive model: the fitness steps are uncorrelated, so both K and J are 0. Therefore $\mathrm{E}_{walks}[\mu(x)]$ is always 0, and uphill steps are taken from the same distribution. The average total fitness gain, $\mathrm{E}_{walks}[f(x)]$, grows linearly in x on average, and the variance $\mathrm{Var}_{walks}[f]$ also grows linearly.

The other simple case is the independent model. Since the fitnesses are all independent, there is a simple relationship between the DFE mean and the (absolute) fitness: $\mu(x) = -F(x)$ for any x in the large L limit, with no additional variation (i.e. $V_\eta = 0$). The difficulty of finding uphill steps is directly related to the current fitness. (Note that the absolute fitnesses are well defined in the independent model since $C(\ell)$ is bounded, as per the discussion in Section 2.1).

We now need to understand the typical uphill steps actually taken, given $\mu(x)$. The distribution of possible steps is just determined by $\mu(x)$ and $C(2)$ for any $C(\ell)$ (with $C(1) = 1$). For large negative $\mu(x)$ ($-\mu(x) \gg \sigma$), the distribution of uphill steps is distributed approximately exponentially with average value

$$\mathrm{E}_{dyn}[s(x)|s(x) > 0, \mu(x)] \approx \frac{\sigma^2}{-\mu(x)} \tag{35}$$

where, as before, $\sigma = \sqrt{C((2)/2}$ is the — history independent — standard deviation of the potential single-step fitness gains $\{s_i(x)\}$ given $\mu(x)$. As denoted by the subscript, this

bioRxiv preprint doi: https://doi.org/10.1101/435669; this version posted October 11, 2018. The copyright holder for this preprint (which was not certified by peer review) is the author/funder, who has granted bioRxiv a license to display the preprint in perpetuity. It is made available under aCC-BY-NC-ND 4.0 International license.

average is over the stochasticity of dynamics alone. Using the above expression, we have, for the independent fitnesses model, an approximate differential equation for F:

$$\frac{dF}{dx} = \frac{\sigma^2}{F} \tag{36}$$

which integrates to $F(x) \sim x^{1/2}$ for large x. The fitness thus increases sublinearly, but still as a power law in the number of steps. For $x \gg 1$, the effects of the initial fitness, $F(0)$, are negligible (corrections to $F(x)$ of order $1/\sqrt{x}$). Thus whether or not we condition over the initial fitness, the long-distance behavior is essentially the same.

For landscapes with exponentially decaying correlations, we can proceed similarly, since far-apart regions of the landscape are approximately independent. Normalizing $C(1) = 1$ as before, Equation 25 gives

$$\frac{dF}{dx} = \mathrm{E}[Z|Z > 0] \tag{37}$$

where Z is normally distributed with expectation $-F(x)/b$ and variance $\sigma^2 = \frac{1}{2}(1 + e^{-1/\xi})$ as calculated previously.

As long as $F(x)/b \ll \sigma$ (equivalent to $F \ll \xi\sigma$ for large ξ), the dynamics is like the additive model with $F(x) \approx \sqrt{\frac{2}{\pi}}\,\sigma x$. The correlations are too weak to influence the dynamics and F increases roughly linearly until $F \sim \xi\sigma$, where the correlations start to matter. For $F \gg \xi\sigma$, the large μ approximation holds and we have

$$\frac{dF(x)}{dx} \approx \frac{\sigma^2\xi}{F(x)} \tag{38}$$

which gives us the approximate trajectory

$$F(x) \approx [2\xi x]^{1/2} \tag{39}$$

at long times for large ξ. The long-distance behavior is thus like the independent-fitness model as could have been anticipated since fitnesses that are much more than ξ apart look roughly independent.

3.3.2 Power-law correlated landscapes

Analyzing adaptive paths on power law landscapes is more complicated, because the correlations matter at all times due to the power laws in the response kernels. Figure 3 shows a typical example of the evolutionary dynamics. The uphill steps get smaller and smaller as the mean, $\mu(x)$, of the DFE decreases.

bioRxiv preprint doi: https://doi.org/10.1101/435669; this version posted October 11, 2018. The copyright holder for this preprint (which was not certified by peer review) is the author/funder, who has granted bioRxiv a license to display the preprint in perpetuity. It is made available under aCC-BY-NC-ND 4.0 International license.

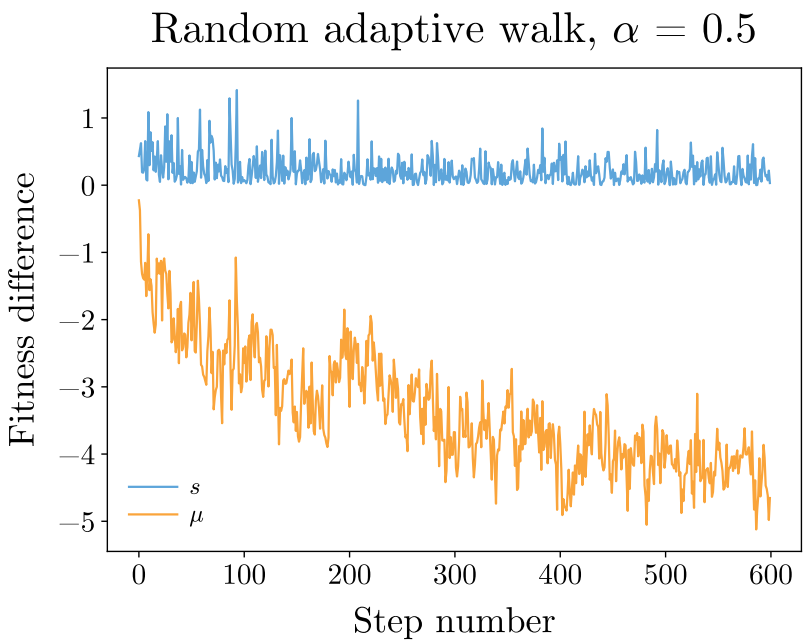

Figure 3: Properties of typical of typical random adaptive walk on a power-law-correlated landscape, with $\alpha = 0.5$. Fitness gains s decrease, on average, as a power of the number of steps, while the mean fitness gain of available steps, μ, is negative with $-\mu$ increasing as a power of the number of steps.

Regardless, we can use the power law forms of the response kernels to self-consistently solve for the dynamics. For power law landscapes, we must deal with fitness differences only since $F(0)$ depends on L ($C(\ell)$ is unbounded). Accordingly, we will solve for the dynamics of the fitness gain $f(x)$ by making the power-law ansatz

$$\mathrm{E}_{walks}[f(x)] = \sum_{y=0}^{x-1} \mathrm{E}_{walks}[s(y)] \sim x^{\beta} \tag{40}$$

and by solving for the scaling forms of $\mathrm{E}_{walks}[\mu(x)]$ and $\mathrm{E}_{walks}[s(x)]$. We conjecture that

$$\mathrm{E}_{walks}[\mu(x)] \sim -x^{\gamma}, \quad \text{while} \quad \mathrm{E}_{walks}[s(x)] \sim x^{\beta-1}. \tag{41}$$

Evaluating the convolutions in Equation 28 (with short-hand notation $*$ for the integrals over the past) using Equation 32, we have $Q * \frac{d\mu}{dy} \sim x^{\gamma-\nu}$ and $J * s \sim -x^{\nu+\beta-1}$, where $\nu = (1-\alpha)/2 < 1$. The neglected terms in Equation 32 are much smaller than than $Q * \frac{d\mu}{dy}$ for large x; therefore the Q term must nearly cancel the $J * s$ term. Thus both those pieces must scale the same way with x, so we conclude that $\beta - 1 + \gamma = 2\nu = 1 - \alpha$.

To get a second equation relating the exponents, we consider the dynamics. Once $-\mu$ becomes large, then s must be selected from the tail of the Gaussian distribution. Typically,

bioRxiv preprint doi: https://doi.org/10.1101/435669; this version posted October 11, 2018. The copyright holder for this preprint (which was not certified by peer review) is the author/funder, who has granted bioRxiv a license to display the preprint in perpetuity. It is made available under aCC-BY-NC-ND 4.0 International license.

we will have

$$s(x) \sim \frac{\sigma^2}{-\mu(x)} \ . \tag{42}$$

Taking random beneficial mutations pushes one into this regime after only a few steps. With $\mathrm{E}_{walks}[\mu(x)] \sim -x^\gamma$ we expect

$$\mathrm{E}_{walks}[s(x)] \sim \sigma^2/\mathrm{E}_{walks}[-\mu(x)] \sim x^{\beta-1} \tag{43}$$

which gives us $\beta - 1 = \gamma$. Here we implicitly assume that the typical $\mu(x)$ is close to $\mathrm{E}_{walks}[\mu(x)]$ (which we will show is supported by the numerics). Combining with the first equation for the exponents, we can solve for β and γ and conclude that

$$\mathrm{E}_{walks}[\mu(x)] \sim -x^\gamma \quad \text{with} \quad \gamma = (1-\alpha)/2 \tag{44}$$

and

$$\mathrm{E}_{walks}[f(x)] \approx \int_0^x \mathrm{E}_{walks}[s(y)]dy \sim x^\beta \quad \text{so that} \quad \beta = (\alpha+1)/2 \ . \tag{45}$$

The exponents interpolate linearly between the extreme cases of the additive ($\alpha = 1$) and independent fitnesses ($\alpha = 0$) models.

These analytic predictions are supported by the numerics. Figure 4 shows the mean and standard deviation of the trajectories of 300 simulations of adaptive walks on different instantiations of the fitness landscape for $\alpha = 0.45$ (left column). As expected, $-\mu$ is constantly increasing, while s decreases accordingly. In the right column, we show log-log plots of $\mu(x)$, $s(x)$, and $f(x)$ for various α. Since $-\mu(x)$ increases more slowly for larger α, $f(x)$ grows more quickly as α increases. Figure 5 shows the scalings of the log derivatives of the mean and variance of each set of trajectories (computed numerically after 100 steps, with Gaussian smoothing of width 5). The estimated power law exponent, γ, of μ deviates from theory as α goes to 1; however, this is also where the estimates are most sensitive to fluctuations and higher order corrections as μ is only slowly increasing in this limit and there are corrections of relative order $1/x^{1-\alpha}$ (as well as $1/x^\alpha$). In all, the scalings from the numerics appear to agree well with the analytic predictions.

The simulations also illustrate the scalings of the variations about the mean of the various quantities. The variance of μ goes to a constant while $|\mu(x)|$ increases, thus justifying the approximation $\mathrm{E}_{walks}[s(x)] \sim -1/\mathrm{E}_{walks}[\mu(x)]$ in the analytical calculation. The variance of s is proportional to $(\mathrm{E}_{walks}[s])^2$, as one should expect for an exponentially distributed random variable; this is roughly correct even though the variations in μ make the distribution of s across realizations is not simply exponential, the standard deviation is still proportional to the expectation. The variance of the fitness scales as $\mathrm{Var}_{walks}[f] \sim \sum_{y=0}^{x} \mathrm{Var}_{walks}[s(y)]$, as would occur if the uphill steps were uncorrelated. The relative variances of both $f(x)$

bioRxiv preprint doi: https://doi.org/10.1101/435669; this version posted October 11, 2018. The copyright holder for this preprint (which was not certified by peer review) is the author/funder, who has granted bioRxiv a license to display the preprint in perpetuity. It is made available under aCC-BY-NC-ND 4.0 International license.

and $\mu(x)$ go to 0 for large x, and therefore the "typical" trajectory is well described by the average trajectory.

The key feature of the dynamics is that the "global" epistatic information — the long-distance correlations in fitness – determine the rate and predictability of evolution, as opposed to local, short-range statistics (which are the ones responsible for things like the number of local maxima). The evolutionary trajectories of different landscapes look similar if their statistics are similar. We will discuss the relationship of fitness trajectories within the same landscape in more detail in Section 4.3.

bioRxiv preprint doi: https://doi.org/10.1101/435669; this version posted October 11, 2018. The copyright holder for this preprint (which was not certified by peer review) is the author/funder, who has granted bioRxiv a license to display the preprint in perpetuity. It is made available under aCC-BY-NC-ND 4.0 International license.

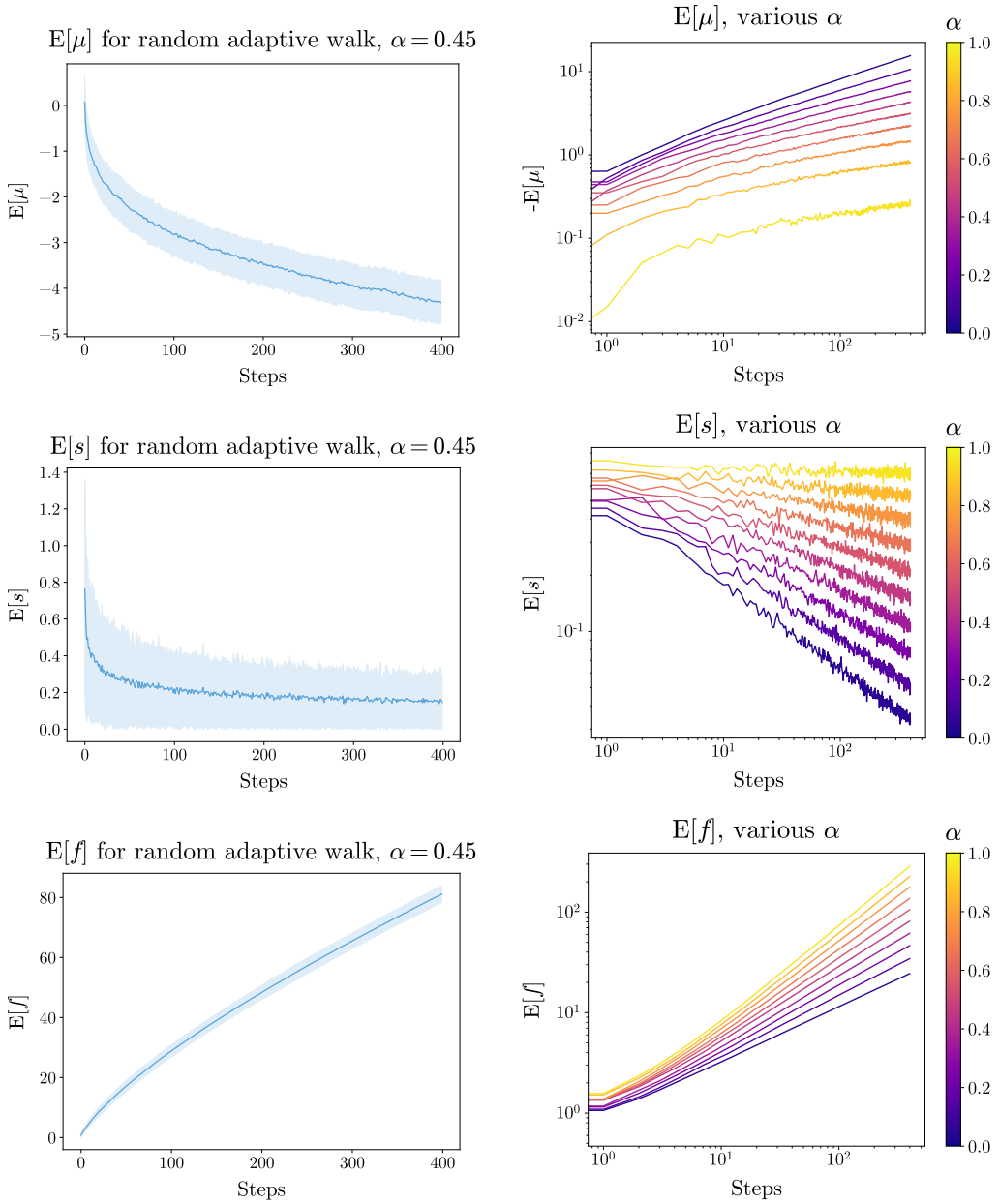

Figure 4: Mean and standard deviation of $\mu(x)$, $s(x)$, and $f(x)$ for adaptive walks with $\alpha = 0.45$ averaged over 300 trajectories (left column). Log-log of averaged trajectories for various α (right column). $\mu(x)$ is negative and decreases more slowly for larger α. This slower decrease leads to larger $s(x)$, and therefore to larger $f(x)$. Relative variability of $\mu(x)$ and $f(x)$ decrease with x, while that of $s(x)$ does not.

bioRxiv preprint doi: https://doi.org/10.1101/435669; this version posted October 11, 2018. The copyright holder for this preprint (which was not certified by peer review) is the author/funder, who has granted bioRxiv a license to display the preprint in perpetuity. It is made available under aCC-BY-NC-ND 4.0 International license.

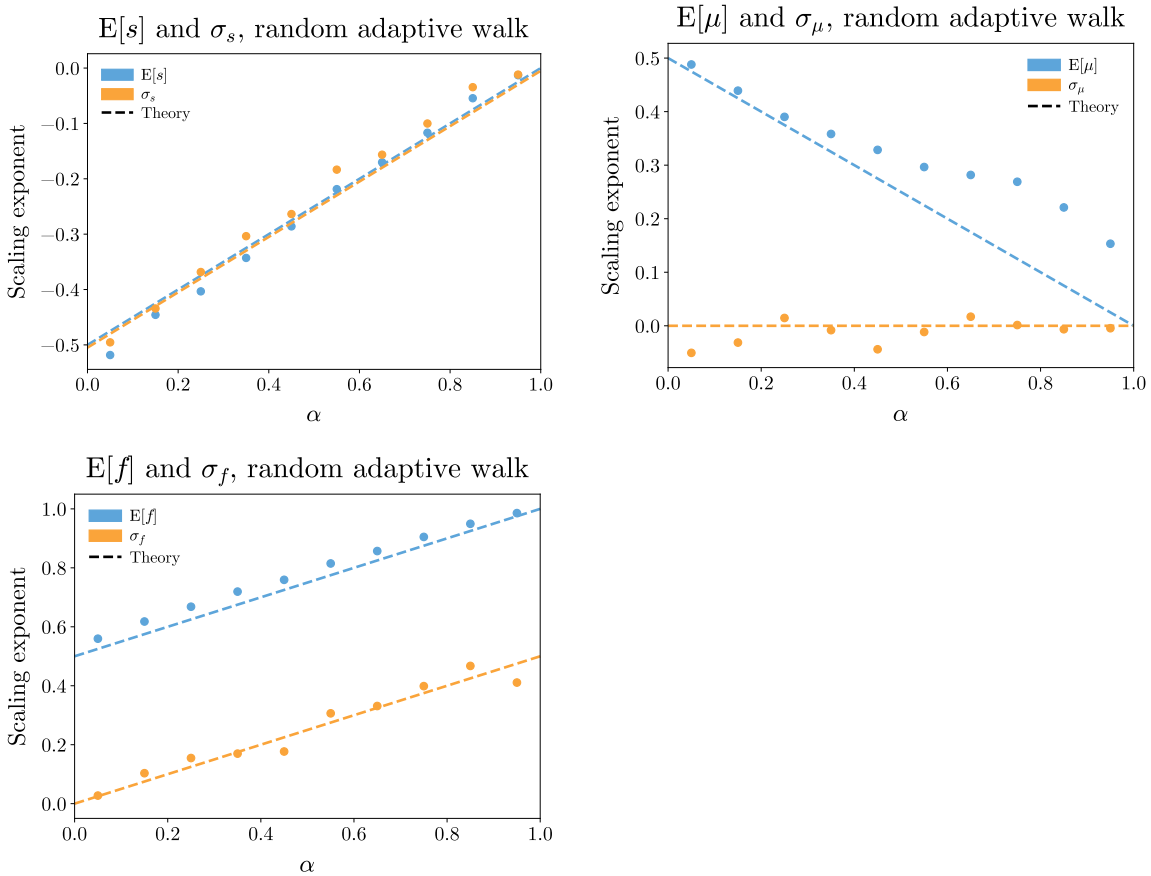

Figure 5: Logarithmic derivatives $d\log(quantity)/d\log(x)$ of trajectories for s, μ, and f. Derivatives computed numerically from trajectories in Figure 4 around $x = 100$. Derivatives of average values in blue, derivatives of standard deviations in orange. All quantities roughly follow power law trajectories. Exponents of s and f increase linearly with α, while μ decreases. Simulations (dots) match theory (dashed lines) well for s for all α and for μ for low α. Deviations are due in part to finite walk-length effects.

bioRxiv preprint doi: https://doi.org/10.1101/435669; this version posted October 11, 2018. The copyright holder for this preprint (which was not certified by peer review) is the author/funder, who has granted bioRxiv a license to display the preprint in perpetuity. It is made available under aCC-BY-NC-ND 4.0 International license.

4 Properties of adaptive walks

The analytical framework introduced in the previous section allows us to understand many features of the evolutionary dynamics quantitatively. The explicit dependence on past evolution means that the long-range statistical structure of the landscape is important for understanding evolutionary trajectories. In particular, evolution drives populations to highly non-generic places on the fitness landscape. We highlight some of the important properties of the dynamics and the evolution-conditioned fitness landscape here.

4.1 Comparisons with typical paths to uphill points

One way to quantify the "non-generic" nature of the evolutionary dynamics is to compare random adaptive trajectories to paths that reach the same fitness gain in the same number of steps. We thus must ask: on a power-law correlated landscape, what does a typical random walk of length x and fitness gain $x^{(\alpha+1)/2}$ look like?

We can use the covariances calculated in Appendix A.1 to find the average trajectory conditioned on the endpoints using formulae for conditional expectations of Gaussian random variables: For power-law correlated landscapes, we find

$$\mathrm{E}[s(y)|f(x)] \approx \frac{\alpha}{2}\left(y^{\alpha-1} + (x-y)^{\alpha-1}\right) x^{(1-\alpha)/2} \tag{46}$$

This is a symmetric trajectory, steepest at the ends. The average step size is at most $x^{(1-\alpha)/2}$, and decreases to $x^{-(1-\alpha)/2}$ in the middle.

Example trajectories for $\alpha = 0.5$ are shown in Figure 6. The conditional random walk trajectories tend to be very lucky at the beginning and end (with high slopes there), and increase only very slowly in the middle. This is in contrast to the adaptive walks, which are typical at the beginning, and then gradually slow down while but continue to gain fitness. In the middle portion of the typical conditioned random walk the average step size is $x^{-(1-\alpha)/2}$, but the variance of the step size is $O(1)$, which means that the walk does not go systematically uphill. There is a probability only slightly less than $\frac{1}{2}$ of steps in the middle being deleterious. Conversely, the late steps are much larger than those of adaptive walks.

Despite these differences, the neighborhood of the endpoint of the typical conditioned walk has $\mu(x) \propto -x^{(1-\alpha)/2}$ just like the adaptive walk. However, even though the scalings of the $\mu(x)$ at the end of the typical walk and the adaptive walk are the same, the coefficients are not; the typical walk has a larger negative $\mu(x)$ by a multiplicative factor. Since the fraction of mutations that are adaptive falls off as a Gaussian in $\mu(x)$, this difference can be very

bioRxiv preprint doi: https://doi.org/10.1101/435669; this version posted October 11, 2018. The copyright holder for this preprint (which was not certified by peer review) is the author/funder, who has granted bioRxiv a license to display the preprint in perpetuity. It is made available under aCC-BY-NC-ND 4.0 International license.

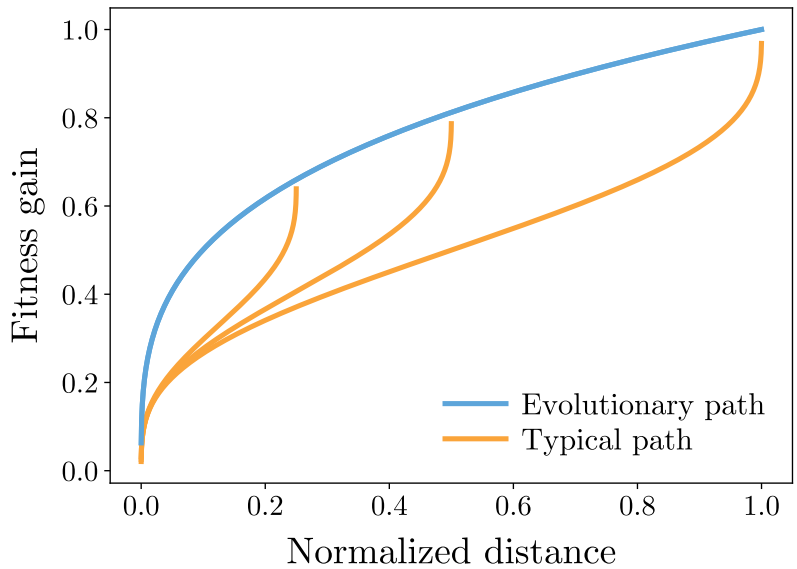

Figure 6: Average evolutionary trajectory compared to typical trajectories of random walks on the landscape constrained to have the same endpoints ($\alpha = 0.5$). Evolution finds a steady path uphill, while typical trajectories with the same fitness gain are lucky at the start and end of the path.

important for future dynamics — adaptive walks are more likely to continue beyond further beyond x before getting stuck.

4.2 Finite L and reaching a local maximum

The results discussed thus far are for the limit of infinite L: we have assumed that there are enough beneficial mutations at any step that the distribution of fitness effects is essentially deterministic given $\mu(x)$, and many uphill steps are always available, even when these constitute a very small fraction of the total of L potential mutations. A crucial consequence of finite L is the tendency to eventually run out of beneficial mutations: this will occur when the fraction of mutations that are beneficial decreases to $O(1/L)$. We can predict the magnitude of the total fitness gained, f_{max}, before a local maximum is reached. This can be calculated directly for the independent fitnesses and independent steps (additive model) cases. For power-law correlated landscapes, we can use our large-distance-scale approximations to find how f_{max} scales with genome size, L.

For the additive model, each site contributes independently to the fitness. Thus the global maximum can be reached and $f_{max} \propto L$. For the independent fitnesses model, at every step,

bioRxiv preprint doi: https://doi.org/10.1101/435669; this version posted October 11, 2018. The copyright holder for this preprint (which was not certified by peer review) is the author/funder, who has granted bioRxiv a license to display the preprint in perpetuity. It is made available under aCC-BY-NC-ND 4.0 International license.

we are presented with L independent choices of new fitnesses, F. A large fitness is unlikely to be found when the probability of any individual neighboring fitness being greater than the current fitness is $< O(1/L)$. This implies that the absolute fitness F_{max} will scale as $F_{max} \sim \sqrt{\log(L)}$, and since a typical starting point has $F(0) \sim O(1)$, $f_{max} \sim \sqrt{\log(L)}$ as well. Note that this f_{max} is a consequence of the Gaussian tail of the fitness distribution: with longer-tailed distributions, as we discuss in Section 6, the fitness can increase further.

The maximum fitness reached can similarly be estimated more generally: simply follow the deterministic dynamics until a value is reached such that there is only $O(1)$ available uphill steps: this occurs when $P(s > 0) \sim O(L^{-1})$. With our Gaussian-random landscapes, this condition is $\exp(-\mu^2/2\sigma^2) = O(L^{-1})$, i.e. when $-\mu \approx \sigma\sqrt{2\log(L)}$. Until then, with high probability there exists a series of uphill steps.

For exponentially correlated landscapes, we showed that $\mathrm{E}[\mu(x)] \propto -\sigma(1 - e^{-1/\xi})^{1/2}x^{1/2}$. Thus the adaptive path can go $(1-e^{-1/\xi})^{-1}\log(L)$ steps, with cumulative fitness gain $f_{max} \propto \sigma(1-e^{-1/\xi})^{-1/2}[\log(L)]^{1/2}$. For $\xi \gg 1$, this is approximately $\sigma\xi^{1/2}[\log(L)]^{1/2}$, the same scaling with L as the independent case. (Of course, if $\xi = O(L)$, then $f_{max} \propto L$.)

For power-law correlated landscapes, we found that $\mu(x) \propto x^{(1-\alpha)/2}$ for a walk of length x, and accordingly $f(x) \propto x^{(1+\alpha)/2}$. Therefore, $f \propto (-\mu)^{(1+\alpha)/(1-\alpha)}$, and we have

$$f_{max} \propto (\log L)^{(1+\alpha)/2(1-\alpha)} \tag{47}$$

This is still logarithmic in L, but can be many times further than the independent case (which corresponds to $\alpha = 0$).

How good are the maxima which adaptive walks reach? Specifically, one can ask: how large is f_{max} compared to the maximum fitness of any genome within the same distance from the starting point as the length of the walk, x? Using Equation 11, we can compute $f_{\mathrm{max(ball)}}$ for a ball of radius x. For power-law landscapes, $f_{\mathrm{max(ball)}} \sim x^{(1+\alpha)/2}\sqrt{\log(L)}$. As the adaptive walk reaches $f_{max} \sim x^{(1+\alpha)/2}$, it only misses out on the factor of $\sqrt{\log(L)}$. Therefore f_{max} and the maximum achievable by any walk of the same length are both powers of $\log(L)$, but the latter has an extra factor of $\sqrt{\log(L)}$.

Another method of quantification is computing $f_{\mathrm{max,up}}$, the maximal fitness gain attainable via any adaptive walk. This can be computed explicitly for the independent fitnesses case (Appendix C.2) to obtain $f_{\mathrm{max,up}} \sim L^{1/4}$. This is a factor of $L^{1/4}$ smaller than the maximum fitness $F^* \sim L^{1/2}$ of any genotype on the hypercube. Therefore the largest possible fitness gains are inaccessible via uphill-only evolution. For non-independent fitnesses, results are likely similar; as we will show in Section 5, even alternate weighting schemes won't let us approach F^* in any power law model (even in a scaling sense).

All the above results, underscore that understanding typical behaviors of adaptive dynamics

bioRxiv preprint doi: https://doi.org/10.1101/435669; this version posted October 11, 2018. The copyright holder for this preprint (which was not certified by peer review) is the author/funder, who has granted bioRxiv a license to display the preprint in perpetuity. It is made available under aCC-BY-NC-ND 4.0 International license.

is very different from understanding "typical" local geometry of the fitness landscape, and even than some of the large-scale properties of the landscape.

4.3 Variability of evolutionary outcomes

The variances computed in Section 3.3 were computed across the entire ensemble of fitness landscapes, by comparing all uphill walks on all landscapes with particular statistics. For power law walks, we noted that $\mathrm{Var}_{walks}[f(x)] \propto \sum_{y<x} \mathrm{Var}_{walks}[s(y)]$ - suggesting that the correlation between individual steps is weak enough to not contribute (at least in a scaling sense) to the overall variability of evolutionary trajectories. However, for natural populations we are usually interested in the variability between two evolutionary trajectories starting from a single genotype on the *same* landscape. This is important to understand populations separated by spatial structure, the variability of evolutionary outcomes, and in experimental settings to understand the statistics of parallel evolutions from a single common ancestor.

The analysis of adaptive walks suggest that the conditioning on past evolution is important to understand this variability; therefore we should consider two adaptive walks starting from a genotype which is itself the result of evolution. More concretely, we consider the following scenario: a population evolves via an adaptive walk for some genetic distance x_b. Then the population is separated into two non-interacting subpopulations, each of which explores a separate direction in the same landscape. We will refer to this trajectory as a *branching path*. The walk starts at a *root* $x = 0$, continues along a shared *trunk*, and then splits into two *branches* at the *branch point* x_b, each branch continuing until the total number of steps in each reaches a total of x. We will be interested in tracking the fitness $f_i(x)$ relative to the root for the two paths $i = 1, 2$, and the difference $\Delta f(x, x_b) \equiv f_1(x) - f_2(x)$ between the fitness of the endpoints of the two paths which branched at x_b. Figure 7 shows the trajectory of f for such a walk on a power-law correlated landscape.

On power-law correlated landscapes, simulations show that long after the branching, the variance between the two branches on the same landscape behaves the same as the variance of a single path across different instantiations of the random landscape (trivially true for the independent fitness model). Specifically, Figure 8 shows the ratio of $\mathrm{Var}[\Delta f(x, x_b)]$ to twice the between-landscapes variance of the post-branch parts of the walk: $2\mathrm{Var}[f(x) - f(x_b)]$ (with the factor of two accounting for the variance of the difference between two — putatively — independent fitness increases.) As expected, $\mathrm{Var}[\Delta f(x, x_b)]$ is smaller than $2\mathrm{Var}[f(x) - f(x_b)]$ due to correlations induced by the shared trunk. However, the ratio approaches unity for $x \gg x_b$, suggesting that, indeed, variance between landscapes behaves the same as variance between branches in the same landscape at large genetic distances. We expect that the ratio approaches unity as a power of $1/(x - x_b)$.

bioRxiv preprint doi: https://doi.org/10.1101/435669; this version posted October 11, 2018. The copyright holder for this preprint (which was not certified by peer review) is the author/funder, who has granted bioRxiv a license to display the preprint in perpetuity. It is made available under aCC-BY-NC-ND 4.0 International license.

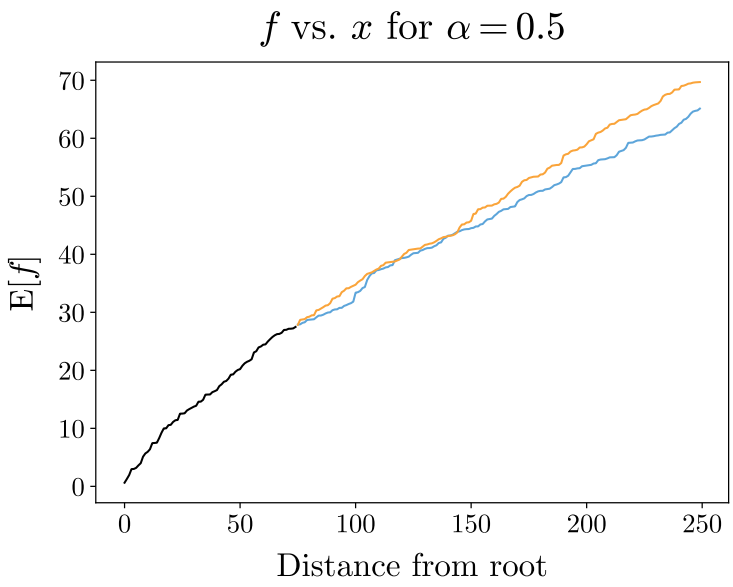

Figure 7: Typical example of cumulative fitness gain f for the two branches of a branched trajectory in a power-law correlated landscape. Paths branch at end of black curve (a distance of $x_0 = 75$ steps from root of walk). Correlations between branches quickly decay, but global structure of epistasis keeps relative variability of f small.

The numerical results suggest that for longer evolutions, there is not much difference between taking multiple paths on the same fitness landscape, or taking paths on different fitness landscapes. For a branching path, the shared part provides some extra correlation, but this only persists for short distances from the branch. The long-term variability between branches only depends on the long-range statistics of the fitness landscape.

5 Greedy and abstemious walks

Thus far, we have considered walks that take uphill steps with probability independent of the fitness increment, s. We now consider different ways of choosing which uphill step to take and how this affects the statistical properties of the walks. We will also be interested in rare (but plausible) adaptive walks whose fitness trajectories are highly anomalous.

bioRxiv preprint doi: https://doi.org/10.1101/435669; this version posted October 11, 2018. The copyright holder for this preprint (which was not certified by peer review) is the author/funder, who has granted bioRxiv a license to display the preprint in perpetuity. It is made available under aCC-BY-NC-ND 4.0 International license.

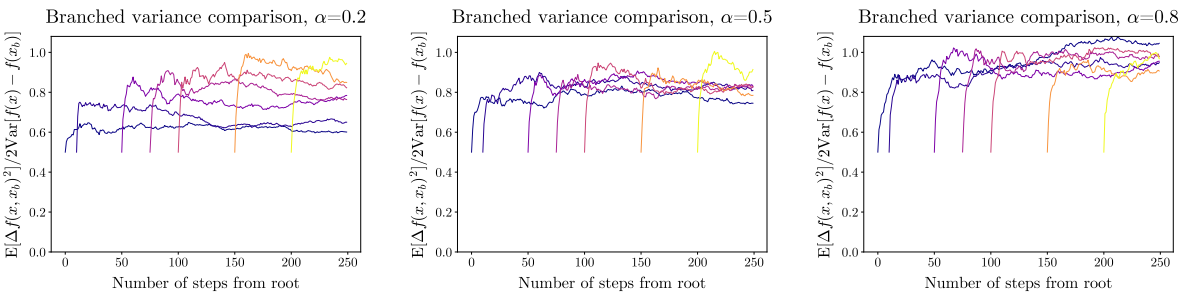

Figure 8: For branched random adaptive walks,ratio of the between-branch variance on a single landscape, to the single branch variance across landscapes: $\mathrm{Var}[\Delta f(x, x_b)]/2\mathrm{Var}[f(x) - f(x_b)]$. The different colors correspond to different distances, x_b, of the branch point from the starting point. Results for power-law correlated landscapes with several values of α are shown. The variance ratios saturate to unity, suggesting that variability between different paths on the same landscape behaves similarly to variability between paths on different landscapes with the same statistics.

5.1 Natural weighting

With birth-death fluctuations in the strong-selection weak-mutation regime, the probability of fixation of a beneficial mutation is proportional to the fitness benefit, s. We only need a slight change in the analysis to understand the dynamics under such a weighting (and indeed, for any power s^κ). Because the distribution of non-negative s is exponential in the limit $-\mu \gg \sigma$, we have:

$$\mathrm{E}_{dyn}[s(x)|\mu(x)] \approx q\sigma^2/(-\mu(x)) \tag{48}$$

where the coefficient q is the ratio of the average step taken to the average positive step available. For weighting s^κ, $q = \Gamma(\kappa+2)$. For unweighted steps $q = 1$; for fixation probability s, $q = 2$. This increase does not change the scalings, but we shall see that it changes the fitness at which the evolution stops by a multiplicative factor.

The effects of q for power law correlated landscapes can be analyzed simply. For $-\mu \gg \sigma$, the change in q is similar to rescaling σ by $\sqrt{q}$; therefore $s(x)$ and $\mu(x)$ scale the same way with q. In particular, we have $-\mu(x) \propto \sqrt{q}x^\nu$ and $f(x) \propto \sqrt{q}x^{1-\nu}$ with $\nu = (1-\alpha)/2$. The evolution reaches a local maximum after X steps when $-\mu(X) \sim \sigma^2\sqrt{\log(L)}$, which gives us $X \sim [\log(L)/q]^{1/2\nu}$. At this point, the fitness increase is

$$f(X) \sim \sqrt{q}X^{1-\nu} \sim \frac{[\log(L)]^{(1-\nu)/2\nu}}{q^{-1+1/2\nu}} \tag{49}$$

Since $1/2\nu = 1/(1-\alpha) > 1$ for all positive α, the smaller the q the higher fitness the adaptive walk reaches; being greedy is deleterious in the long run. Going from randomly

bioRxiv preprint doi: https://doi.org/10.1101/435669; this version posted October 11, 2018. The copyright holder for this preprint (which was not certified by peer review) is the author/funder, who has granted bioRxiv a license to display the preprint in perpetuity. It is made available under aCC-BY-NC-ND 4.0 International license.

chosen mutations to fixation probability proportional to s decreases the maximum fitness reached by a factor of $2^{-\alpha/(1-\alpha)}$. The suppression is strongest for α near 1. (Note that for $\alpha = 1$ this result does not apply as the maximum fitness is of order L independent of q which only determine in which order the steps are likely to be taken).

In larger populations, the fixation of mutations tends to be greedier than in the strong-selection, weak-mutation regime. Multiple mutations will arise in each generation and compete with each other, giving fixation probabilities growing more rapidly than linearly in s (indeed, can be highly non-linear). However large populations are polymorphic with the population spread out over many genomes — effectively taking many paths in parallel — and the behavior is much more complex; we discuss it in more detail in Section 8.

5.2 Slow but steady adaptive walks

The above analysis suggests that to reach as high as possible fitness in an adaptive walk, one should carefully — and artificially, although using only local information and memory — chose which uphill steps to take, being as *abstemious* as possible.

The independent fitness model is simplest. If from each point the smallest available step is taken, then the walk can continue for of order L steps of size $\sim 1/L$ before $-\mu(x)$ becomes of order σ and the number of available steps starts being limited. Along such a walk, L^2 neighbors will have been "seen". The maximum fitness seen will be $\sigma\sqrt{4\log(L)}$; if a fitness of this magnitude is selected, this will increase the fitness at the endpoint by $\sqrt{2}$ compared to a random adaptive walk (which effectively selects the maximum of L fitnesses). A good strategy is to take steps until such a fitness is seen (which will happen with high probability), take the anomalously good step, and – most likely – get stuck there.

For power law-walks, the behavior is much more interesting. The analysis in the previous sub-section is correct for any fixed q for large L; what happens when we have $q \sim L^{-\zeta}$ for some positive $\zeta < 1$? In particular, to better characterize the topology of the landscape, we would like to know what slow steady paths are likely to exist. Unfortunately, as the number of steps, x, starts to become of order L, the tree approximation we have been using breaks down. A major complication is then that some fraction of possible steps — of order x out of L — would reverse mutations that have already occurred. This changes the correlations and the response function forms we have derived no longer obtain. But there is a simple way out: if we only consider mutations that have not already occurred, then the symmetry under permutation still implies that the $L - x$ allowable next steps will still have a distribution well characterized by the now-restricted $\mu(x)$ as long as $L - x$ is large. Thus we should be able to take a total number of steps, X, at least some fraction of L.

bioRxiv preprint doi: https://doi.org/10.1101/435669; this version posted October 11, 2018. The copyright holder for this preprint (which was not certified by peer review) is the author/funder, who has granted bioRxiv a license to display the preprint in perpetuity. It is made available under aCC-BY-NC-ND 4.0 International license.

For very small q, $\mu(x)$ will remain small until large x. The distribution of available s is thus not far from symmetric and a positive s can be chosen with typical value of order q (as long as $q \gg 1/L$). The contribution from the $s(y)$ history to the conditional mean, $\mu(x)$, is then simply $-qx^{\nu}$. For Equation 28 to be true the $s(y)$ history must cancel the $\mu(x)$ history, so Equations 30 and 31 require that $-\mu \sim qx^{2\nu}$. The walk can continue in this way until $-\mu(x = X_1) \sim \sigma$ which occurs for $X_1 \sim 1/q^{1/2\nu}$ at which point the fitness gain has already reached

$$f(X_1) \sim qX_1 \sim q^{1-1/2\nu} \gg \sigma. \tag{50}$$

We can now choose q just small enough that $X_1 = \mathcal{O}(L)$: $q \sim 1/L^{2\nu} = L^{-1+\alpha}$ (which is larger than $O(L^{-1})$ as required), so that $f(X_1) \sim L^{1-2\nu} = L^{\alpha}$ — a remarkably good outcome!

The walk can be continued into the regime where $-\mu \gg \sigma$ as well. To do this while keeping the total length X of order L, one needs

$$q \sim \frac{\log(L)}{L^{2\nu}} \tag{51}$$

and this walk reaches a height

$$f(X) \sim \; L^{1-2\nu}\sqrt{\log(L)} = L^{\alpha}\sqrt{\log(L)} \tag{52}$$

Note that the logarithmic factor should really be $\log(qL)$ as qL is the size of the pool of neighbors with s in the bottom q fraction of the positive ones. But as $\log(qL) \approx (1 - 2\nu)\log(L)$ this only decreases the maximum fitness reached by an order one factor, and the walk could keep going a bit longer by loosening the restriction of q. However it will still be highly restricted by conditioning on the past and we expect that not much extra can be gained by gradually relaxing the q restriction: this could be analyzed by our methods but as it would at best change the coefficient of the bound, we do not do so.

As explained in Section 2.3 the absolute maximum fitness on the hypercube is of order $L^{(1+\alpha)/2}$. For $\alpha = 1$, the additive model, the above estimate — up to the log factor which is unreliable in this case — is the same as this; of course, any strategy works perfectly here. Note that for the independent case, $\alpha = 0$, the analysis above breaks down, as $2\nu = 1$, but naive extrapolation does give $\sqrt{\log(L)}$ with no power of L, as for natural walks which have $q = 2$.

For power-law correlated landscapes how well can one do if even longer walks are allowed, so that many mutations are reversed with some — presumably many — reversing multiple times? This is a complex question which we will not endeavor to answer here. But the method of conditioning on the past should enable some exploration even in this regime. We leave as an intriguing open question whether, using only *local* information, the lower bound of the maximum reachable fitness in Equation 52 can be beaten. Note that there are already

bioRxiv preprint doi: https://doi.org/10.1101/435669; this version posted October 11, 2018. The copyright holder for this preprint (which was not certified by peer review) is the author/funder, who has granted bioRxiv a license to display the preprint in perpetuity. It is made available under aCC-BY-NC-ND 4.0 International license.

subtleties in actually *finding* a path by choosing from the lowest q fraction of the available positive steps. This could be done by trying many steps and picking the lowest uphill one: in the regime where $-\mu$ is still of order σ, only roughly $2/q$ steps need to be tried. But once this is done, then in principle the future possibilities are conditioned on the s's tested but not chosen. This means that the rate of loss of mutations that have already been chosen or tested is greater by this factor and the argument using the permutation symmetry of the untried mutational directions breaks down. We suspect that this would not actually affect the scaling of the fitness achievable, but that would require a much trickier estimate of the effects of the conditioning-by-testing. What we have shown, is the *existence* of an uphill path that can reach a fitness gain of order $f^\alpha\sqrt{\log(L)}$, but not quite how to find it with local information.

What if global information is available? From a random initial genome, how high fitness increase will the best possible path reach? In the independent case, a direct computation (Appendix C.2) suggests that this goes as $L^{1/4}$. More generally, answering this question is likely to be very difficult analytically because of the strong correlations among different directions, and is numerically intractable without generating the whole landscape and exploring — exponentially hard in L.

6 Beyond Gaussian landscapes

A key question about all our results is the generalizability of the quantitative and qualitative features to other models of epistasis. In particular, how sensitive are the adaptive walks to the assumptions of Gaussianity of the random landscape? Addressing this generally is beyond the scope of this paper, but we can begin to explore by considering *mixed landscapes* whose fitness function is a linear combination of an epistatic Gaussian function and a non-Gaussian additive part. More precisely, the fitness F_{tot} is given by

$$F_{tot}(g) = F_C(g) + F_A(g) \tag{53}$$

where F_C is a distance dependent landscape, and F_A is an additive landscape. Both parts of the landscape depend on the same parts of the genome, but they are statistically independent. Note that this is different than having a fraction of the sites on the genome not participating in the epistasis with mutations at those sites simply adding to the fitness: in that case adaptive walks can always continue until all the non-epistatic mutations are exhausted. In contrast, the models we consider have many local maxima and adaptive walks can not necessarily take $O(L)$ steps. The RMF model is the simplest example, with F_C the independent fitnesses model.

bioRxiv preprint doi: https://doi.org/10.1101/435669; this version posted October 11, 2018. The copyright holder for this preprint (which was not certified by peer review) is the author/funder, who has granted bioRxiv a license to display the preprint in perpetuity. It is made available under aCC-BY-NC-ND 4.0 International license.

One way to understand models of this mixed-type is to think of the additive piece as being a modification of the dynamical rules. Recall the general transition rule for steps, to be taken with probability $P(g \to g') = \phi(s_{g\to g'})/Z$. With a mixed landscape, we can decompose the fitness benefit, s, of each potential mutation into an additive part, s_A, and the part from the correlated landscape, which we will call s_C. Then, the probability of taking a step becomes

$$P(g \to g') = \phi(s_C(g \to g') + s_A(g \to g'))/Z \tag{54}$$

After convoluting with the distribution of s_A, we can consider this to be a modified transition rule for steps, s_C, to be taken in the correlated part of the landscape. With $\phi(s)$ still a step function, the additive part of the landscape can compensate for the non-additive part; the path can take negative steps in the correlated landscape so long as a sufficiently positive step in the additive part is available to make the total fitness step positive.

The effects of the loosening of the requirements for steps in the correlated part of the landscape, will keep the DFE mean, μ_C, of the correlated part of the steps from getting too negative and allow for long evolutionary trajectories. In the limit of infinite L, $\mu_C(x)$ will saturate for large x and from then on the statistics of the available steps will no longer change. In Appendix C.3, we use the modified transition rule together with the response kernels to directly study combinations of an additive model with a power-law-correlated model, first analyzing the saturation of μ_C.

A key question, is the behavior large finite L: when can the additive part stop walks getting stuck at local maxima? We first consider the simplest case: the RMF model ($\alpha = 0$) [36]. In this case, it is simple to show that a Gaussian additive part with relative variance σ_A^2/σ_C^2 larger than $O([\log(L)]^{-1})$, will ensure that with high probability there are always uphill steps available. In Appendix C.3 we show that this result also holds for power-law correlated landscapes. This quantifies the crossover from walks that get stuck like those we have analyzed, to walks of length $O(L)$. In the limit of very large L, this is equivalent to the previously observed "phase transition"" [36, 41] — really a cross-over that only exists with mixed scaling of the statistics with L. For any fixed non-zero σ_A^2/σ_C^2, in the limit of large L adaptive walks can take $O(L)$ steps.

It is instructive to compare how much of an additive part is needed to avoid random adaptive paths getting stuck, with the probability that there *exists* an uphill path of length $O(L)$. An upper bound for the relative variance needed is only $\sigma_A^2/\sigma_C^2 \sim O(L^{-2})$. Here, the strategy is to pick a step with positive s_A, and random s_C with $|s_C| < s_A$. We can do this with high probability so long as $\sigma_A \gg L^{-1}$. With this strategy, the induced $\mu(x)_C$ is random and $O(1)$, so the walk can continue until all positive additive steps are taken. Such a walk would only have fitness gain of $O(1)$; it remains an open question if a more refined strategy can lead to large fitness gains.

bioRxiv preprint doi: https://doi.org/10.1101/435669; this version posted October 11, 2018. The copyright holder for this preprint (which was not certified by peer review) is the author/funder, who has granted bioRxiv a license to display the preprint in perpetuity. It is made available under aCC-BY-NC-ND 4.0 International license.

The effects of additive parts of the fitness function are more dramatic if the additive parts of the step-sizes are broadly distributed, especially when there are rare mutations that have very large fitness effects. As an explicit example, we consider a distribution of s_A with a power law tail so that the cumulative distribution function is

$$\int_s^\infty P(s_A = s')ds' \approx \left(\frac{s}{\sigma_A}\right)^{-\psi+1} \tag{55}$$

for large s. For $\psi > 3$, the scale σ_A sets the standard deviation; for smaller ψ, the variance is infinite. When the μ_C of the correlated landscape is large and negative, adaptive mutations must involve rare values in the tail of s_A. If there is a large negative step s_C in the correlated landscape, the probability that the mutation is net adaptive is given by

$$P(s > 0|s_C) \approx \left(\frac{-s_C}{\sigma_A}\right)^{-\psi+1} \tag{56}$$

So long as this probability is greater than $O(L^{-1})$, one of the L possible mutants, is likely to have sufficiently large s_A and the rare, high effect mutation will prevent getting stuck at a local maximum. The correlations in the landscape reflected in the response kernel structure, implies that taking deleterious steps in the correlated part of the landscape makes the DFE mean μ tend to increase becoming less negative. Therefore if the large additive steps are rare but not too rare, there will be a dynamical balance: evolution proceeds by usually taking small uphill steps in the correlated landscape, and occasionally uses the broadly distributed piece to keep going and "release the pressure" on the correlated landscape. This dynamics is studied in detail in Appendix C.4. We find that the effects of the additive piece are strong enough to allow this process to continue if

$$\frac{\sigma_A}{\sigma_C} \sim L^{-1/(\psi-1)} \tag{57}$$

(with σ_C^2 the variance of the correlated parts of the steps). Thus only a very small additive piece is needed to un-block long adaptive walks. (The limit $\psi \to \infty$ is like the Gaussian case which requires $\sigma_A \propto 1/\sqrt{\log(L)}$.) For $\psi = 2$, we only need an additive piece of $O(L^{-1})$ for long walks — just enough to offset the smallest possible s_C when $\mu = O(1)$.

Note that with a long-tailed distribution of available mutations, the behavior can depend strongly on the probability, $\phi(s)$, of a mutation fixing. If $\phi(s) \propto s$, then for $\psi < 2$ the largest effect ("jackpot") mutations would be chosen which modifies the nature of the walks and their dependence on L.

The analysis of the additive-plus-correlated landscapes shows explicitly how long-term evolutionary dynamics can depend sensitively on the tails of the distribution of fitness effects of

bioRxiv preprint doi: https://doi.org/10.1101/435669; this version posted October 11, 2018. The copyright holder for this preprint (which was not certified by peer review) is the author/funder, who has granted bioRxiv a license to display the preprint in perpetuity. It is made available under aCC-BY-NC-ND 4.0 International license.

mutations. Rare large effect mutations can drive evolution in parts of the landscape where the "typical" modest effect mutations — the bulk of the DFE — are deleterious. And such rare large mutations can unlock new sections of the fitness landscape and enable the typical DFE to again drive the evolution. As we will discuss below, these phenomena do not require an additive part of the landscape: they can occur whenever the distribution of effects of available mutations around some genomes has a long tail.

7 Time dependence of walks and landscapes

7.1 Adaptive walks in time

The properties discussed thus far all depended only on the *geometry* of the random adaptive walks. The pseudo-"dynamics" was in terms of number of mutations. However we are also interested in how the evolution progresses in *time*. The simplest way to convert the mutation steps to actual dynamics, which is essentially correct for modest size populations, is to take the time between mutations to be exponentially distributed with characteristic rate $1/\tau_M$ proportional to the total population mutation rate (the product of the mutation rate per site, L, and the population size). If a mutation is deleterious, it is purged with probability one in a time much shorter than τ_M. If the mutation is adaptive, it fixes in time much shorter than τ_M. We will henceforth set $\tau_M = 1$.

With this dynamics, evolution on any Gaussian landscape slows down dramatically with time. Figure 9 shows an example of the fitness gain as a function of time, plotted together with the DFE mean $\mu(x(t))$. When μ is a large and negative (which it will systematically go to as the number of mutations increases), the waiting time for the next mutation is very long. More precisely, we let $\tau_U(x)$ be the time taken for the xth uphill step. The average time $\bar{\tau}_U(x) = \mathrm{E}[\tau_U(x)|\mu(x)]$ goes as $\bar{\tau}_U(x) \propto 1/P(s(x) > 0|\mu(x))$, which with our Gaussian fitnesses gives

$$\bar{\tau}_U(x) \sim e^{\mu(x)^2/2\sigma^2} \tag{58}$$

when $-\mu \gg \sigma$ (Appendix D.1). There is a super-exponential slowdown in the beneficial mutation rate due to the rarity of uphill directions; $\bar{\tau}_U(x)$ will reach $O(L)$ as the number of beneficial mutations becomes $O(1)$ and at that point the walk is likely to stop at a local fitness maximum.

While there are still many available beneficial mutations, the logarithm $\log(\tau_U(x))$ is roughly normal (deviations discussed in Appendix D.1), with mean and variance that increase as $x^{1-\alpha}$ (Figure 9, right panel). The broad distribution of the waiting time between mutations means

bioRxiv preprint doi: https://doi.org/10.1101/435669; this version posted October 11, 2018. The copyright holder for this preprint (which was not certified by peer review) is the author/funder, who has granted bioRxiv a license to display the preprint in perpetuity. It is made available under aCC-BY-NC-ND 4.0 International license.

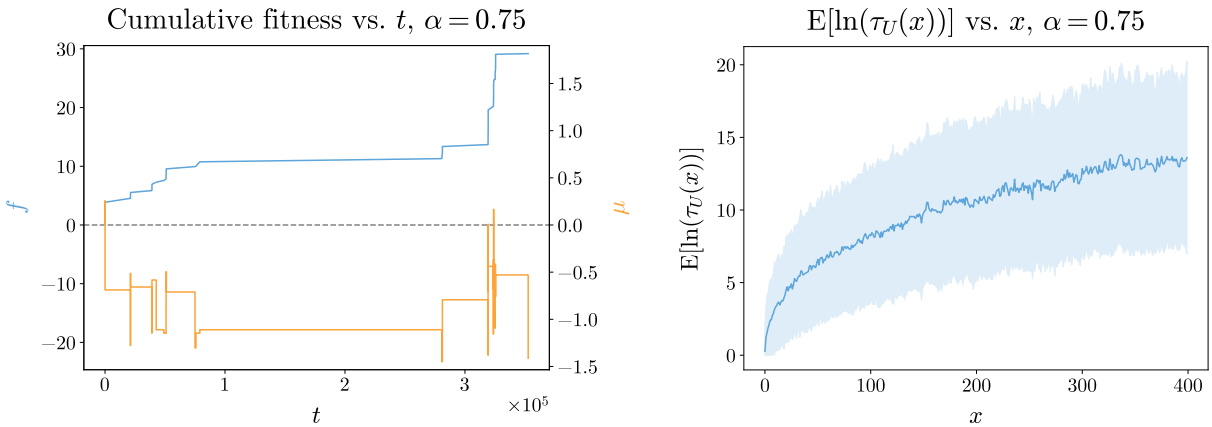

Figure 9: Time dependence of adaptive walks. Left panel shows an example of the fitness gain versus time, $F(x(t))$, of a typical adaptive walk (blue) on a power-law correlated landscape with $\alpha = 0.75$, along with the dynamics of the DFE mean, $\mu(x(t))$ (orange). The typical time between steps, $\tau_U(x)$, goes as $\exp[\mu[x(t)]^2/2\sigma^2]$, so that the logarithm of the waiting time for a beneficial mutation to arise and fix has mean and variance that both increase rapidly — although not monotonically — as the evolution progresses (right panel). Time is in units of total population mutation rate.

that there is not a steady slowing down: initially, there will be a small number of quick, large effect mutations, but after a while there will be a mixture of long and short intervals as seen in Figure 9, before the evolution stops. Of course, if fluctuation effects are included, deleterious mutations can fix, or, in larger populations, "tunneling" through deleterious intermediaries can occur: the dynamics then becomes more complicated.

7.2 Time-dependent landscapes

In nature, and even in the lab, environments are never completely static and whether or not mutations are beneficial can be very sensitive to even small changes in the environment [31]. As this can result from changing the subtle balance between the deleterious and beneficial consequences of a mutation, random fitness changes are a natural caricature of these effects. More generally, we would like to understand the effects of conditioning on evolutionary history in environments that have been somewhat different than the current one. Thus we are led to consider evolution in slowly changing fitness landscapes — sometimes dubbed "seascapes".

To make progress, we again focus on Gaussian correlated fitness functions, but now with temporal correlations as well. The response kernel framework can be used to analyze fit-

bioRxiv preprint doi: https://doi.org/10.1101/435669; this version posted October 11, 2018. The copyright holder for this preprint (which was not certified by peer review) is the author/funder, who has granted bioRxiv a license to display the preprint in perpetuity. It is made available under aCC-BY-NC-ND 4.0 International license.

ness landscapes that change simply in time — we comment later on more complex time dependence.

We consider fitness landscapes with simple time-dependent correlations $C(\ell, t)$ given by

$$C(\ell, t) = e^{-|t|/\tau_E} C(\ell) \tag{59}$$

for the variance in fitness difference between two genomes x mutations apart, measured at times t apart. At any given instant in time the correlation structure is the same as before; however, fitnesses at different times become decorrelated on a timescale of τ_E. The exponential time decay corresponds to a memoryless process, which simplifies both analytical and computational understanding (see Appendix D.2 for details).

Time dependence qualitatively changes the nature of random adaptive walks — especially their dynamics. The system approaches a statistical steady state for which the distribution of the time to take an uphill step $\tau_U(x)$ loses explicit dependence on the mutational distance from where it started. The average time between steps, $\bar{\tau}_U \equiv \mathrm{E}[\tau_U]$, plays an important role in the overall dynamics — but there are a whole spectrum of time scales. The behavior in the random seascape is controlled by the balance between finding uphill steps, in $\tau_U(x)$, and significant decorrelation of the landscape tending to decrease $-\mu(x)$ back towards zero on time scale τ_E. Calculations in Appendix D.3 show that for τ_E large, our focus, we expect the steady-state value of the DFE mean, μ_c, to scale like

$$\mu_c \sim \sigma \left(\tau_E/\bar{\tau}_U\right)^{(1-\alpha)/2} \tag{60}$$

This is because $\xi_D \equiv \tau_E/\bar{\tau}_U$ serves as an effective length scale: it is the number of steps taken in a time τ_E, and gives the number of mutations in the past that still have significant effect on the current DFE, via contribution to the current $\mu(x)$.

From Equation 58, we know that μ_c only depends logarithmically on τ_U. Equation 60 then implies that in the dynamical steady state, to logarithmic accuracy, $\log(\tau_U(x)) \approx \log(\bar{\tau}_U) \approx \log(\tau_E)$ so that, for self-consistency we must have

$$\mu_c \approx -\sigma[2\log(\tau_E)]^{1/2} \tag{61}$$

independent of α due to the sharp Gaussian tails of the distributions.

Numerical simulations confirm this predicted scaling: Figure 10 shows μ_c versus $\log(\tau_E)^{1/2}$. Each simulation was run for a fixed number of uphill steps $X = 200$. For low α, the relationship is linear over a large range. For larger α, the behavior is linear for modestly large τ_E, but for longer τ_E, namely those where $|\mu_c| \ll X^{-(1-\alpha)/2}$, μ did not saturate in the number of steps allotted for the simulations. The data in Figure 10 is thus plotted only for τ_E less than this characteristic crossover value.

bioRxiv preprint doi: https://doi.org/10.1101/435669; this version posted October 11, 2018. The copyright holder for this preprint (which was not certified by peer review) is the author/funder, who has granted bioRxiv a license to display the preprint in perpetuity. It is made available under aCC-BY-NC-ND 4.0 International license.

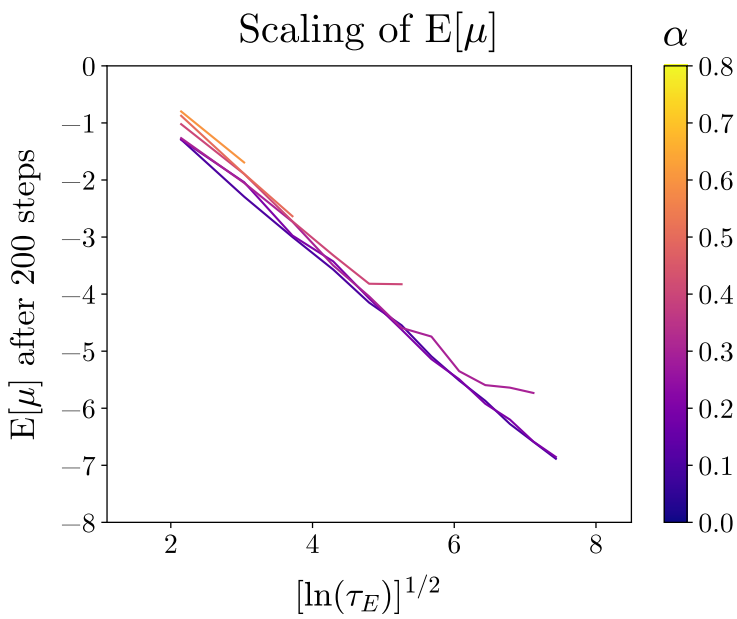

Figure 10: Scaling of the steady state average available fitness step, μ_c, with $\log(\tau_E/\tau_U)^{1/2}$ for walk of length $X = 200$. Relationship is linear until $\ln(\tau_E) \sim X^{(1-\alpha)/2}$, where simulations have not saturated (not shown). For large α and τ_E, μ did not saturate for any simulations with this X due to slower growth of $-\mu(x)$.

The typical fitness gain in one step, $s(t)$, is of order $\sigma^2/|\mu_c|$. This, times the average rate of fixing of beneficial mutations, $\sim 1/\bar{\tau}_U$, is the "fitness flux" — the apparent rate of increase of fitness. If μ_c is small — when the landscape changes quickly relative to mutations — then the fitness flux is high. Conversely, the fitness gain in any one environment — that is, the maximal fitness of any genotype reached during evolution as measured in the fitness landscape at a fixed time — scales as $\frac{1}{\tau_E}(\sigma^2/|\mu_c|)$. The quicker the environment changes, the less adaptation occurs relative to any fixed environment.

But the details of the dynamical behavior are much more interesting and subtle. Due to the broad distribution of $\tau_U(x)$, to understand the qualitative behavior of the dynamics we must analyze the distribution of mutation times and not just the average $\bar{\tau}_U$. This can be done asymptotically for large τ_E. For ease of notation, we define the following quantities: $\mu(x)$ is taken to be the mean available fitness step just after the previous step has been taken; its scaled minus-average, $m \equiv -\mu_c/\sigma \gg 1$, and its scaled variance $W \equiv \mathrm{Var}[\mu(x)]/\sigma^2$, so that the quantity $h(x) \equiv (\mu_c - \mu(x))/\sigma$ has average zero and variance W (h is not exactly Gaussian, but is close enough for these calculations).

In Appendix D.4, we show that for τ_E large, there are two classes of mutations: those that

bioRxiv preprint doi: https://doi.org/10.1101/435669; this version posted October 11, 2018. The copyright holder for this preprint (which was not certified by peer review) is the author/funder, who has granted bioRxiv a license to display the preprint in perpetuity. It is made available under aCC-BY-NC-ND 4.0 International license.

occur in time much smaller than τ_E, so that the landscape does not change significantly between mutations, and those with long enough weighting times (but still smaller than τ_E) such that some decorrelation has occurred. More precisely, when the fraction of beneficial mutations, $R(h) \sim \exp(-(m+h)^2/2)$, is larger than $b \equiv m^2/\tau_E$, beneficial mutations will occur in a time much smaller than τ_E. This is typically the case; however, for anomalously large $-\mu(x)$, the waiting time is dominated by waiting for $-\mu(x)$ to decrease (due to the loss of correlations with time) until the adaptive fraction, R, increases sufficiently that a beneficial mutation occurs.

For mutations that have to wait for environmental change, the waiting time is $\tau_U \approx \frac{\tau_E(h-H)}{m}$ where H is the crossover value of h, for which $R(h=H)=b$. Because $H \gg \sqrt{W}$, this only occurs rarely and the distribution of $h-H$ decays exponentially in this regime. The mean $\bar{\tau}_U$ is found to be dominated by the "slightly-stuck" situations, places at which $h(x)-H \sim W/H$: this thus gives $\bar{\tau}_U$ in terms of the parameters.

We have found that the typical $\tau_U(x)$ is much smaller than the ones which dominate the average, the slow steps that have to wait for environmental change which are only a fraction $m^{-\kappa_H}$ of the total steps, where $\kappa_H = \frac{1+\alpha}{1-\alpha} + \log(W/m)$. The evolutionary dynamics, we thus see, will be characterized by series of fast steps when $\mu(x)$ is comparable to μ_c or somewhat smaller, interspersed with occasional slow steps. The slow steps occur when just after the previous mutational step $\mu(x)$ is substantially less than μ_c (by more than σH), in which case the population must wait for the landscape to change before a beneficial mutation is found and fixes.

Figure 11 shows a typical example of the dynamics of fitness gain with exponential temporal correlations. There is a period of rapid adaptation before the time dependence of the environment comes into play: the fitness flux is large and μ is still decreasing (right panel). As the dynamics slows down the time dependence matters; μ and the fitness flux (whose integral is plotted in the figure) saturate and then fluctuate stochastically with steady-state distributions. One can also see the heterogeneity in the fitness flux; the fitness looks as if it is taking very discrete steps. Looking more closely (right panel), one can see that there are periods during which mutations occur rapidly, and occasional anomalously long gaps between successive mutations.

Figure 11 also shows the fitness gain with respect to a landscape at a fixed time. Measured in the initial landscape, the fitness first increases and then does a random walk with diffusion constant $\sigma^2/\bar{\tau}_U$ as the dynamics become uncorrelated from that initial landscape. The transition from uphill behavior in the initial landscape to the random walk behavior depends on $C(\ell)$. If negative correlations with previously observed genotypes are strong, the dynamics drives the original-landscape fitness back to zero before commencing the random walk. If

bioRxiv preprint doi: https://doi.org/10.1101/435669; this version posted October 11, 2018. The copyright holder for this preprint (which was not certified by peer review) is the author/funder, who has granted bioRxiv a license to display the preprint in perpetuity. It is made available under aCC-BY-NC-ND 4.0 International license.

correlations with other genotypes are weak, then the random walk commences almost immediately and is centered around the highest fitness value reached during the uphill dynamics. This can be seen most easily by examining the independent and the additive models, respectively. In the independent model, once the steps are no longer biased towards being uphill, any single step will tend to take the fitness to a random genotype (with fitness distribution centered around zero). Conversely, for the additive model, future steps are independent of the previous fitness gains; therefore, the average value of the fitness in the present landscape at future times will be the average value of the current fitness — the evolution "remembers" that it gained fitness when the landscape was the one driving the dynamics. Models that lie between the two extremes — such as the exponentially and power-law correlated landscapes — will either have smaller memory of the fitness gain, or memory that decays more slowly with time than for the independent model.

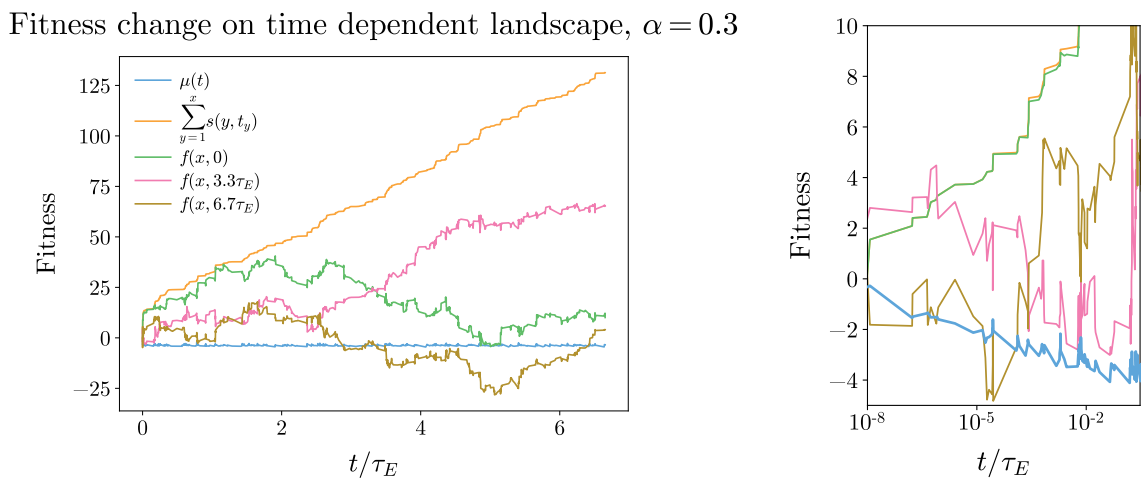

Figure 11: Dynamics of μ and fitness gains, f, for uphill random walks in exponentially time-correlated power-law random landscapes, with time in units of the landscape correlation time $\tau_E = 10^8$. Rapid adaptation occurs at start of evolution until μ saturates (blue in right panel) as the statistical steady-state is reached. The right panel shows a blow-up of this early-time transient behavior. The left panel shows the cumulative fitness flux $\sum_{y=1}^{x} s(y, t_y)$ (sum of fitness gains evaluated at times of mutations) which increases linearly in time (orange line). But for any fixed time, t^*, fitness gains in the landscape at t^*, $f(x(t), t^*)$, are guaranteed to be positive only for times near t^*. Gain in initial landscape, $t^* = 0$, (green line in both panels) is correlated with fitness flux at start but then becomes a random walk with diffusion coefficient $\sigma^2/\bar{\tau}_U$. Fitness gains in later landscapes, at $t^* = 3.3\tau_E$ and at $t^* = 6.7\tau_E$ are also shown (in red and brown, respectively): they are random, then correlated with fitness flux, then random again.

All the above analyses hold for when there are significant anticorrelations in the landscape.

bioRxiv preprint doi: https://doi.org/10.1101/435669; this version posted October 11, 2018. The copyright holder for this preprint (which was not certified by peer review) is the author/funder, who has granted bioRxiv a license to display the preprint in perpetuity. It is made available under aCC-BY-NC-ND 4.0 International license.

This requires there to be significant anticorrelation over the dynamically induced lengthscale ξ_D. For landscapes that are additive up to a length-scale ξ (like the exponentially-correlated landscapes), the behavior of the dynamics is qualitatively different for $\xi_D < \xi$ than for $\xi_D > \xi$. If $\xi_D < \xi$ then the previous analyses hold, and there is intermittent dynamics where the population occasionally has to wait a long time for the landscape to change before taking a step. However, if $\xi > \xi_D$, then the landscape is effectively additive and μ_c is always small (zero for the perfectly additive model). In this case evolution always proceeds steadily as beneficial mutations are always available. Such seascapes forget past fitnesses quickly enough that their correlations remain small and do not drive $\mu(x)$ to large negative values.

An important question is: In what sense are the fitness landscape neighborhoods in steady-state atypical? They do not look like neighborhoods of "typical" points with the same DFE mean $\mu(x) \approx \mu_c$. To see this, consider what happens when the dynamics starts at some random point on the fitness landscape with $\mu(0) < \mu_c$. Figure 12 shows that the dynamics very quickly "resets" to what it would be if originally had $\mu(0) = 0$. The initially large negative μ decays away due to a combination of the exponential time decorrelation at rate τ_E, but also due to the history of the trajectory. As at early times, there have not been a large number of genotypes visited in the near past that had large negative μ, thus the response kernel does not have enough "memory" to drive down future μ. (This is analogous to the future evolution of a "typical" random trajectory conditioned only on the end point fitness, discussed in Section 4.1.) This lack of a past history causes the dynamics to "forget" its initialization.

Further evolution then drives μ down towards μ_c slowly; stabilization around μ_c requires the development of a history of large negative μ in the near past. After some time of order τ_E, μ will reach, and then fluctuate around, μ_c. At this point, the last few steps (more precisely, the last ξ_D steps) will all have had $\mu \approx \mu_c$. The population, now in dynamical steady state, has arrived at a location on the fitness landscape that has a sort of "ridge". In the neighborhood of the current genome, most directions tend to decrease the fitness F sharply while relaxing μ to less negative values. But there are some special directions — back along the evolutionary trajectory — in which both F and μ do not change very much. The history of evolution has led the population to a region that has different geometry than a typical region with the same DFE mean μ.

Though many of our results depend on the Gaussian nature of the landscape, the nature of local landscapes in dynamical steady state is less sensitive to it — and therefore may be a general phenomenon. The "ridge-like" character only requires that the current average potential step is correlated with the past evolutionary trajectory as a whole. This type of dependence on the past means that to reach any sort of dynamical steady state in a stochastically varying high-dimensional seascape, the population must be in a region of the

bioRxiv preprint doi: https://doi.org/10.1101/435669; this version posted October 11, 2018. The copyright holder for this preprint (which was not certified by peer review) is the author/funder, who has granted bioRxiv a license to display the preprint in perpetuity. It is made available under aCC-BY-NC-ND 4.0 International license.

current landscape for which its whole past trajectory is consistent with the steady state, so that the memory of past history affects it in a steady-state manner. This criterion is very different than just matching the statistics of the single-mutation DFE.

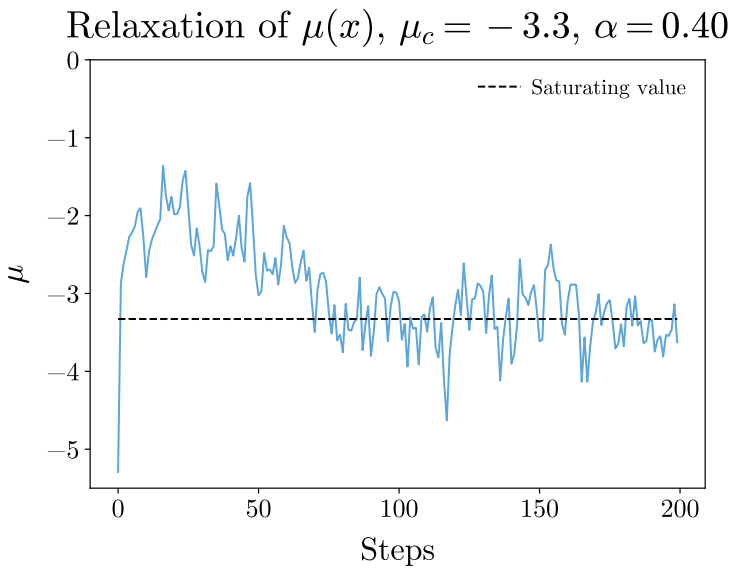

Figure 12: Dynamics of walk started from a randomly chosen point with anomalously negative $\mu(0) < \mu_c$ in exponentially time-correlated power-law landscape. Large negative value of the mean-available fitness step, μ, is "forgotten" as it quickly becomes greater than the steady state average value, μ_c, then approaches this from above (as occurs with random initialization, $\mu(0) = 0$, not shown), and then fluctuates around μ_c. This illustrates that history of a trajectory, rather than just the local neighborhood parametrized by μ, matters, and in steady state, the genomes are not at all like typical points with $\mu \approx \mu_c$.

The analysis of simple exponentially-decaying temporal correlations of the landscape suggests that even very slow time dependence qualitatively changes the nature of evolutionary dynamics and the character of local landscapes conditioned on the past evolutionary history. Exponential time correlations "blur out" the effects of the static-landscape structure. We have seen that at long timescales in randomly changing environments, evolution reaches a dynamical steady state where it does not improve too much in any one landscape; however, the population is always improving in the current environment. This means that the rate of fixation of new mutations, the fitness flux, does not decrease, on average. But in direct head to head competition with an ancestor in the original environment, the fitness difference of the evolving population would increase only slowly and then vary randomly. In spite of this seemingly simple behavior, the complex dependence on the past remains, as evidenced by the fact that neighborhoods at steady state have "flatter" directions than random points

bioRxiv preprint doi: https://doi.org/10.1101/435669; this version posted October 11, 2018. The copyright holder for this preprint (which was not certified by peer review) is the author/funder, who has granted bioRxiv a license to display the preprint in perpetuity. It is made available under aCC-BY-NC-ND 4.0 International license.

in the landscape with the same DFE (i.e. $\mu \approx \mu_c$): the latter tend to have uniformly large negative curvature.

7.3 General time dependent Gaussian landscapes

Many of the concrete features discussed above depend on the simple exponential time-correlations of the landscapes. But within the Gaussian framework, one can consider more general time correlation, parametrized by a *time-dependent amplitude spectrum*. In short, each Fourier mode — roughly corresponding to each length-scale — has its own time dependence. The most general form of correlations consistent with the distance-dependent correlation structure is given by

$$C(\ell, t) = 2 \int_0^1 \left[\rho_A(z, 0) - (1 - 2z)^\ell \rho_A(z, t)\right] dz \tag{62}$$

with $\rho_A(z, t)$ any function of time with non-negative temporal Fourier coefficients, $\hat{\rho}_A(z, \omega)$ which could be used to parametrize it.

Though we can formally write down the general time correlation, our current methods are not sufficient to analyze cases beyond simple exponential time correlations — each $\rho_A(z, t)$ having the same pure exponential time-dependence — as in the previous section. Because, in general, every order of epistasis has a different time dependence, generating the landscape on the fly becomes problematic since the conditional probabilities of the μ no longer have simple response kernel forms; they depend on the entire history of the known landscape. In principle, one could compute "space-time" response kernels which were a function of distance as well as time. However this would quickly become problematic numerically as in steady state the landscape could need to change significantly between each mutational step so that the number of variables would grow at least as x^2 for a walk of length x, leading to matrix inversion on the order of x^6 per step for a total complexity for a walk of length X of X^8 which, while still polynomial, rapidly becomes intractable. This is likely still true if the space-time kernels were computed iteratively, although the complexity might then be held at X^6.

Further development of, heuristic, asymptotic, and approximate numerical methods are needed to study general-time dependent Gaussian random landscapes. Because of the complex environmental and evolutionary histories, and strong effects of conditioning on the history, the behavior is potentially especially interesting. For example, relatively rapid changes of the small-scale properties of the landscapes could open up possibilities to continue evolving in the much more slowly changing large-scale structure of the landscapes.

bioRxiv preprint doi: https://doi.org/10.1101/435669; this version posted October 11, 2018. The copyright holder for this preprint (which was not certified by peer review) is the author/funder, who has granted bioRxiv a license to display the preprint in perpetuity. It is made available under aCC-BY-NC-ND 4.0 International license.

8 Discussion

8.1 Lessons from the theory

Our study of evolution on random landscapes with distance-dependent correlations has given us some key insights into the interplay between evolution and epistasis. The distance-dependent correlation structure enables model definition based on features about which one might have intuition, such as the relationship between genetic and phenotypic relatedness, rather than being constrained to convenient mathematical constructs (such as the independent plus additive structure of the RMF models, or pairwise interaction models). The simple relationship between the locally-defined (distance-dependent correlations) and globally-defined (rescaled amplitude spectrum) descriptions of epistasis facilitate classification and understanding of models; for example, we showed that the *NK* models, in the appropriate scaling limit correspond to correlations that decay exponentially in genetic distance.

Our analysis of random adaptive walks on high-dimensional landscapes gives direct insight into how epistasis can shape evolution and *vice versa*. One key point is that the evolutionary dyanamics depends more on *long range* properties than *short range*, local information. Intuition that the "ruggedness" of landscapes — in particular distributions of local maxima – determine how epistasis affects evolution is, in high dimensions, misleading at best. The high dimensionality of the landscape, and consequent large number of possible mutations, means that rare beneficial mutations can occur even when most mutations are deleterious. Subsequently such mutations can drive large gains in fitness. This is especially true when the distribution of fitness of potential mutations (DFE) is broadly distributed, as we showed in the analysis of mixed models.

A primary result of our analysis is that *the evolutionary history matters*. The current DFE is determined by the past evolutionary trajectory as a whole, not just the recent past. Except in special cases — in particular with exponentially decaying correlations — it is not enough to condition over summary statistics like the current fitness, or the fitness gain over the last few mutational steps. For landscapes in which the fitness differences between genetically distant genomes can be large — in particular the illustrative class we have studied for which fitness differences typically grow as a power of genetic distance — mutations that occurred far in the past collectively contribute in important ways to the present DFE. This reflects the general conclusion that evolution is sensitive to large-scale properties and largely insensitive to local structure.

The dependence on the past leads to highly *non-generic* points on the landscape near which

bioRxiv preprint doi: https://doi.org/10.1101/435669; this version posted October 11, 2018. The copyright holder for this preprint (which was not certified by peer review) is the author/funder, who has granted bioRxiv a license to display the preprint in perpetuity. It is made available under aCC-BY-NC-ND 4.0 International license.

the statistics of interactions between mutations in the neighborhood of the current genome are very different than the neighborhoods of more generic, but superficially similar, genomes, such as those with similarly DFEs. For example, at a random point the double-mutant DFE (fitness difference to all genotypes distance 2 away) is determined solely by the current (single mutant) DFE, but when evolution has occurred, the double-mutant DFE depends on an integral over the past evolution (a generalization of the dependence of $\mu(x)$ on the past that we have analyzed in detail).

Differences in these longer-range statistics determine the properties of future evolution conditioned on past evolution. We have shown that adaptive walks tend to take populations to places on the fitness landscape where they can continue uphill. Adaptive walks, while taking individual steps that are not special — other than being uphill — are overall rare and special paths through the landscape. In particular we have shown that they are very different than typical uphill paths that take the same number of steps and have the same total fitness increase.

Uphill evolution can continue as long as there are some beneficial mutations available. The depletion of beneficial mutations depends on the entire past trajectory. Our results suggest that there might be long-term benefits to "abstemious" walks where smaller fitness gains are accrued at each step; at least in the landscapes studied here, "greedy" walks tend to lead populations to dead ends much faster.

In some families of landscapes, in particular with an additive part of the fitness function, an adaptive walk can "unstick" itself from genomes near which there are very few beneficial mutations and move to where there are more. This is easier if the additive parts of the step distribution are long-tailed: evolution can proceed in a mixed additive-plus-correlated landscape by mostly steps that are uphill in the correlated landscape, only occasionally using a rare, large additive mutation to get unstuck.

Similar behavior occurs when the landscape changes slowly in time. In the statistical steady state that is reached after a long time, a large fraction of mutational steps — almost all in the limit of very slow rate of environmental change — are uphill in the current landscape and occur fast enough that the landscape is effectively static. Only a small fraction of the steps "wait" for more beneficial mutations to become available because of the slightly changed environment — but these few mutations occur slowly enough that they dominate the average time between mutations fixing and thus the average fitness flux.

Collectively, the various features of evolution on epistatic landscapes show that the statistical properties of fitness landscapes are insufficient for understanding evolutionary dynamics: what really matters is the statistical properties of the landscape (and more generally seascape) conditioned on past evolution — in general very different than unconditioned

bioRxiv preprint doi: https://doi.org/10.1101/435669; this version posted October 11, 2018. The copyright holder for this preprint (which was not certified by peer review) is the author/funder, who has granted bioRxiv a license to display the preprint in perpetuity. It is made available under aCC-BY-NC-ND 4.0 International license.

neighborhoods of the landscape. This conclusion is much broader than the particular class of landscapes we have analyzed.

8.2 Possible experimental connections

The genomic fitnes landscapes we have analyzed are, of course, far from those that occur in nature. However some insights can be gleaned for experimental microbial evolution and some other real systems.

Richard Lenski has carried out *long-term evolution experiments* in *E. Coli* in a nominally simple environment with selective pressure designed to be due solely to glucose limitation [28] This experiment has run continuously for over 65,000 generations, with 12 replicate lines. Quantitative analysis of the populations has shown that the fitness relative to the ancestor has been steadily increasing throughout the evolution, but the rate of fitness increase has slowed down, initially strongly and then more gradually [52]. The fitness trajectories have been fit by a rough model of diminishing returns epistasis that predicts logarithmic time dependence of the fitness trajectories [16, 52]. The shapes of fitness trajectories will certainly depend on properties of the landscape, but our conclusion that they will depend on large genetic-distance scale properties, rather than just simple features such as overall diminishing-returns epistasis, suggests that better models are needed.

The time dependence of the fitness, and the similarity among Lenksi's 12 separate lines, can not be compared to our analysis, even roughly. The experimental populations are large enough that many mutations arise, interfere, and add before any can fix. This tends to make the evolution of large populations much steadier than the highly sporadic nature of the evolution in small populations for which, as we have seen, the epistatic interactions can make the number of available beneficial mutations change stochastically as the evolution proceeds. Large populations are likely to average over some of these variations because of the multiple directions that they explore in parallel. In addition, the likely non-Gaussian nature of the evolution-conditioned DFEs likely makes the dynamics in both time and number of mutations quantitatively different.

A surprising feature of Lenski's data, revealed by following trajectories of mutations by deep sequencing of populations every 500 generations, suggests that the rate of fixation of new mutations does not change much after the initial decrease (with the exception of the emergence of hypermutator strains) [18]. This could occur if the environment were gradually changing so that the increases in fitness relative to the ancestor were not indicative of changes relative to the current population — i.e. the fitness flux could decrease much more slowly than the rate of increase of fitness in the original environment. Evidence from the mutation

bioRxiv preprint doi: https://doi.org/10.1101/435669; this version posted October 11, 2018. The copyright holder for this preprint (which was not certified by peer review) is the author/funder, who has granted bioRxiv a license to display the preprint in perpetuity. It is made available under aCC-BY-NC-ND 4.0 International license.

frequency trajectories for the development of ecological interactions (including coexistence of evolved strains for much longer times than could be attributed to them by chance) [18], support this candidate explanation. This would mean that the systems are evolving in a landscape that is more like an externally time-dependent "seascape" than a static landscape. It is worth noting that even if the time-dependence of the environment had been steady and systematic instead of determined by the evolution itself, one would nevertheless have expected a period of rapid adaptation in an effectively static landscape followed by reduced adaptation in any one environment but nevertheless a relatively steady accumulation of further mutations. Lenski's experiments do not seem to have reached a state in which the fitness increases in the original environment — measured by competing with labeled ancestors that dominate the population [52] — have become random. But that is not what would be expected if, in addition to mutations with epistatic interactions that depend on the environment, there were also a small but still available supply of unconditionally beneficial mutations (most simply with additive effects) that have not yet been depleted: these would cause steady increase in fitness even measured in the original environment.

An opposite extreme of genome-wide adaptive evolution is to artificially construct a large number of closely related genomes, and directly measure *empirical fitness landscapes*. Great advances in genomics have made it possible to map out portions of a fitness landscape by creating all possible variants at a small number of sites in the genome of an organism, and measure the relative fitness of each variant (see the recent review article [9]). Examples include a set of mutations in a single protein, β-lactamase, which increase antibiotic resistance [50], biosynthetic loci on yeast [21], and 24 loci on an RNA whose "fitness" is defined by its binding affinity to a GTP agarose resin [24]. Researchers can fit the landscapes to models or, more generally, decompose them, via their Fourier spectrum, as sums of all possible orders of epistatic interactions. A recent meta-analysis showed that the Fourier amplitude spectra of some low-dimensional ($L = 4 - 7$) complete landscapes range from nearly additive to highly epistatic (70% of variance from non-linear terms) [47]. Previous analyses had mainly focused on fitting Rough Mount Fuji or *NK* models to the empirical landscapes [35, 47], with limited success.

In addition to the question of what more general can be learned from empirical landscapes in particular contexts, there is the much broader question of whether evolution on high dimensional landscapes is fundamentally different than on low-dimensional ones. Most empirical landscapes are very low dimensional with the number of sites varied usually ranging from 10-20. Larger studies have been carried out — see [30] for a recent example where variants at 69 sites of an tRNA gene were considered – but they are far less comprehensive, only probing modest pairwise-distances — in the tRNA gene, only 9 or so. With a small number of sites, ℓ, changed, high order epistatic effects — in the more general representation, larger

bioRxiv preprint doi: https://doi.org/10.1101/435669; this version posted October 11, 2018. The copyright holder for this preprint (which was not certified by peer review) is the author/funder, who has granted bioRxiv a license to display the preprint in perpetuity. It is made available under aCC-BY-NC-ND 4.0 International license.

larger length-scale components — are not probed. The combinatorial explosion of genomes and hence interactions with ℓ means that even rare, strong, interactions can contribute to the overall landscape for even modest ℓ. The higher order interactions can dominate the long-distance statistics of fitness landscapes, which our modeling and analysis suggests can be a crucial driver of evolution via multiple successive mutations. Recent computational work on fitness landscapes from data suggests that epistatic interactions determine *available* evolutionary paths even in low-dimensional landscapes [44].

There are several problems with drawing lessons from empirical landscapes involving only very small parts of the genome. Such restricted studies leave out the potential for rare mutations on other parts of the genome that might have weak epistatic interactions with the sub-system studied, but sufficient to "unblock" the sub-system's fitness landscape and enable evolution to avoid getting stuck at local maxima. Further issues are that the studies are conditioned on both past evolution, and the sub-space studied often has special properties. For example, for the β- lactamase protein, the collection of mutations analyzed were known to be jointly beneficial, while for the yeast study analyzed in [47], mutations were individually deleterious. We have shown that the properties of the fitness landscape in the neighborhood of a particular genome, depend heavily on conditioning: this includes on whatever is already known about relationships among mutations being considered.

Overall, we suspect that while studying regions of the genome involved in important processes is valuable for evolution of specific traits in narrow contexts, such studies unfortunately give few insights about how even intermediate-term evolution is affected by, and determines, epistasis.

Can one overcome the biases caused by choice of "wild-type" genome and sets of mutations around it? One system where this should be possible is with yeast for which a wide range of genomic technology has been developed and the ability to bring random combinations of mutations together is enabled by controlled mating. Empirical studies of epistasis have been made with *yeast crosses*, where two genetically distinct strains of yeast are mated repeatedly to generate a large number of offspring which are genetically "between" — in the sense of genetic distance — their two parents [3]. In this particular experiment, the two parental strains differ on 0.5% of their genome (roughly $3 \cdot 10^4$ possible SNPs). The fitness of a large number of the created recombinant variants — upwards of $4 \cdot 10^3$ in [4] — were assayed in a variety of environments. The resulting fitness measurements in each environment were combined with genotyping information to estimate the fraction of fitness variation between types that is explained by additive fitness effects: the unexplained variance is then a statistical estimate of the total epistatic contribution to the fitness landscape in that environment. The findings vary across environments; some have $> 90\%$ of the variance explained by an additive model, while others have closer to 50%.

bioRxiv preprint doi: https://doi.org/10.1101/435669; this version posted October 11, 2018. The copyright holder for this preprint (which was not certified by peer review) is the author/funder, who has granted bioRxiv a license to display the preprint in perpetuity. It is made available under aCC-BY-NC-ND 4.0 International license.

Unfortunately, even from the very large number of yeast-crosses studied, and the very high-dimensional sub-space spanned by the set of mutations by which the parents differ, extracting information about the important statistical properties of the fitness landscape is problematic. One issue is that the distribution of pairwise genetic distances between variants tends to be narrow. In [3] the distribution of distances was peaked at 50% of the genomic distance between the ancestors with a standard deviation of $\sim 5\%$. Thus the data provide information primarily about the overall scale of the fitness landscape at one, particular, long distance. The crucial distance dependence is thus not explored. Another issue is parametrizing the distribution of the fitness landscape by a few simple summary statistics — here decomposing into additive and "unexplained" variance. While the models we have analyzed were, for tractability, assumed Gaussian, that is certainly not expected in nature and more information on *distributions* of fitness differences, rather than just covariances, is needed. (Indeed, we found this already in our analysis of mixed models with Gaussian epistatic parts and non-Gaussian additive parts for which the tail of the distribution was particularly important.)

Regardless of the difficulties of extraction of the most useful information, experiments that combine substantial numbers of mutations to make large numbers of combinations have the potential to tell us much about the statistics of genomic-scale — rather than protein scale — fitness landscapes. An advantage of using crosses of well-adapted strains to produce the subset of mutations to explore, is that effort is not wasted on large numbers of unconditionally deleterious mutations. Another approach would be to take a set of mutations that arose individually in evolution experiments and make many recombinants of these, either engineered or by crosses of evolved mutants that already differ by a substantial — but far less than the strain-cross experiments — number of mutations. Explorations of the distributions of fitness differences as a function of genetic distance could be explored with either approach, as well as, crucially, how these vary with small changes of environment. As datasets become more sophisticated, one can start to develop better caricatures of fitness landscapes and seascapes using the data to guide development of models and insights from theory to guide experimental design. The time is ripe for more detailed back and forth between theory and experiment.

8.3 Theory beyond Gaussian landscapes

Studying adaptive walks on landscapes with distance-dependent correlations has given us considerable insight into the interplay between evolution and epistasis; however we are limited by the simplifying assumptions of the family of models, especially by the Gaussian assumption which is what enabled us to generate landscapes on the fly and analyze the effects of past history via the response-kernel framework. Real fitness landscapes are surely not

bioRxiv preprint doi: https://doi.org/10.1101/435669; this version posted October 11, 2018. The copyright holder for this preprint (which was not certified by peer review) is the author/funder, who has granted bioRxiv a license to display the preprint in perpetuity. It is made available under aCC-BY-NC-ND 4.0 International license.

Gaussian [29]; and in the future one needs to study caricatures that include non-Gaussian statistics, especially the potential for anomalously large effect mutations that can arise even after much evolution has already occurred in the same environment, as seen during experimental microbial evolution [5]. In addition, to gain better understanding of the conditioning on past history, one needs to study different forms of time dependent seascapes than the very simple exponential decay of temporal-correlations that we analyzed.

One way to go beyond the Gaussian simplification while keeping the desirable distance-dependent structure of correlations, would be to define the elements of the amplitude spectrum using other distributions. This is equivalent to transforming to the Fourier basis, then generating independent distributions for each Fourier mode. A natural extension of the Gaussian model would be Levy distributions; these would give a family of self similar random variables which are broadly distributed with power-law tails.

Seascapes can similarly be generated in the Fourier basis with each mode a stochastic process in time instead of a static random variable. Even within the Gaussian-correlated models, one can have a broad range of time scales with longer distance correlations of the landscape changing more slowly. The response-kernel framework we have developed should enable progress to made on such models. More generally, one could consider dynamics that have more complex temporal structure than simple random walks, for example, having periods of relative tranquility punctuated by large, abrupt changes — loosely, a temporal analog of Levy distributions. This sort of model can be implemented within the framework described in Appendix 7.3.

Unfortunately, as soon as one goes beyond Gaussian randomness, one loses the ability to efficiently sample landscapes (or seascapes) on the fly as the evolution proceeds. In general, one needs to define 2^L Fourier coefficients — intractable for numerical explorations. We propose that further progress can be made by defining *sparsified* models of fitness landscapes which keep only a small number of interactions while matching some of the believed-to-be important statistical structure of the landscapes. By analogy with sparse random matrices, where $O(N \log(N))$ non-zero elements in an $N \times N$ matrix are sufficient to give the same eigenvalue spectrum as with all elements random, preliminary calculations suggest that at least the pair correlation structure of a Gaussian landscape, in particular a power-law correlated one, can be preserved with a number of Fourier coefficients polynomial in L. With this, our analytical framework could not be used, but numerical simulation would be computationally inexpensive to perform as with such a sparsified representation one could cheaply evaluate the landscape at any point in (genotype) space and time. An important question is what features of the sparsified landscapes determine the long-term evolution: even with Gaussian random coefficients, the rare regions into which evolution takes the population may be very different in a sparisifed than a fully Gaussian landscape with the same amplitude spectrum.

bioRxiv preprint doi: https://doi.org/10.1101/435669; this version posted October 11, 2018. The copyright holder for this preprint (which was not certified by peer review) is the author/funder, who has granted bioRxiv a license to display the preprint in perpetuity. It is made available under aCC-BY-NC-ND 4.0 International license.

It is worth noting that sparsified representations can also provide a way to capture approximately the features of low-dimensional empirical landscapes, without assuming any particular form.

With non-Gaussian statistics, many of the statistical features of adaptive walks will change, some quite dramatically. We have already seen that a broadly distributed additive piece greatly aids evolution. Non-Gaussian walks will have different relationships between the past evolution and the distribution of available steps, as well as different dependences on how they get stuck for large but finite L.

8.4 Beyond weak-mutation strong-selection dynamics

We have in this paper considered only the simplest evolutionary process: a population that is small enough that mutations arise only infrequently, but large enough that drift is unimportant, especially that deleterious mutations cannot fix. Such a population takes a simple uphill adaptive walk. We end by discussing several important effects that are ignored in this simplified caricature.

Small populations do not need to evolve solely uphill because weakly deleterious mutations can drift to fixation with probability of order $e^{-N\delta}$ for a deleterious mutation of selective disadvantage δ in a population of size N. This means that the population never gets completely stuck. Its dynamics is essentially identical to stochastic motion on the landscape with a "temperature" of $1/N$. There is a rich literature analyzing stochastic thermal dynamics on random landscapes [7, 8, 27] which would be instructive to extend to power-law correlated landscapes such as those we have studied. In spite of never getting fully stuck, the dynamics is likely to continue to slow down (at least at low temperatures), but how it does so is worth exploring. Long-tailed distributions of magnitudes of fitness steps would add another interesting feature.

Large populations are much more interesting. They can also escape local maxima but instead by "tunneling" through intermediate lower fitness points to reach a higher fitness one. This process involves only part of the population and its rate is a complicated function of the population size and fitness differences especially when the move to a higher fitness involves more than one intermediate lower-fitness step [51]. But the overall effect can be crudely approximated by allowing double (or triple, etc.) steps to find points of higher fitness. As the number of double net-uphill steps is much larger than single uphill steps when the mean available fitness, μ, is strongly negative, the effects of tunneling processes on the evolution can be large even before a local fitness maximum is reached.

But this is only one of the complexities of large population caused by the diversity engendered

bioRxiv preprint doi: https://doi.org/10.1101/435669; this version posted October 11, 2018. The copyright holder for this preprint (which was not certified by peer review) is the author/funder, who has granted bioRxiv a license to display the preprint in perpetuity. It is made available under aCC-BY-NC-ND 4.0 International license.

by multiple independent mutations occurring each generation with competition between these — clonal interference — and several mutations occurring on the same lineage before any can fix. Large populations explore many directions in the landscape in parallel. Tunneling via a deleterious intermediary is a mutation-limited example of this. But even with only uphill steps, which will dominate when there are still many available beneficial mutations, the population will explore many directions simultaneously. The rate of evolution is then limited primarily by selection rather than mutation. The competition that will make one of the directions eventually win is played out over a longer time scale — extensively studied for additive models [12, 14, 34] — and involves luck in both when and which several steps of further beneficial mutations occur.

Naively, being able to explore multiple directions in the fitness landscape before committing to any would suggest that, even if only beneficial mutations are allowed, large populations will increase their fitness more before getting stuck than small populations will. But there is another effect that goes in the opposite direction. Large populations are much greedier: the mutations that are likely to fix are much more heavily weighted toward larger effect — exponentially so – than in small populations [14, 17]. We have shown that greedier adaptive walks get stuck at lower fitness local-maxima. Which of the two competing effects dominates in determining when large populations get stuck is certainly a key question. More generally, understanding the evolution on epistatic landscapes of large populations that are continually diversifying and pruning, is an important avenue for further research which should be enabled by the progress we have made thus far.

Beyond their interest for natural evolution, questions about how fast and how far evolution proceeds and how these depend on the nature of the evolutionary process, including strength of competition, sizes of population or multiple partially separated sub-populations, etc are also of practical interest as evolution is being used in both bioengineering [33, 46] as well as machine learning [43] in order to optimize a wide spectrum of systems.

bioRxiv preprint doi: https://doi.org/10.1101/435669; this version posted October 11, 2018. The copyright holder for this preprint (which was not certified by peer review) is the author/funder, who has granted bioRxiv a license to display the preprint in perpetuity. It is made available under aCC-BY-NC-ND 4.0 International license.

Bibliography

[1] Jeffrey E. Barrick, Dong Su Yu, Sung Ho Yoon, Haeyoung Jeong, Tae Kwang Oh, Dominique Schneider, Richard E. Lenski, and Jihyun F. Kim. Genome evolution and adaptation in a long-term experiment with Escherichia coli. *Nature*, 461(7268):1243–1247, October 2009. ISSN 0028-0836. doi: 10.1038/nature08480.

[2] Jesús Blazquez, María-Isabel Morosini, María-Cristina Negri, and Fernando Baquero. Selection of Naturally Occurring Extended-Spectrum TEM β-Lactamase Variants by Fluctuating β-Lactam Pressure. *Antimicrobial Agents and Chemotherapy*, 44(8):2182–2184, January 2000. ISSN 0066-4804, 1098-6596. doi: 10.1128/AAC.44.8.2182-2184.2000.

[3] Joshua S. Bloom, Ian M. Ehrenreich, Wesley T. Loo, Thúy-Lan Võ Lite, and Leonid Kruglyak. Finding the sources of missing heritability in a yeast cross. *Nature*, 494 (7436):234–237, February 2013. ISSN 0028-0836. doi: 10.1038/nature11867.

[4] Joshua S. Bloom, Iulia Kotenko, Meru J. Sadhu, Sebastian Treusch, Frank W. Albert, and Leonid Kruglyak. Genetic interactions contribute less than additive effects to quantitative trait variation in yeast. *Nature communications*, 6, 2015.

[5] Zachary D. Blount, Christina Z. Borland, and Richard E. Lenski. Historical contingency and the evolution of a key innovation in an experimental population of Escherichia coli. *Proceedings of the National Academy of Sciences*, 105(23):7899–7906, June 2008. ISSN 0027-8424, 1091-6490. doi: 10.1073/pnas.0803151105.

[6] Alan J. Bray and David S. Dean. Statistics of Critical Points of Gaussian Fields on Large-Dimensional Spaces. *Physical Review Letters*, 98(15):150201, April 2007. doi: 10.1103/PhysRevLett.98.150201.

[7] L. F. Cugliandolo and J. Kurchan. Analytical solution of the off-equilibrium dynamics of a long-range spin-glass model. *Physical Review Letters*, 71(1):173–176, July 1993. doi: 10.1103/PhysRevLett.71.173.

[8] Leticia F. Cugliandolo and Pierre Le Doussal. Large time nonequilibrium dynamics of a particle in a random potential. *Physical Review E*, 53(2):1525–1552, February 1996. doi: 10.1103/PhysRevE.53.1525.

[9] J. Arjan GM de Visser and Joachim Krug. Empirical fitness landscapes and the predictability of evolution. *Nature Reviews Genetics*, 15(7):480–490, 2014.

bioRxiv preprint doi: https://doi.org/10.1101/435669; this version posted October 11, 2018. The copyright holder for this preprint (which was not certified by peer review) is the author/funder, who has granted bioRxiv a license to display the preprint in perpetuity. It is made available under aCC-BY-NC-ND 4.0 International license.

[10] J. Arjan GM de Visser, Su-Chan Park, and Joachim Krug. Exploring the effect of sex on empirical fitness landscapes. *the american naturalist*, 174(S1):S15–S30, 2009.

[11] Michael M. Desai and Daniel S. Fisher. Beneficial mutation–selection balance and the effect of linkage on positive selection. *Genetics*, 176(3):1759–1798, 2007.

[12] Michael M. Desai, Aleksandra M. Walczak, and Daniel S. Fisher. Genetic diversity and the structure of genealogies in rapidly adapting populations. *Genetics*, 193(2):565–585, 2013.

[13] David Deutscher, Isaac Meilijson, Martin Kupiec, and Eytan Ruppin. Multiple knockout analysis of genetic robustness in the yeast metabolic network. *Nature Genetics*, 38(9): 993–998, September 2006. ISSN 1546-1718. doi: 10.1038/ng1856.

[14] Daniel S. Fisher. Asexual evolution waves: Fluctuations and universality. *Journal of Statistical Mechanics: Theory and Experiment*, 2013(01):P01011, 2013.

[15] S. A. Frank. Generative models versus underlying symmetries to explain biological pattern. *Journal of Evolutionary Biology*, 27(6):1172–1178, June 2014. ISSN 1420-9101. doi: 10.1111/Jeb.12388.

[16] Benjamin H. Good and Michael M. Desai. The Impact of Macroscopic Epistasis on Long-Term Evolutionary Dynamics. *Genetics*, page genetics.114.172460, January 2014. ISSN 0016-6731, 1943-2631. doi: 10.1534/genetics.114.172460.

[17] Benjamin H. Good, Igor M. Rouzine, Daniel J. Balick, Oskar Hallatschek, and Michael M. Desai. Distribution of fixed beneficial mutations and the rate of adaptation in asexual populations. *Proceedings of the National Academy of Sciences*, February 2012. ISSN 0027-8424, 1091-6490. doi: 10.1073/pnas.1119910109.

[18] Benjamin H. Good, Jeffrey E. Barrick, Michael J. McDonald, Michael M. Desai, and Richard E. Lenski. The dynamics of molecular evolution over 60,000 generations. *Nature*, 551(7678):45, October 2017. ISSN 1476-4687. doi: 10.1038/nature24287.

[19] Nelson G. Hairston and Theresa A. Dillon. Fluctuating Selection and Response in a Population of Freshwater Copepods. *Evolution*, 44(7):1796–1805, November 1990. ISSN 1558-5646. doi: 10.1111/j.1558-5646.1990.tb05250.x.

[20] Alex R. Hall, Pauline D. Scanlan, Andrew D. Morgan, and Angus Buckling. Host–parasite coevolutionary arms races give way to fluctuating selection. *Ecology Letters*, 14(7):635–642, July 2011. ISSN 1461-0248. doi: 10.1111/j.1461-0248.2011.01624.x.

bioRxiv preprint doi: https://doi.org/10.1101/435669; this version posted October 11, 2018. The copyright holder for this preprint (which was not certified by peer review) is the author/funder, who has granted bioRxiv a license to display the preprint in perpetuity. It is made available under aCC-BY-NC-ND 4.0 International license.

[21] David W. Hall, Matthew Agan, and Sara C. Pope. Fitness Epistasis among 6 Biosynthetic Loci in the Budding Yeast Saccharomyces cerevisiae. *Journal of Heredity*, 101 (suppl 1):S75–S84, January 2010. ISSN 0022-1503, 1465-7333. doi: 10.1093/jhered/esq007.

[22] Mark Isalan, Caroline Lemerle, Konstantinos Michalodimitrakis, Carsten Horn, Pedro Beltrao, Emanuele Raineri, Mireia Garriga-Canut, and Luis Serrano. Evolvability and hierarchy in rewired bacterial gene networks. *Nature*, 452(7189):840–845, April 2008. ISSN 0028-0836. doi: 10.1038/nature06847.

[23] Elizabeth R. Jerison, Sergey Kryazhimskiy, James Kameron Mitchell, Joshua S. Bloom, Leonid Kruglyak, and Michael M. Desai. Genetic variation in adaptability and pleiotropy in budding yeast. *eLife*, 6:e27167, 2017.

[24] José I. Jiménez, Ramon Xulvi-Brunet, Gregory W. Campbell, Rebecca Turk-MacLeod, and Irene A. Chen. Comprehensive experimental fitness landscape and evolutionary network for small RNA. *Proceedings of the National Academy of Sciences*, 110(37): 14984–14989, October 2013. ISSN 0027-8424, 1091-6490. doi: 10.1073/pnas.1307604110.

[25] Rees Kassen and Thomas Bataillon. Distribution of fitness effects among beneficial mutations before selection in experimental populations of bacteria. *Nature Genetics*, 38 (4):484–488, April 2006. ISSN 1061-4036. doi: 10.1038/ng1751.

[26] Stuart A. Kauffman and Edward D. Weinberger. The NK model of rugged fitness landscapes and its application to maturation of the immune response. *Journal of Theoretical Biology*, 141(2):211–245, November 1989. ISSN 0022-5193. doi: 10.1016/S0022-5193(89)80019-0.

[27] Jorge Kurchan and Laurent Laloux. Phase space geometry and slow dynamics. *Journal of Physics A: Mathematical and General*, 29(9):1929, 1996. ISSN 0305-4470. doi: 10.1088/0305-4470/29/9/009.

[28] Richard E. Lenski, Michael R. Rose, Suzanne C. Simpson, and Scott C. Tadler. Long-term experimental evolution in Escherichia coli. I. Adaptation and divergence during 2,000 generations. *American naturalist*, pages 1315–1341, 1991.

[29] Sasha F. Levy, Jamie R. Blundell, Sandeep Venkataram, Dmitri A. Petrov, Daniel S. Fisher, and Gavin Sherlock. Quantitative evolutionary dynamics using high-resolution lineage tracking. *Nature*, 2015.

[30] Chuan Li, Wenfeng Qian, Calum J. Maclean, and Jianzhi Zhang. The fitness landscape of a tRNA gene. *Science*, 352(6287):837–840, May 2016. ISSN 0036-8075, 1095-9203. doi: 10.1126/science.aae0568.

bioRxiv preprint doi: https://doi.org/10.1101/435669; this version posted October 11, 2018. The copyright holder for this preprint (which was not certified by peer review) is the author/funder, who has granted bioRxiv a license to display the preprint in perpetuity. It is made available under aCC-BY-NC-ND 4.0 International license.

[31] Yuping Li, Sandeep Venkataram, Atish Agarwala, Barbara Dunn, Dmitri A. Petrov, Gavin Sherlock, and Daniel S. Fisher. Hidden Complexity of Yeast Adaptation under Simple Evolutionary Conditions. *Current Biology*, 28(4):515–525.e6, February 2018. ISSN 0960-9822. doi: 10.1016/j.cub.2018.01.009.

[32] Marta Luksza and Michael Lässig. A predictive fitness model for influenza. *Nature*, 507 (7490):57–61, March 2014. ISSN 1476-4687. doi: 10.1038/nature13087.

[33] Joshua K. Michener and Christina D. Smolke. High-throughput enzyme evolution in Saccharomyces cerevisiae using a synthetic RNA switch. *Metabolic Engineering*, 14(4): 306–316, July 2012. ISSN 1096-7176. doi: 10.1016/j.ymben.2012.04.004.

[34] Richard A. Neher and Oskar Hallatschek. Genealogies of rapidly adapting populations. *Proceedings of the National Academy of Sciences*, 110(2):437–442, January 2013. ISSN 0027-8424, 1091-6490. doi: 10.1073/pnas.1213113110.

[35] Johannes Neidhart, Ivan G. Szendro, and Joachim Krug. Exact results for amplitude spectra of fitness landscapes. *Journal of Theoretical Biology*, 332:218–227, September 2013. ISSN 0022-5193. doi: 10.1016/j.jtbi.2013.05.002.

[36] Johannes Neidhart, Ivan G. Szendro, and Joachim Krug. Adaptation in Tunably Rugged Fitness Landscapes: The Rough Mount Fuji Model. *Genetics*, 198(2):699–721, October 2014. ISSN 0016-6731, 1943-2631. doi: 10.1534/genetics.114.167668.

[37] Stefan Nowak and Joachim Krug. Analysis of adaptive walks on NK fitness landscapes with different interaction schemes. *Journal of Statistical Mechanics: Theory and Experiment*, 2015(6):P06014, 2015.

[38] H. Allen Orr. The Distribution of Fitness Effects Among Beneficial Mutations. *Genetics*, 163(4):1519–1526, April 2003. ISSN 0016-6731, 1943-2631.

[39] Su-Chan Park and Joachim Krug. $$\backslash$ delta $-exceedance records and random adaptive walks. *arXiv preprint arXiv:1603.05102*, 2016.

[40] Su-Chan Park, Johannes Neidhart, and Joachim Krug. Greedy adaptive walks on a correlated fitness landscape. *arXiv preprint arXiv:1507.03511*, 2015.

[41] Su-Chan Park, Ivan G. Szendro, Johannes Neidhart, and Joachim Krug. Phase transition in random adaptive walks on correlated fitness landscapes. *Physical Review E*, 91 (4):042707, 2015.

[42] Patrick C. Phillips. Epistasis—the essential role of gene interactions in the structure and evolution of genetic systems. *Nature Reviews Genetics*, 9(11):855–867, 2008.

bioRxiv preprint doi: https://doi.org/10.1101/435669; this version posted October 11, 2018. The copyright holder for this preprint (which was not certified by peer review) is the author/funder, who has granted bioRxiv a license to display the preprint in perpetuity. It is made available under aCC-BY-NC-ND 4.0 International license.

[43] Esteban Real, Sherry Moore, Andrew Selle, Saurabh Saxena, Yutaka Leon Suematsu, Quoc Le, and Alex Kurakin. Large-scale evolution of image classifiers. *arXiv preprint arXiv:1703.01041*, 2017.

[44] Zachary R. Sailer and Michael J. Harms. High-order epistasis shapes evolutionary trajectories. *PLOS Computational Biology*, 13(5):e1005541, May 2017. ISSN 1553-7358. doi: 10.1371/journal.pcbi.1005541.

[45] D. Sherrington. D. Sherrington and S. Kirkpatrick, Phys. Rev. Lett. 35, 1792 (1975). *Phys. Rev. Lett.*, 35:1792, 1975.

[46] Tong Si, Jiazhang Lian, and Huimin Zhao. Strain Development by Whole-Cell Directed Evolution. In *Directed Enzyme Evolution: Advances and Applications*, pages 173–200. Springer, Cham, 2017. ISBN 978-3-319-50411-7 978-3-319-50413-1. doi: 10.1007/978-3-319-50413-1_7.

[47] Ivan G. Szendro, Martijn F. Schenk, Jasper Franke, Joachim Krug, and J. Arjan GM De Visser. Quantitative analyses of empirical fitness landscapes. *Journal of Statistical Mechanics: Theory and Experiment*, 2013(01):P01005, 2013.

[48] Athanasios Typas, Robert J. Nichols, Deborah A. Siegele, Michael Shales, Sean R. Collins, Bentley Lim, Hannes Braberg, Natsuko Yamamoto, Rikiya Takeuchi, Barry L. Wanner, Hirotada Mori, Jonathan S. Weissman, Nevan J. Krogan, and Carol A. Gross. High-throughput, quantitative analyses of genetic interactions in *E. coli*. *Nature Methods*, 5(9):781–787, September 2008. ISSN 1548-7105. doi: 10.1038/nmeth.1240.

[49] Sandeep Venkataram, Barbara Dunn, Yuping Li, Atish Agarwala, Jessica Chang, Emily R. Ebel, Kerry Geiler-Samerotte, Lucas Hérissant, Jamie R. Blundell, Sasha F. Levy, Daniel S. Fisher, Gavin Sherlock, and Dmitri A. Petrov. Development of a Comprehensive Genotype-to-Fitness Map of Adaptation-Driving Mutations in Yeast. *Cell*, 166(6):1585–1596.e22, September 2016. ISSN 0092-8674, 1097-4172. doi: 10.1016/j.cell.2016.08.002.

[50] Daniel M. Weinreich, Nigel F. Delaney, Mark A. Depristo, and Daniel L. Hartl. Darwinian evolution can follow only very few mutational paths to fitter proteins. *Science (New York, N.Y.)*, 312(5770):111–114, April 2006. ISSN 1095-9203. doi: 10.1126/science.1123539.

[51] Daniel B. Weissman, Michael M. Desai, Daniel S. Fisher, and Marcus W. Feldman. The rate at which asexual populations cross fitness valleys. *Theoretical population biology*, 75(4):286–300, 2009.

bioRxiv preprint doi: https://doi.org/10.1101/435669; this version posted October 11, 2018. The copyright holder for this preprint (which was not certified by peer review) is the author/funder, who has granted bioRxiv a license to display the preprint in perpetuity. It is made available under aCC-BY-NC-ND 4.0 International license.

[52] Michael J. Wiser, Noah Ribeck, and Richard E. Lenski. Long-Term Dynamics of Adaptation in Asexual Populations. *Science*, 342(6164):1364–1367, December 2013. ISSN 0036-8075, 1095-9203. doi: 10.1126/science.1243357.

[53] Alex Wong. Epistasis and the Evolution of Antimicrobial Resistance. *Frontiers in Microbiology*, 8, February 2017. ISSN 1664-302X. doi: 10.3389/fmicb.2017.00246.

bioRxiv preprint doi: https://doi.org/10.1101/435669; this version posted October 11, 2018. The copyright holder for this preprint (which was not certified by peer review) is the author/funder, who has granted bioRxiv a license to display the preprint in perpetuity. It is made available under aCC-BY-NC-ND 4.0 International license.

A distance-dependent correlations

A.1 Correlation function derivatives

Suppose that we have a fitness function F on a high dimensional hypercube, with distance dependent correlation C given by

$$C(|g-g'|) = \mathrm{E}[(F(g)-F(g'))^2] \tag{63}$$

where $|g-g'|$ is the number of sites where g and g' differ. We define F to be covariate Gaussian with 0 mean so C completely determines the ensemble.

Consider the pair of fitness differences $F(a)-F(b)$ and $F(c)-F(d)$, oriented so that the shortest path $a \to b$ runs in the same direction as $c \to d$. Then we have

$$\mathrm{E}[(F(a)-F(b))(F(c)-F(d))] = \mathrm{E}[F(a)F(c)] + \mathrm{E}[F(b)F(d)] - \mathrm{E}[F(a)F(d)] - \mathrm{E}[F(b)F(c)] \tag{64}$$

Since all the $\mathrm{E}[F_a^2]$ are the same, and there are 2 positive and 2 negative terms in each, we can rewrite each term as $C(x)$ for the appropriate x. Then we have

$$\mathrm{E}[(F(a)-F(b))(F(c)-F(d))] = \frac{1}{2}\left(C(|a-d|) + C(|b-c|) - C(|a-c|) - C(|b-d|)\right) \tag{65}$$

One case of interest is when c and d are adjacent, and the edge $c \to d$ is contained inside the line between a and b. Let $\ell_f = |a-b|$ and $\ell_0 = |c-a|$. Then we have

$$\mathrm{E}[(F(a)-F(b))(F(c)-F(d))] = \frac{1}{2}\left(C(|\ell_0+1|) + C(|\ell_f-\ell_0|) - C(|\ell_0|) - C(|\ell_f-\ell_0-1|)\right) \tag{66}$$

Which in a continuous approximation gives us

$$\mathrm{E}[(F(a)-F(b))(F(c)-F(d))] = \frac{1}{2}\left(\left.\frac{dC}{dx}\right|_{x=\ell_0} + \left.\frac{dC}{dx}\right|_{x=\ell_f-\ell_0}\right) \tag{67}$$

This tells us that the total fitness gain on a path is correlated with the fitness effect of a single mutation by $\frac{dC}{dx}$ for a random path. For power law walks, we have

$$\frac{1}{2}\left(\left.\frac{dC}{dx}\right|_{x=\ell_0} + \left.\frac{dC}{dx}\right|_{x=\ell_f-\ell_0}\right) \approx \frac{\alpha}{2}\left[(\ell_0)^{\alpha-1} + (\ell_f-\ell_0)^{\alpha-1}\right] \tag{68}$$

That is, for a random path the total fitness gain is most correlated with the fitness gains at the end, and least correlated with the fitness gains in the middle.

bioRxiv preprint doi: https://doi.org/10.1101/435669; this version posted October 11, 2018. The copyright holder for this preprint (which was not certified by peer review) is the author/funder, who has granted bioRxiv a license to display the preprint in perpetuity. It is made available under aCC-BY-NC-ND 4.0 International license.

Now consider the case where a is adjacent to b, and c is adjacent to d. Let us also suppose that the shortest path from a to d runs through c. This gives us $|a-b| = |c-d| = 1$, $|a-c| = |b-d|$ and $|a-d| = |a-c|+1$. Let $\ell = |a-c|$. Then we have

$$\mathrm{E}[(F(a)-F(b))(F(c)-F(d))] = \frac{1}{2}\left[C(\ell+1) - 2C(|\ell|) + C(\ell-1)\right] \tag{69}$$

We can approximate as

$$\mathrm{E}[(F(a)-F(b))(F(c)-F(d))] = \frac{1}{2}\frac{d^2C}{dx^2}\bigg|_{x=\ell} \tag{70}$$

This approximation is good when C changes slowly with genetic distance. For sublinear C, $\frac{dC}{dx} > 0$ but $\frac{d^2C}{dx^2} < 0$ - giving negative correlations between mutational steps on the same path.

A.2 Fourier transform and amplitude spectrum

To diagonalize the covariance given by C, we pass to the Fourier basis on the hypercube. This is due to the fact that the covariance respects the symmetries of the hypercube; the theory of Pontryagin duality guarantees us that the Fourier basis is the eigenbasis of any correlation function that respects the discrete symmetries of the hypercube.

The Fourier coefficients can be written as

$$f_{\mathbf{k}} = \frac{1}{2^L}\sum_g e^{i\pi\mathbf{k}\cdot g}F(g) \tag{71}$$

Here with a slight abuse of notation, $\mathbf{k}$ is a vector with k ones and $L-k$ zeros. The coefficient $f_{\mathbf{k}}$ represents the interaction of those k sites with $\mathbf{k}_i = 1$. We can reconstruct the fitness from the Fourier coefficients by

$$F(g) = \sum_{\mathbf{k}} f_{\mathbf{k}} \prod_{i:\mathbf{k}_i=1} g_i \tag{72}$$

where g_i is the ith site labeled with values ± 1 (instead of $\{0,1\}$), and the sum is over all possible $\mathbf{k} \in \{0,1\}^L$.

Since the sites are symmetric under permutation for any distance-dependent correlation function, the statistical properties of $f_{\mathbf{k}}$ only depend on k (the number of interacting sites. We can therefore define the *amplitude spectrum* A_k by

$$A_k \equiv \langle f_{\mathbf{k}}^2 \rangle \tag{73}$$

bioRxiv preprint doi: https://doi.org/10.1101/435669; this version posted October 11, 2018. The copyright holder for this preprint (which was not certified by peer review) is the author/funder, who has granted bioRxiv a license to display the preprint in perpetuity. It is made available under aCC-BY-NC-ND 4.0 International license.

where the average is taken over the ensemble, for all $\mathbf{k}$ with k ones.

The collection of all possible non-negative combinations of spectra A_k determines all possible distance-dependent correlation functions. In other words, we can generate the set of allowable $C(x)$ by defining different distributions of Fourier coefficients. The amplitude spectrum has been previously used and defined as a metric for epistasis [35]. A_k gives us a measure of the magnitude of epistasis at order k. In the case of our Gaussian models, the amplitude spectrum is exactly analogous to the power spectrum for stationary Gaussian signals.

One undesirable feature of the amplitude spectrum is that it depends on the total genome size L. We would like to be able to write the spectrum in a scale-invariant way so that we can understand what models look like in the large L limit. Accordingly, we define the *rescaled amplitude spectrum* ρ_A by

$$\rho_A(z) = L\binom{L}{Lz}A_{Lz} \tag{74}$$

where Lz is rounded to the nearest integer. This normalization is chosen so that weighted sums over the amplitude spectrum can be converted to an integral. For example, consider a function $f : [0,1] \to \mathbb{R}$. The amplitude weighted average can be computed as

$$\sum_{k=0}^{L}\sum_{I_{\gamma k}} A_k f(k/L) = \sum_{k=0}^{L}\binom{L}{k}A_k f(k/L) \approx \int_0^1 f(z)\rho_A(z)dz \tag{75}$$

For simple models we can compute the A_k easily and therefore the ρ_A as well. For the additive model, only terms at order 1 contribute; we have

$$\rho_A(z) = \delta(z - L^{-1}) \tag{76}$$

For independent fitnesses, each mode has equal weight (since it is a graded sum of independent random variables). The combinatorics of terms at each order sets the distribution; we have

$$\rho_A(z) = \frac{L}{2}2^{-L}\binom{L}{Lz} \approx \delta(z - 1/2) \tag{77}$$

In order to have correlations with super-exponential long range structure, $\rho_A(z)$ needs to have a divergence at 0. As an example, consider power law correlations. In general, going from correlations to amplitude spectra is difficult; it requires inversion of the matrix M whose elements are given by

$$M_{ij} = \int_0^1 (1-2z)^{i+j}dz = \frac{1}{i+j+1}\cdot[(i+j+1) \mod 2] \tag{78}$$

bioRxiv preprint doi: https://doi.org/10.1101/435669; this version posted October 11, 2018. The copyright holder for this preprint (which was not certified by peer review) is the author/funder, who has granted bioRxiv a license to display the preprint in perpetuity. It is made available under aCC-BY-NC-ND 4.0 International license.

However, we can guess at a form of ρ_A which corresponds to power law scaling in C. We want a $\rho_A(z)$ such that

$$\int_0^1 \left((1-(1-2z)^\ell\right) \rho_A(z)dz \propto \ell^\alpha \tag{79}$$

Differentiating with respect to ℓ gives us the condition

$$-\int_0^1 (1-2z)^\ell \log(1-2z)\rho_A(z)dz \propto \ell^{\alpha-1} \tag{80}$$

For large ℓ, we expect the integral to be dominated by small z. The integrand, sans ρ_A, peaks around $z = O(\ell^{-1})$, and has significant value over a range that is $O(\ell^{-1})$ as well. The value it takes on is $O(\ell^{-1})$ as well. This suggests that $O(\ell^{-2})\rho_A(\ell^{-1}) = O(\ell^{\alpha-1})$ or

$$\rho_A(z) \propto z^{-1-\alpha} \tag{81}$$

for small z. This is peaked at $z = 0$, and is consistent with the approximation that the integrand in Equation 80 is peaked around ℓ^{-1}. Note that the exponent of $\rho_A(z)$ is less than -1. Therefore, power law distance-dependent correlations have a power law distributed power spectrum, with most of the weight at low orders.

Note that though $\rho_A(z)$ is weighted towards $z = 0$, for large L we can still have a significant weight at higher order ($k > 1$) Fourier modes. This suggests quantitatively that higher order epistasis matters increasingly for increasing genetic distances, at least in models that have a consistent large L limit (as all distance-dependent correlation models do). We also again come to the lesson that there is some flexibility in the exact form of $\rho_A(z)$ with regards to its effect on $C(x)$; the form of the divergence at 0 sets the long tail behavior.

A.3 Computing correlations from amplitude spectra

The amplitude spectrum has been described previously, but the rescaled limit — crucial for giving landscapes whose structure is well behaved in the large L limit — has, to our knowledge, not been studied previously.

Suppose we wish to calculate the correlation $\mathrm{E}[F(g)F(g')]$ between two genomes g and g' such that $|g - g'| = \ell$, given the amplitude spectra. Then we have

$$\mathrm{E}[F(g)F(g')] = \sum_{\mathbf{k}} S(\mathbf{k}, g, g')A_k \tag{82}$$

where

$$S(\mathbf{k}, g, g') = \begin{cases} 1 & \text{if } g \text{ and } g' \text{ differ at an even number of sites where } \mathbf{k}_i = 1 \\ -1 & \text{otherwise} \end{cases} \tag{83}$$

bioRxiv preprint doi: https://doi.org/10.1101/435669; this version posted October 11, 2018. The copyright holder for this preprint (which was not certified by peer review) is the author/funder, who has granted bioRxiv a license to display the preprint in perpetuity. It is made available under aCC-BY-NC-ND 4.0 International license.

The sum over the $\mathbf{k}$ can be rewritten as

$$\sum_{\mathbf{k}} S(\mathbf{k}, g, g') = \sum_{d=0}^{\min(k,\ell)} (-1)^d \binom{\ell}{d} \binom{L-\ell}{k-d} \tag{84}$$

This sum cannot be evaluated exactly, but can be evaluated approximately in two cases. First, for $L, \ell \gg k$ — low order epistasis but macroscopic distances — we have

$$\sum_{I_{\gamma k}} S(\mathbf{k}, g, g') = \sum_{d=0}^{k} (-1)^d \binom{\ell}{d} \binom{L-\ell}{k-d} \tag{85}$$

Use of Stirling's approximation gives

$$\sum_{I_{\gamma k}} S(\mathbf{k}, g, g') \approx \frac{1}{k!} \sum_{d=0}^{k} (-1)^d \ell^d (L-\ell)^{k-d} \binom{k}{d} \tag{86}$$

which can then be evaluated via generating functions as

$$\sum_{I_{\gamma k}} S(\mathbf{k}, g, g') \approx \binom{L}{k} \left(1 - 2\frac{\ell}{L}\right)^k \tag{87}$$

To evaluate the full sum with this approximation, we use the rescaled amplitude spectrum:

$$\mathrm{E}[F(g)F(g')] \approx \int_0^1 \left(1 - 2\frac{\ell}{L}\right)^{Lz} \rho_A(z) dz \text{ for } L, \ell \gg Lz \tag{88}$$

This approximation is useful if most of the weight of ρ_A is at low orders. If terms of some particular lower order dominate, the correlations drop off polynomially, with fitnesses becoming uncorrelated at $\ell = L/2$ and anti-correlated at $\ell = L$.

The second and more useful case is when $L, k \gg \ell$ — short-distances (compared to L, but arbitrarily high order epistasis. Then we have

$$\sum_{I_{\gamma k}} S(\mathbf{k}, g, g') = \sum_{d=0}^{\ell} (-1)^d \binom{\ell}{d} \binom{L-\ell}{k-d} \tag{89}$$

Stirling's approximation then gives

$$\sum_{I_{\gamma k}} S(\mathbf{k}, g, g') \approx \binom{L}{k} \sum_{d=0}^{\ell} (-1)^d \binom{\ell}{d} \frac{(L-\ell)!}{L!} \frac{k!}{(k-d)!} \frac{(L-k)!}{(L-\ell-(k-d))!} \tag{90}$$

bioRxiv preprint doi: https://doi.org/10.1101/435669; this version posted October 11, 2018. The copyright holder for this preprint (which was not certified by peer review) is the author/funder, who has granted bioRxiv a license to display the preprint in perpetuity. It is made available under aCC-BY-NC-ND 4.0 International license.

which simplifies to

$$\sum_{I_{\gamma k}} S(\mathbf{k}, g, g') \approx \binom{L}{k} \sum_{d=0}^{\ell} (-1)^d \binom{\ell}{d} \left(\frac{k}{L}\right)^d \left(\frac{L-k}{L}\right)^{\ell-d} \tag{91}$$

and a similar generating function computation gives

$$\sum_{I_{\gamma k}} S(\mathbf{k}, g, g') \approx \binom{L}{k} \left(1 - 2\frac{k}{L}\right) \tag{92}$$

In terms of the rescaled amplitude spectrum we have

$$\mathrm{E}[F(g)F(g')] \approx \int_0^1 (1-2z)^{\ell} \rho_A(z) dz \text{ for } Lz \gg \ell \tag{93}$$

Here we arrive at a nice intuition for how terms of different order affect the correlation structure. Epistasis of order Lz contributes a term with exponential decay of correlations with lengthscale $\log(|1-2z|)^{-1}$. Terms of order less than $L/2$ contribute positively to correlations, while higher order terms contribute alternating signs on average.

Arbitrary combinations of different orders of epistasis can be represent in the large L limit, with $\ell \ll L$ – the regime of interest for almost all we study in this paper — by the general scaled linear combinations of Equation 93 .

A.4 Time-dependent covariance

We can use the Fourier decomposition to come up with simple characterizations of time-dependent fitness correlations. If we have a time-translationally invariant covariance of the form

$$M_f(x, t, y, s) = f(|x-y|, |t-s|) \tag{94}$$

then the covariance matrix M_f is diagonalized in the space-time Fourier basis. In other words, with both spatial diagonalization and time diagonalization factors. For each wavevector $\vec{k}$ and frequency ω, we can write

$$M_f(x, t, y, s) = \sum_{\vec{k},\omega} \hat{M}_f(\vec{k}, \omega) e^{i\vec{k}\cdot(\vec{x}-\vec{y})} \cos(\omega|t-s|) \tag{95}$$

where $\hat{M}_f(\vec{k}, \omega)$ are the Fourier coefficients. This is the normal space-time Fourier transform, where the positivity condition on the Fourier coefficients forces the time part to be cosines only.

Another way to think about it is that each spatial mode $\vec{k}$ has its own (time-)translation invariant temporal correlations. The fact that each "mode" can vary independently in time makes analytical and computational work on time-dependent models more complicated.

bioRxiv preprint doi: https://doi.org/10.1101/435669; this version posted October 11, 2018. The copyright holder for this preprint (which was not certified by peer review) is the author/funder, who has granted bioRxiv a license to display the preprint in perpetuity. It is made available under aCC-BY-NC-ND 4.0 International license.

B Response kernel approach

B.1 Dependence of DFE on past evolutionary history

A key property needed to understand evolutionary processes is the distribution of fitness effects (DFE) of all single mutants away from a given genotype. Consider a genome g on a distant-dependent correlated landscape, and let s_i be the fitness gain from a mutation at site i. The s_i are distributed as a covariate Gaussian, with zero mean, variance $C(1)$ and correlation $C(1) - \frac{1}{2}C(2)$.

We can write each difference $s(y)$ as a sum of two Gaussian random variables:

$$s_i = Z_c + Z_i \tag{96}$$

Here Z_c is the "shared" part of the variability - a random variable with variance $C(1) - \frac{1}{2}C(2)$ identical across all the sites. The Z_i give the "private" part of the variability - Gaussian random variables with variance $\frac{1}{2}C(2)$, independent for all sites. This type of decomposition is always possible with identically correlated Gaussian random variables.

In the limit of large L, we can approximate Z_c with the *average available fitness step*, $\mu(g) \equiv \frac{1}{L}\sum_i s_i$. We have:

$$s_i = \mu(g) + Z_i + O(L^{-1/2}) \tag{97}$$

In this limit, the (empirical) DFE is approximately Gaussian with mean $\mu(g)$ and variance $\frac{1}{2}C(2)$. Since $C(2)$ is a constant set by the landscape, once $\mu(g)$ is known, the entire DFE is known as well.

This gives us the following strategy for constructing adaptive walks:

- Draw the value of $\mu(x)$ from its distribution.
- Use the resulting DFE to take an evolutionary step.
- Define $x + 1$ as shorthand for the genome after the step is taken.
- Draw the next $\mu(x + 1)$ conditioned on past evolution and repeat

where x labels the number of steps taken. Note that the DFE conditioned on $\mu(x)$ (and the previous evolution) is still Gaussian, even though the actual step taken $s(x)$ is not. This simplifies the dynamics considerably, as each step in the evolution involves first evaluating a conditional Gaussian random variable, and then drawing from a simple distribution — the positive s part of the Gaussian DFE.

bioRxiv preprint doi: https://doi.org/10.1101/435669; this version posted October 11, 2018. The copyright holder for this preprint (which was not certified by peer review) is the author/funder, who has granted bioRxiv a license to display the preprint in perpetuity. It is made available under aCC-BY-NC-ND 4.0 International license.

This suggests that in order to understand the dynamics along a single adaptive walk, in the limit of large L all we need to understand the DFE at any point is its conditional mean $\mu(x)$ at that point. This approximation starts to break down when we ask about events which have probability $O(L^{-1})$ in the Gaussian distribution; in particular, extremal values of the empirical distribution are no longer in the large number regime and need to be treated with care. But the continuous Gaussian approximation for the DFE holds so long as the number of possible adaptive mutations is large.

B.2 Deriving response kernels on power-law correlated landscapes

We now analyze how the DFE around the current genome is conditioned on the past history of the adaptive walk to that genome. Assume the walk has taken a sequence of steps, $y = 1, 2, ...x - 1$ leading to the current point labelled x with these steps having fitness changes $s(y)$, each taken from the local DFE of average available fitness steps, with average $\mu(y)$. In this section we will describe how to compute the response kernels J and K such that

$$\mu(x) = \sum_{y=0}^{x-1} K(x,y)\mu(y) + J(x,y)s(y) + \eta(x) \tag{98}$$

where $\eta(x)$ is the additional random part of the DFE average: $\eta(x)$ has mean zero and variance, $V_\eta(x)$. We make the continuous approximation for the sums:

$$\mu(x) = \int_0^x J(x,y)\mu(y) + K(x,y)s(y)dy + \eta(x) \tag{99}$$

Note that the J and K are non-zero only for $x > y$.

For most cases it will suffice to use this continuum approximation; but there are a few special cases of landscapes with particular correlation function, $C(\ell)$ which are more easily understood with the discrete equations.

It is useful to define and use the following correlation functions in order to obtain self-consistent equations for J and K:

$$A(x,y) = \mathrm{E}[\mu(x)\mu(y)] \tag{100}$$

$$B(x,y) = \mathrm{E}[\mu(x)\eta(y)] \tag{101}$$

$$G(x,y) = \mathrm{E}[\mu(x)s(y)] \tag{102}$$

$$D(x,y) = \mathrm{E}[s(x)s(y)] \tag{103}$$

bioRxiv preprint doi: https://doi.org/10.1101/435669; this version posted October 11, 2018. The copyright holder for this preprint (which was not certified by peer review) is the author/funder, who has granted bioRxiv a license to display the preprint in perpetuity. It is made available under aCC-BY-NC-ND 4.0 International license.

In addition, we define the convolution operator $*$ by

$$A * B\,(x,y) \equiv \int_0^x A(x,z)B(z,y)dz, \tag{104}$$

and the transpose, T, by

$$A(x,y)^{\mathrm{T}} \equiv A(y,x). \tag{105}$$

(In terms of the discrete sums, these are simply matrix multiplication and transpose.)

By explicitly computing A, B, and G using Equation 99 multiplied by on of μ, s, or η at a different point on the path, and averaging, we get:

$$A = B^T + K * A + J * G^{\mathrm{T}} \tag{106}$$

$$G = B^T + K * G + J * D \tag{107}$$

$$B = V_\eta \delta(x-y) + K * B + J * B \tag{108}$$

Note that K shows up once in each equation, convolved with the quantity on the left hand side. With some foresight, we rewrite $K = \delta + P$ to cancel the left hand sides. In terms of P we are left with:

$$0 = B^T + P * A + J * G^{\mathrm{T}} \tag{109}$$

$$0 = B^T + P * G + J * D \tag{110}$$

$$0 = V_\eta \delta(x-y) + P * B + J * B \tag{111}$$

Up until now, the equations are exact (and also for the discrete sums). We now take the large x limit keeping terms to leading order in powers of $1/x$ and similarly for y and $x-y$. We now define a useful quantity related to the second derivative of $C(\ell)$ in the large ℓ regime:

$$M \equiv m\,\mathrm{sign}(x-y)\mathcal{P}[1/(x-y)^{2-\alpha}] \tag{112}$$

with m a positive coefficient given by the normalization of C, and the principal part, $\mathcal{P}$, ensuring that $\int dy M(x,y) = 0$. Then in the large x limit, from the definitions we have:

$$D \approx -M - M^{\mathrm{T}} \tag{113}$$

$$A \approx \sigma^2 \delta(x-y) + M + M^{\mathrm{T}} \tag{114}$$

$$G \approx -M + M^{\mathrm{T}} + \mathcal{O}(d\delta/dy) \tag{115}$$

with σ^2 proportional to V_η. Corrections to all of these correlations are smaller by one power of $1/x$ except for A: the symmetry under the transpose means that there is only a second derivative of $\delta(x-y)$ correction to the δ function part of A (like a correction of $O(1/x^2)$).

bioRxiv preprint doi: https://doi.org/10.1101/435669; this version posted October 11, 2018. The copyright holder for this preprint (which was not certified by peer review) is the author/funder, who has granted bioRxiv a license to display the preprint in perpetuity. It is made available under aCC-BY-NC-ND 4.0 International license.

We now make the ansatz (readily shown to be correct) that J scales as $x^{\nu-1}$, with $0 \leq \nu \leq \frac{1}{2}$, and that P is much smaller for large x. Then from Equation 111 we have

$$B \approx -V_\eta J^{-1} \tag{116}$$

with inversion taken over $*$ (like matrix inversion). In Equation 110, the $P * G$ term is negligible and in Equation 109, $P * A \approx \sigma^2 P$ plus smaller corrections. Writing an expression for B^{T} and substituting, we get

$$B^{\mathrm{T}} \approx J * (M + M^{\mathrm{T}}) \approx -\sigma^2 P + J * (M^{\mathrm{T}} - M) \tag{117}$$

which can thus determine J and $P = -2J * M/\sigma^2$, subject to conditions that they are only non-zero for $x > y$, as is B – the latter not automatic. Counting powers of x we see that $B \sim P \sim x^{-1-\nu}$ and, from the form of M, that must have

$$\nu = \frac{1-\alpha}{2} \ . \tag{118}$$

One can directly get the scaling behavior and this result for ν by considering the behavior for $(x - y) \ll x$. This can be obtained straightforwardly by approximating the kernels as functions of only $x - y$, taking $x \to \infty$ and then Fourier transforming and decomposing functions into sums of parts that are analytic in upper and lower half-planes corresponding to being zero for either $x < y$ or $x > y$. Armed with these forms (and some knowledge of such singular integral equations), exact solutions can be guessed:

$$J(x, y) \approx -c_J \,\mathrm{sign}(x - y) \frac{y^\nu}{(x - y)^{1-\nu} x^\nu} \ , \tag{119}$$

$$K(x, y) \approx \delta(x - y) + c_K \,\mathrm{sign}(x - y) \frac{x^\nu}{y^\nu} \mathcal{P}(1/(x - y)^{1+\nu}) \ , \tag{120}$$

and

$$B \propto -\mathrm{sign}(x - y) \frac{y^\nu}{x^\nu} \mathcal{P}(1/(x - y)^{1+\nu}) \tag{121}$$

with c_J and c_K positive coefficients that can be written in terms of Beta functions and combinations of V_η and σ^2 to set the scales. Note that with the correct value of ν — indeed only with that value of ν — the $x > y$ part of $J * (M + M^T) = B^T$ vanishes as it must.

The sign of P is rather misleading due to the principal part. If the convolution integral is done by parts, we have that

$$\int_0^x dy K(x, y)\mu(y) = \mu(x) - \frac{c_q}{x^\nu}\mu(x) - \int_0^x dy Q(x, y) \frac{d\mu}{dy} \tag{122}$$

bioRxiv preprint doi: https://doi.org/10.1101/435669; this version posted October 11, 2018. The copyright holder for this preprint (which was not certified by peer review) is the author/funder, who has granted bioRxiv a license to display the preprint in perpetuity. It is made available under aCC-BY-NC-ND 4.0 International license.

with the kernel for $\frac{d\mu}{dy}$,

$$Q(x,y) \equiv \int_0^y dz P(x,z) \tag{123}$$

and Q and the coefficient c_q both positive. Thus the effects of K are: $\delta(x-y)$, a negative — but needed — correction to this, and a negative convolution with $d\mu/dy$, the latter two being the same order for large x.

In order to show that the solutions to the integral equations are of the form given, two integrals need to be done. To show that B is proportional to the inverse of J — i.e. that $J * B = \int_0^x dz J(x,z)B(z,y) = -V\delta(x-y)$ — one only needs to note that the z dependent parts of the z^ν/x^ν and y^ν/z^ν factors from J and B cancel. To do the integrals $J * M$ and $J * M^T$, the substitution $z = xy/(x+y-\zeta)$ changes the integral over z from 0 to x to an integral over ζ from $-\infty$ to x, eliminates the z^ν part from J, brings out (combining with the $x^{-\nu}$ from J) an overall factor of x^ν/y^ν, replaces $x-z$ and $y-z$ with $x-\zeta$ and $y-\zeta$, and cancels all factors of $x+y-\zeta$ thereby making the integrand the simple standard form $(x-\zeta)^{\nu-1}(\zeta-y)^{-1-2\nu}$ and the integrals over the different parts of the range of ζ and for $x > y$ and $x < y$ all simply expressible in terms of Beta functions. The structure is now exactly the same as it would be if the limit $|x-y| \ll x$ were taken initially and Fourier and Weiner-Hopf analysis used. Note, however, that for $\mu(y)$ and $s(y)$ powers of y, as we find, the contributions from the kernels are dominated by intermediate range of y/x and thus the approximation $x-y \ll x$ is incorrect by multiplicative constants, butt gives the correct scalings with x.

B.3 Adaptive walks on exponentially correlated landscapes

Here we analyze adaptive walks on landscapes with correlations

$$C(\ell) = \frac{1}{b}(1 - e^{-\ell/\xi}) \tag{124}$$

where $b = 1 - e^{-1/\xi}$ normalizes so that $C(1) = 1$ for all ξ. That is, the fitness of genomes at a distance $\ell \ll \xi$ are highly correlated, and the fitness of genomes at long-distance $\ell \gg \xi$ are close to statistically independent. In particular we are interested in the case where $\xi \gg 1$, which arises from the NK model.

The exponential-correlations give the advantage that the response functions can be computed exactly. We want to know the conditional distribution of the fitness at a distance x along the walk. It is easiest to compute in terms of $F(x)$ along the path, where F is the absolute fitness function (well-defined since $C(\ell)$ is bounded). For arbitrary genomes g and g' we have

$$\mathrm{E}[F(g)F(g')] = e^{-|g-g'|/\xi} \tag{125}$$

bioRxiv preprint doi: https://doi.org/10.1101/435669; this version posted October 11, 2018. The copyright holder for this preprint (which was not certified by peer review) is the author/funder, who has granted bioRxiv a license to display the preprint in perpetuity. It is made available under aCC-BY-NC-ND 4.0 International license.

where for convenience we have normalized the landscape so that the absolute fitness at any point has 0 mean and variance $\frac{1}{2}$ (instead of with $C(1) = 1$ as in the main text). On any path, we can compute the conditional mean of the fitness at the end of the path $F(x)$ in terms of the previously observed fitnesses as:

$$\mathrm{E}[F(x)|F(y), y < x] = \sum_{y=0}^{x-1} K_F(x, y)F(y) \tag{126}$$

where $K_F(x)$ obeys the equation

$$\sum_{y=0}^{x-1} K_F(x, y)\mathrm{E}[F(y)F(z)] = \mathrm{E}[F(x)F(z)] \tag{127}$$

for all y on the path. We can solve for K_F directly. Subsitution gives

$$\sum_{y=0}^{x-1} K_F(x, y)e^{-|y-z|/\xi} = e^{-|x-z|/\xi} \tag{128}$$

Solving for $K_F(x, y)$ for all $z < x$ we get

$$K_F(x, y) = e^{-1/\xi}\delta_{1y} \tag{129}$$

That is, the final fitness $F(x)$ is correlated directly only with the previous fitness $F(x-1)$ with correlation $e^{-1/\xi}$.

Evolution in an exponentially correlated landscape is in some sense a Markov process; only the last fitness value reached contributes to the statistics of the current neighborhood. The correlation coefficient $e^{-1/\xi}$ has the right limits; when $\xi \gg 1$, the landscape is effectively additive on short distances and the correlations vanish. When $\xi \ll 1$ the landscape is of the independent type and the average step available is exactly $-F(x)$.

Though we have computed correlations in terns of the absolute fitnesses $F(x)$, in exponentially correlated landscapes this gives complete information about $\mu(x)$. We can see this by computing the simple conditional variance $\mathrm{Var}[F(x)|\mu(x)]$:

$$\mathrm{Var}[F(x)|\mu(x)] = \mathrm{Var}[F(x)] - \mathrm{cov}(F(x), \mu(x))^2/\mathrm{Var}[\mu(x)] \tag{130}$$

We can compute $\mathrm{Var}[F(x)] = \frac{1}{2}C(\infty)$ (since long range correlations vanish), $\mathrm{Var}[\mu(x)] = C(1) - \frac{1}{2}C(2)$, and $\mathrm{cov}(F(x), \mu(x)) = -\frac{1}{2}C(1)$. Combining, we have

$$\mathrm{Var}[F(x)|\mu(x)] = 0 \tag{131}$$

Therefore we have:

$$F(x) = -\mu(x)/(1 - e^{-1/\xi}) \tag{132}$$

bioRxiv preprint doi: https://doi.org/10.1101/435669; this version posted October 11, 2018. The copyright holder for this preprint (which was not certified by peer review) is the author/funder, who has granted bioRxiv a license to display the preprint in perpetuity. It is made available under aCC-BY-NC-ND 4.0 International license.

One can think of this as an extension of the situation in the independent fitnesses case. There, since $\mu(x) = \frac{1}{L}\sum_{x'} F(x') - F(x)$, where x' are all one-step neighbors of x, independence and the central limit theorem gives $\frac{1}{L}\sum_{x'} F(x') \sim O(L^{-1/2})$, and we have, for large L, $\mu(x) = -F(x)$.

The combination of Equation 132 as well as $s(x) = F(x) - F(x-1)$ cause knowledge of the $F(x)$ to be equivalent to knowledge of the $s(x)$ *and* $\mu(x)$. Therefore Equation 129 can be used to compute the response functions J and K. However, there is an additional complication: there are $2x$ total s and μ for a walk of length x, but only x total values of F. This redundancy leads to zero-modes in the $s - \mu$ covariance matrix, and a degeneracy of degree x in the response function.

Using this degeneracy, we can write the response function in a variety of ways. The two most interpretable are:

$$\mathrm{E}[\mu(x)|\text{ past}] = -b\sum_{y=0}^{x-1} s(y) + \mu(0) \tag{133}$$

and

$$\mathrm{E}[\mu(x)|\text{ past}] = -bs(x-1) + \mu(x-1) \tag{134}$$

where $b = 1 - e^{-1/\xi}$, and we normalize so that $C(1) = 1$ as in the main text. The first form suggests a flat weighting over past $s(x)$ with an additional dependence on $\mu(0)$ — likely not important for long walks for which the first term continues to grow. The second form shows dependent only on the immediately preceding properties of the adaptive walk. The factor b accounts for the fact that the landscape is somewhere between additive and independent. For $\xi \gg 1$ (so that have almost additive effects of fitness steps), $b \to 0$ and the dependence is only on $\mu(x)$, which is also 0 in that limit, giving $\mathrm{E}[\mu(x)|\text{ past}] = 0$ as expected. For $\xi \ll 1$ (effectively independent fitnesses), $b \to 1$ and we recover the response function of the behavior of the independent landscape.

C Statistics of random and evolution-conditioned maxima

C.1 Local maxima

The expected number of maxima on a random fitness function on the hypercube depends on the local correlation properties only. We can compute this expectation in the following manner. Suppose that the fitnesses in some neighborhood of a genotype (ie that genotype

bioRxiv preprint doi: https://doi.org/10.1101/435669; this version posted October 11, 2018. The copyright holder for this preprint (which was not certified by peer review) is the author/funder, who has granted bioRxiv a license to display the preprint in perpetuity. It is made available under aCC-BY-NC-ND 4.0 International license.

and all single mutations away) are covariate Gaussian. Let s_i be the fitness benefit of a mutant at site i. We assume that the s_i have 0 mean, variance 1, and identical correlation r. In the limit of large L, the $\{s_i\}$ are independent given their mean $\mu(g)$. The distribution of $\mu(g)$ is a Gaussian random variable with mean 0 and variance r.

In the limit of large L the empirical distribution of the $\{s_i\}$ is given by a Gaussian with mean μ and variance $1-r$. Note that g is a local max if all s_i are negative, which happens with probability

$$P_{loc-max} = \int \frac{1}{\sqrt{2\pi r}} e^{-\mu^2/2r} \Phi^L \left(-\frac{\mu}{\sqrt{1-r}} \right) d\mu \tag{135}$$

with Φ the error function. We use a saddle-point approximation to compute P. The log of the integrand $\phi(\mu)$

$$\phi(\mu) = -\frac{\mu^2}{2r} + L \log \left[\Phi \left(-\frac{\mu}{\sqrt{1-r}} \right) \right] \tag{136}$$

Differentiating gives

$$\phi'(\mu) = -\frac{\mu}{r} - L \left[\Phi \left(-\frac{\mu}{\sqrt{1-r}} \right) \right]^{-1} \frac{e^{-\mu^2/2(1-r)}}{\sqrt{2\pi(1-r)}} \tag{137}$$

The peak is at $\mu = \mu^*$ determined by:

$$-\frac{\mu^*}{rL} \Phi \left(-\frac{\mu^*}{\sqrt{1-r}} \right) = \frac{e^{-(\mu^*)^2/2(1-r)}}{\sqrt{2\pi(1-r)}} \tag{138}$$

Clearly, $\mu^* < 0$. If $|\mu^*| \gg \sqrt{1-r}$, then $\Phi\left(-\frac{\mu^*}{\sqrt{1-r}}\right) \approx 1$ (leading correction $O(e^{-(\mu^*)^2/2(1-r)})$). In this approximation, we have

$$-\frac{\mu^*}{rL} = \frac{e^{-(\mu^*)^2/2(1-r)}}{\sqrt{2\pi(1-r)}} \tag{139}$$

And then, approximately

$$\mu^* \approx -\sqrt{2(1-r)(\log(L) - \log\log(L))} \tag{140}$$

We can use this approximation to calculate $\Phi\left(-\frac{\mu^*}{\sqrt{1-r}}\right)$. We need this calculation to be accurate to $o\left(\frac{\log(L)}{L}\right)$ in order to compute P to logarithmic accuracy in large L. Error function asymptotics give

$$\Phi \left(-\frac{\mu^*}{\sqrt{1-r}} \right) \approx 1 - \frac{e^{-(\mu^*)^2/2(1-r)}}{\sqrt{2\pi}(-\mu^*/\sqrt{1-r})} \tag{141}$$

bioRxiv preprint doi: https://doi.org/10.1101/435669; this version posted October 11, 2018. The copyright holder for this preprint (which was not certified by peer review) is the author/funder, who has granted bioRxiv a license to display the preprint in perpetuity. It is made available under aCC-BY-NC-ND 4.0 International license.

Substitution gives

$$\Phi\left(-\frac{\mu^*}{\sqrt{1-r}}\right) \approx 1 - \frac{1}{rL}\frac{\sqrt{2\pi(1-r)}\mu^*}{\sqrt{2\pi}(\mu^*/\sqrt{1-r})} = 1 - \frac{1-r}{r}\frac{1}{L} \tag{142}$$

The second derivative of the log integrand ϕ is

$$\phi''(\mu) = -\frac{1}{c} + L\frac{\mu}{1-c}\left[\Phi\left(-\frac{\mu}{\sqrt{1-c}}\right)\right]^{-1}\frac{e^{-\mu^2/2(1-c)}}{\sqrt{2\pi(1-c)}} - L\left[\Phi\left(-\frac{\mu}{\sqrt{1-c}}\right)\right]^{-2}\frac{e^{-\mu^2/(1-c)}}{2\pi(1-c)} \tag{143}$$

The value at μ^* is

$$\phi''(\mu^*) = -\left(\frac{1}{r} + \frac{(\mu^*)^2}{r(1-r)} + \frac{(\mu^*)^2}{r^2 L}\right) \tag{144}$$

which is dominated by the middle term and is approximately

$$\phi''(\mu^*) \approx -\frac{2(\log(L))}{r} \tag{145}$$

where we drop the $\log\log(L)$ term as it doesn't contribute to leading order in $\log(L)$.

The saddle point approximation then gives us

$$P_{loc-max} \approx \sqrt{\frac{2\pi}{-\phi''(\mu^*)}}e^{\phi(\mu^*)} \tag{146}$$

We can evaluate this to get

$$P_{loc-max} \approx \sqrt{\frac{1}{2r\log(L)}}e^{-(\mu^*)^2/2r}\left(1 - \frac{1-r}{rL}\right)^L \tag{147}$$

For large L, substituting in μ^* gives us

$$P_{loc-max} \approx \sqrt{\frac{1}{2r}}L^{-(1-r)/r}e^{-(1-r)/r} \tag{148}$$

up to poly-log factors. Note that for the independent fitnesses model, $r = \frac{1}{2}$, and $P_{loc-max} = \frac{1}{L+1}$, matching the approximate calculation.

The result for P implies that for most landscapes, the probability of a single genome being at a local max is some power of L. The total number of maxima thus scales roughly like $L^{(1-r)/r}2^L$. As the correlation between step sizes decreases, the number of maxima does as well; the limit $r \to 0$ corresponds to independent steps and there is a single local max on the whole fitness landscape (so $P = 2^{-L}$).

bioRxiv preprint doi: https://doi.org/10.1101/435669; this version posted October 11, 2018. The copyright holder for this preprint (which was not certified by peer review) is the author/funder, who has granted bioRxiv a license to display the preprint in perpetuity. It is made available under aCC-BY-NC-ND 4.0 International license.

Note that for power-law correlated fitness landscapes, r does not determine the long-distance dynamics of uphill random walks. There are fitness landscapes with very different local structures which nonetheless have similar long-term evolutionary dynamics. In the limit of large genome size, L, the dynamics is dominated by the long-distance behavior of $C(\ell)$, which gives rise to the tails of the response kernels. Classifying the "ruggedness" of landscapes via expected properties of maxima is therefore not very useful for understanding evolution on epistatic landscapes.

C.2 Maxima reached by uphill walks

We can estimate the max fitness increase reached by uphill walks. First consider the independent fitnesses landscape. The cumulative distribution function, CDF, of an uphill walk of length X is given by $\Phi(F)^X$. Let the number of uphill paths of length X be given by $N_U(X)$. If the uphill paths are statistically independent, the maximum fitness, f_{max}, couol be approximated by solving

$$1 - \Phi(f_{max})^X = N_U(X)^{-1} \tag{149}$$

Correlations due to shared subpaths will cause this approximation to overestimate f_{max}. On the hypercube, we have $N_U(X) = \frac{[1-\Phi(F(0))]^X}{X!}\binom{L}{X}$. Solving for the CDF approximately, we get

$$1 - \Phi(f_{max}) \approx [1 - \Phi(F(0))]^{-X} \frac{X!}{X} \binom{L}{X}^{-1} \tag{150}$$

The maximum is dominated by the combinatorics of the number of paths, rather than the structure of the paths themselves. If $\Phi(F(0))$ is not too close to 1, the right hand side is minimized at $X \approx \sqrt{L}$, giving us the optimal CDF value $\sim -\sqrt{L}$, which and gives a max fitness gain of

$$f_{\text{max,up}} \propto L^{1/4} \tag{151}$$

in the independent Gaussian case, compared to the global max of $O(L^{1/2})$. Uphill paths have trouble reaching the global max, and random adaptive walks do not go nearly as high. The only way to go higher would be to allow some deleterious mutations as well (which we will not analyze here).

Performing calculations as above for correlated landscapes is more difficult and we will not attempt it here. However, we expect interpolation between the independent fitnesses and additive cases. The maximum absolute fitness $F^* \equiv \max_g F(g)$ on the landscape can be crudely estimated as

$$F^* \approx L^{(1+\alpha)/2} \tag{152}$$

bioRxiv preprint doi: https://doi.org/10.1101/435669; this version posted October 11, 2018. The copyright holder for this preprint (which was not certified by peer review) is the author/funder, who has granted bioRxiv a license to display the preprint in perpetuity. It is made available under aCC-BY-NC-ND 4.0 International license.

using the observation that the fitness difference between any pair of points at a distance x is $\sim x^{\alpha/2}$, and there are roughly $\exp(cL)$ "independent" pairs of points we can choose. We expect something similar to the independent fitnesses case, where $f_{\text{max,up}}$ scales as a power of L, but not as much as F^*. As before, to reach the global maximum one must have an extremely fortuitous choice of starting location. However we will see in the next section that small perturbations of the long range statistics can drastically increase chances of reaching points near the global maximum fitness.

C.3 Mixed landscapes with narrowly distributed additive piece

A small additive piece of the fitness function can have large effects on the global dynamics of evolution. The net effect on the dynamics is also sensitive to the distribution of the additive part. To show this concretely, we work with mixtures of a power law and an additive piece and consider different tails for the additive piece.

Let s_C be the steps in the correlated part of the landscape, and let s_A be the steps in the additive part so the total fitness gain is $s = s_A + s_C$. We first consider an the additive part normally distributed with variance σ_A^2. The distribution of s_C and s_A is jointly Gaussian. The conditional means can be computed directly:

$$\mathrm{E}[s_C|\mu_C, s > 0] = \frac{\sigma_A^2}{\sigma^2 + \sigma_A^2}\mu_C + \frac{\sigma^2}{|\mu_C|}, \ \mathrm{E}[s|\mu_C] \approx \frac{\sigma_A^2 + \sigma^2}{|\mu_C|} \tag{153}$$

for $|\mu_C| \gg \sqrt{\sigma^2 + \sigma_A^2}$. For $\mu_C < 0$, $\mathrm{E}[s_C|s > 0]$ is reduced compared to what it would be in the absence of the additive piece. This change in the relationship between s and μ_C changes the dynamics, making it easier to find uphill steps.

We can use the above equations to compute the dynamics on a power law plus additive landscape. From Equation 28 we have, schematically

$$\frac{d\mathrm{E}[\mu_C(x)]}{dx} = \int_0^x -a(x-y)^{-(3-\alpha)/2}\mu_C(y) - b(x-y)^{-(1+\alpha)/2}\left(\frac{\sigma_A^2}{\sigma^2 + \sigma_A^2}\mu_C(y) - \frac{\sigma^2}{\mu_C(y)}\right) dy \tag{154}$$

where the expectation is taken over the ensemble.

If $\mu_C(x)$ and $s_C(x)$ saturate, then we know $s(x)$ must saturate to 0 (since $J(x)$ has a divergent integral). We solve for the equilibrium μ_C^* by setting the 2nd and 3rd terms equal to each other. If $\mathrm{E}[\mu_C(x)]$ is constant for all x, those two terms will be much larger than the $(x-y)^{-(3-\alpha)/2}$ term. Define $p_A \equiv \frac{\sigma_A^2}{\sigma^2+\sigma_A^2}$ be the fraction of the landscape that is additive. This gives us the saturating value $\mu_C^* = -\frac{\sigma}{\sqrt{p_A}}$. We can find the approximate length X at which

bioRxiv preprint doi: https://doi.org/10.1101/435669; this version posted October 11, 2018. The copyright holder for this preprint (which was not certified by peer review) is the author/funder, who has granted bioRxiv a license to display the preprint in perpetuity. It is made available under aCC-BY-NC-ND 4.0 International license.

saturation occurs for small values of p_A by using the relationship $\mathrm{E}[\mu_C(x)] \propto -\sigma x^{(1-\alpha)/2}$ for the power law walk. We have

$$X \propto p_A^{-1/(1-\alpha)} \tag{155}$$

After the walk reaches saturation, we have $\mathrm{E}[s] = 0$ and the saturated total step s_{sat} goes as $\sigma\frac{\sqrt{p}}{1-p}$. Thus $\mathrm{E}[F(x))]$ goes like a power law for roughly $p_A^{-1/(1-\alpha)}$ steps, after which it goes roughly linearly at a rate $\sigma\frac{\sqrt{p_A}}{1-p_A}$ per step.

We can also compute how far up the walk is expected to go for finite L. We can find the minimal value of p_A for which the walk length is $O(L)$ for fixed L. This occurs when $\mu_C^*/\sqrt{\sigma^2+\sigma_A^2} = O([\log(L)]^{1/2})$, which occurs when

$$p_A = O([\log(L)]^{-1}) \tag{156}$$

For large enough p the population gain fitness linearly with step size; for p_A smaller than the critical value, the power law correlations perform better as they still have $\mathrm{E}[F(x)] \propto x^{(1+\alpha)/2}$. This critical value goes to zero as L increases (albeit slowly). The dynamics goes similarly for more narrowly distributed s_A as well.

For Gaussian and sub-Gaussian distributions, the primary effect of the additive piece is to let s relax to 0. The adaptive walk "chooses" to use the additive component of the landscape as the primary source of its adaptive steps, while not moving much in the correlated landscape. A balance can be found where μ_C does not change; this means that in the correlated landscape, the trajectory goes along a path of constant curvature. This small additive piece can have a large global effect on evolutionary dynamics.

The transition to $O(L)$ fitness gains due to the additive piece has been previously seen in the case of RMF models (additive mixture with $\alpha = 0$). Previous work has shown phase transitions from linear to sublinear fitness gains of random adaptive walks as the amount of additive piece is changed in the limit of infinite L. [36, 41] The phase transition occurs at $p = 0$ for sub-exponential tails of the random piece if the additive piece is constant. These new results explicitly show the crossover for finite but large L, showing the scale of the amount of additive piece needed to go long distances decays slowly with L if s_A is narrowly distributed.

Even in cases where the additive component does not change the "typical" dynamics, it may change extremal ones. Consider the case of an additive, narrowly distributed component plus a correlated component. Now suppose we wished to find the "best" uphill path starting at a particular node. If we had full knowledge of the landscape, one simple strategy would be the following: for every step, find a direction where $s \approx 0$ and $s_A \approx \sigma_A$. If we can easily find such a step, is has $s > 0$ and also ensures that μ_C will not increase. Then, at the next step we should be able to easily find such a step again.

bioRxiv preprint doi: https://doi.org/10.1101/435669; this version posted October 11, 2018. The copyright holder for this preprint (which was not certified by peer review) is the author/funder, who has granted bioRxiv a license to display the preprint in perpetuity. It is made available under aCC-BY-NC-ND 4.0 International license.

So long as $\sigma_A \gg L^{-1}$, we should be able to find a step in the correlated landscape such that $s < 0$ and $|s| < \sigma_A$. This means that the critical p for the existence of at least one path which gets close to the global maximum is at most L^{-1}, as opposed to the $[\log(L)]^{-1}$

C.4 Mixed landscapes with broadly distributed additive piece

Consider the case of a mixed landscape where the additive piece goes as

$$P(s > 0|s) = \left(\frac{|s|}{\sigma_A}\right)^{-\beta+1} \tag{157}$$

In the main text, we considered the case where large steps were relatively plentiful; however the regime where the probability of a large step is $O(L^{-1})$ has some additional structure as well.

Consider a simplified model of a correlated plus additive landscape, where with probability p_{add} any single uphill direction has an arbitrarily large uphill part. When $p_{add} = n_{add}L^{-1}$ for some $n_{add} = O(1)$, there is some waiting time to find the uphill direction. If the probability of any uphill step on the correlated landscape alone is p_{cor}, then an uphill step using the additive piece occurs with probability $\frac{p_{add}}{p_{cor}+p_{add}}$, or every $\frac{p_{cor}L+n_{add}}{n_{add}}$ steps.

The dynamics then proceeds as follows: the population follows its normal trajectory on the correlated landscape until it finds and picks a large uphill direction. It then takes the large uphill direction, and takes a step μ in the correlated landscape. On average then, this leads to the following equilibrium equation for μ:

$$0 = \int a(x-x')^{-(3-\alpha)/2}\mu_c + b(x-x')^{-(1+\alpha)/2}\left(\frac{p_{add}}{p_{cor}+p_{add}}\mu_c + \frac{p_{cor}}{p_{cor}+p_{add}}\frac{\sigma^2}{|\mu_c|}\right)dx' \tag{158}$$

where $p_{cor} \approx \frac{\sigma}{|\mu_c|}e^{-\mu_c^2/2\sigma^2}$. The equilibrium condition is given when the second and 3rd terms cancel; we have

$$\frac{\sigma^3}{|\mu_c|^3}e^{-\mu_c^2/2\sigma^2} = p_{add} \tag{159}$$

which gives us $\mu_c \approx -\sigma\sqrt{2|\log(p_{add})|}$, or $p_{cor} = 2|\log(p_{add})|p_{add}$. For small p_{add} (as we expect in the crossover regime), $p_{cor} \gg p_{add}$.

The walks are of extensive (linear in L) length when $Lp_{cor} = O(1)$ (more accurately, when $1 - Lp_{cor} = o(L^{-1})$). Therefore, to have dynamics of this type that nonetheless go a long-distance, we need $|\log(p_{add})| = O(1)$ - guaranteed when $p_{add} = O(L^{-1})$. A necessary condition for this ansatz to hold is that the additive piece gets used before the correlated piece

bioRxiv preprint doi: https://doi.org/10.1101/435669; this version posted October 11, 2018. The copyright holder for this preprint (which was not certified by peer review) is the author/funder, who has granted bioRxiv a license to display the preprint in perpetuity. It is made available under aCC-BY-NC-ND 4.0 International license.

would normally get stuck; that is we need $\ell_{cor} \gg \ell_{add}$ where

$$\ell_{cor} \approx \frac{1}{1 - Lp_{corr}}, \ \ell_{add} \approx \frac{p_{corr} + p_{add}}{p_{add}} = 2|\log(p_{add})| \tag{160}$$

which means that walks in the correlated bit must go at least length $\log(L)$ for this method of equilibration to work.

This again shows us that the global and sometimes extremal statistics of the landscape matter far more than the local ones. Different extremal statistics lead not only to different crossovers in behavior, but potentially to different phases as well.

D Dynamics on static and time-varying landscapes

D.1 Time dependence of power law walks

We assume a model where mutations arise from a Poisson process, with characteristic time $\tau_M = 1$ between mutations. Deleterious mutations are purged instantly; adaptive mutations fix instantly.

Under this model, the time $\tau_U(x)$ to take the $x+1$ th step is distributed exponentially with mean time $1/p_U(x)$, where $p_U(x)$ is the probability of any given step being uphill. Note that in the large L limit, $p_U(x)$ only depends on the current average available fitness gain $\mu(x)$, as the variance of available steps (given $\mu(x)$ is constant. For $|\mu|/\sigma \gg 1$, we have approximately

$$p_U(x) \propto \frac{\sigma}{|\mu(x)|} e^{-\mu(x)^2/2\sigma^2} \tag{161}$$

This means that $t(x)$ is superexponential in $\mu(x)$ — the adaptive walk is very slow. Additionally, $\tau_U(x)$ is very broadly distributed. In fact, $\log(\tau_U(x))$ is roughly normal. We can decompose its variance as

$$\mathrm{Var}[\log(\tau_U(x))] = \mathrm{E}[\mathrm{Var}[\log(\tau_U(x))|p_U(x)]] + \mathrm{Var}[\mathrm{E}[\log(\tau_U(x))|p_U(x)]] \tag{162}$$

From the convexity of log, we have approximately

$$\mathrm{Var}[\log(\tau_U(x))] \leq \mathrm{E}[\mathrm{Var}[\log(\tau_U(x))|p_U(x)]] + \mathrm{Var}\left[\mu(x)^2/\sigma^2\right] \tag{163}$$

for large $\mu(x)$. Since $\tau_U(x)|p_U(x)$ is exponentially distributed, for large $\mu(x)$ the width of the distribution is narrow relative to the mean and the first term negligible relative to the second. We expect, then, that $\log(\tau_U(x))$ is distributed similarly to $\mu(x)^2$; its mean and variance should both scale as $x^{1-\alpha}$.

bioRxiv preprint doi: https://doi.org/10.1101/435669; this version posted October 11, 2018. The copyright holder for this preprint (which was not certified by peer review) is the author/funder, who has granted bioRxiv a license to display the preprint in perpetuity. It is made available under aCC-BY-NC-ND 4.0 International license.

Figure 13 shows the exponents of power law fits to the mean and standard deviations of $\mathrm{E}[\log(t(x))]$. These exponents show good agreement for low α where the approximate arguments above are expected to hold. They deviate at high α where $\mu(x)$ grows slowly enough that neglected terms matter more (at least for the range of x explored).

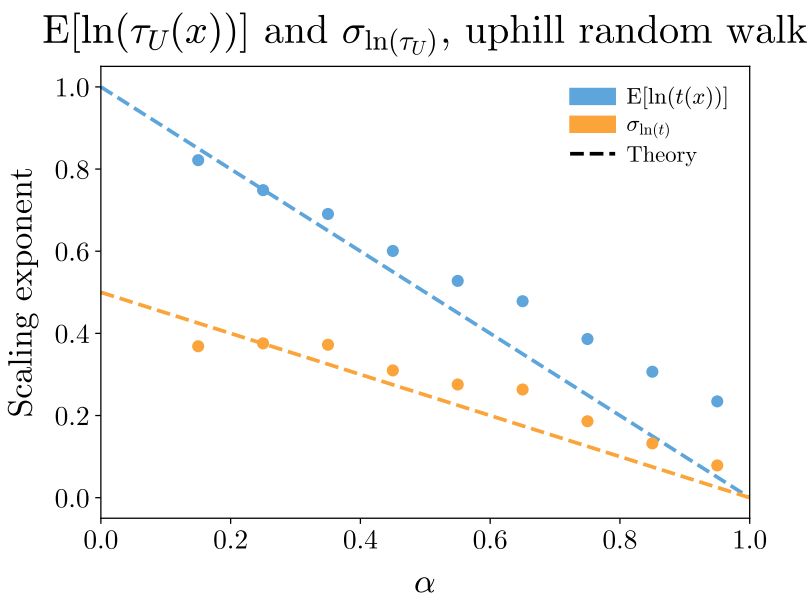

Figure 13: Average log derivatives of mean and standard devation of $\log(\tau_U(x))$. For low α, mean and variance scale like $\mu(x)^2$.

This suggests then that the time taken to reach fitness gain $f(x)$ is dominated by the last step. We can write $\log(\tau_U(f))$ as

$$\log(\tau_U(f)) \propto f^{2(1-\alpha)/(1+\alpha)} \tag{164}$$

for the time taken to reach a fitness f. As we will discuss later, this is clearly too slow to be a reasonable model of evolution in most scenarios. Bu this result is very sensitive to the Gaussian tails of our random fitness functions. It may be possible to find distributions with alternate extremal statistics that give similar $f(x)$ but faster τ_U: we leave this for future research.

D.2 Exponential time correlation

In this section we develop the results needed to analyze the exponentially time-correlated landscapes. Consider random variables $F(x,t)$, each with mean zero and covariance structure

bioRxiv preprint doi: https://doi.org/10.1101/435669; this version posted October 11, 2018. The copyright holder for this preprint (which was not certified by peer review) is the author/funder, who has granted bioRxiv a license to display the preprint in perpetuity. It is made available under aCC-BY-NC-ND 4.0 International license.

given by

$$\mathrm{E}[F(x,t)F(y,s)] = C(x,y)e^{-|t-s|/T} \tag{165}$$

for some correlation function C. Here t and s denote time, while x and y denote some other type of coordinate (spatial coordinate for physical systems, genotypes for the case of fitness landscapes).

Conditional draws from this distribution simplify in two cases. The first is drawing the current conditional values at some set of spatial coordinates, given a joint observation in the past. More precisely, consider a set of locations $\{x\}$, with each x having some set of observation times $\{t_{x,i}|i>0\}$ sorted from most recent to furthest in the past ($t_{x,i} > t_{x,j}$ for $i<j$). Suppose we wish to draw the conditional variables $\{F(x,t_{x,0})\}$ for some later times $\{t_{x,0}\}$. If all the latest observations happened at the same time (that is, $t_{x,1} = t_1$ for all x, x'), then the response function $K(x,t_{x,0};x',t_{x,i})$ (contribution of $F(x',t_{x,i})$ to conditional expectation of $F(x,t_{x,0})$) is given by

$$K(x,t_{x,0};x',t_{x,i}) = \delta_{1i}\delta_{xx'}e^{-|t_{x,0}-t_1|/T} \tag{166}$$

In other words, the expectation only depends on the latest observed value at the same location. If the newly observed time $t_{x,0}$ is also the same value t_0 for all x, the conditional covariance $\tilde{C}_{t_0}(x,x')$ at t_0 can also be written simply as

$$\tilde{C}_{t_0}(x,x') = (1-e^{-2(t_0-t_1)/T})C(x,x') \tag{167}$$

Therefore the conditional distribution is a weighted sum of the last observed function values and an independent draw from the time-independent ensemble.

The second important case is where the x previously observed have the same structure, but there are some new location z being observed at time t_0. In this case, if the $\{F(x,t_0)\}$ are drawn first, then the response function is given by

$$K(z,t_0;x,t_{x,i}) = \delta_{i0}K(z,x) \tag{168}$$

That is, only the values $F(x,t_0)$ contribute to the conditional distribution, with the same weighting they would without time dependence. Likewise, the conditional covariance is given by $\tilde{C}_{t_0}(z,z') = \tilde{C}(z,z')$, or more simply the conditional covariance without time dependence. This means that the new x can be drawn using only the values $F(x,t_0)$, with the same statistics as the case without time dependence.

Therefore we can generate exponentially time-correlated functions as follows:

1. Pick a set of points $\{x\}$ for which the most recent values of F were all generated at the same timepoint t_1.

bioRxiv preprint doi: https://doi.org/10.1101/435669; this version posted October 11, 2018. The copyright holder for this preprint (which was not certified by peer review) is the author/funder, who has granted bioRxiv a license to display the preprint in perpetuity. It is made available under aCC-BY-NC-ND 4.0 International license.

2. Pick a new time t_0 in the future.
3. Generate a new draw of a set of random variables F' on x with correlation structure C.
4. Add the values $\sqrt{1-e^{-2|t_{x,0}-t_{x,1}|/T}}F'$ to $e^{-|t_{x,0}-t_{x,1}|/T}F(t_1)$.
5. Generate any new values $F(y,t_0)$ on unexplored y as desired, conditioning only on previously observed $F(x,t_0)$.
6. Go back to 1.

In order to simulate evolution on time-dependent landscapes, we chose a time interval small compared to the correlation time of the landscape ($\Delta t \ll \tau_E$), and carried out steps $1-4$ above. We then computed the probability that an uphill step would occur in the window of size Δt given the current $\mu(x,t)$. With that probability, we drew an uphill step as we would in the time-independent case, and drew the new conditional DFE mean $\mu(x+1,t)$. Otherwise, we went back to step 1 and updated all values to time $t+\Delta t$.

Every uphill step with exponential time correlations is just as efficient as it is without time dependence. The additional cost is the updates to the landscape when uphill steps are not taken. For average time $\bar{\tau}_U$ for an uphill step, this introduces a cost of $O(\frac{\bar{\tau}_U}{\Delta t}X^4)$ to simulate an evolution with X uphill steps.

D.3 Power law landscapes with exponential time correlations

After a transient period, dynamics in a landscape with exponentially time-decaying correlations leads to an equilibration of the DFE mean μ around some critical value μ_c. If the landscape has power law correlations, we must solve an integral equation to find μ_c.

For slowly varying landscapes, $|\mu_c/\sigma| \gg 1$ and the average values of s and μ will control the overall dynamics. We also assume that the time for each uphill step is not too broadly distributed near the steady state. Using the response function asymptotics, we have the approximate differential equation

$$\frac{d\mu}{dx} \approx \int_0^x e^{-|x-y|/\xi_D}\left(-a|x-y|^{-(3-\alpha)/2}\mu(y) - b|x-y|^{-(\alpha+1)/2}s(y)\right)dy \tag{169}$$

for $\xi_D = \frac{\tau_E}{\bar{\tau}_U}$. Here we average over the new random part of the landscape we get from the time dependence of the landscape. The derivative vanishes at steady state. If we replace $\mu(y)$

bioRxiv preprint doi: https://doi.org/10.1101/435669; this version posted October 11, 2018. The copyright holder for this preprint (which was not certified by peer review) is the author/funder, who has granted bioRxiv a license to display the preprint in perpetuity. It is made available under aCC-BY-NC-ND 4.0 International license.

with μ_c and $s(y)$ with $-\frac{\sigma^2}{\mu_c}$, and take the limit of large x, the integrals are well approximated by Γ functions and we get

$$\mu_c^2 \approx \sigma^2 \frac{a}{b} c_\alpha \xi_D^{(1-\alpha)/2} \tag{170}$$

for some constant c_α.

D.4 Distribution of uphill steps with exponential temporal correlations

We now analyze the steady state stochastic dynamics for large τ_E, and show that the approximations of Appendix D.3 hold in this limit. The important quantities are $\mu(x)$, defined more precisely to be the average-available-fitness-step just after the previous step, its scaled minus-average, $m \equiv -\mu_c/\sigma \gg 1$ and its scaled variance $W \equiv \mathrm{Var}[\mu(x)]/\sigma^2$, so that the quantity $h(x) \equiv (\mu_c - \mu(x))/\sigma$ has mean zero and variance W. (Note that h is not exactly Gaussian due to the distributions of the earlier s's, but the deviations will not change the overall conclusions.) The probability per time, $r(t)$, of a beneficial mutation occurring a time t after the previous mutation, is increased by the exponential decay of the average available fitness step, $\mathrm{E}[\mu(x,t)|\mu(x)] = e^{-t/\tau_E}\mu(x)$ so that $\mu(x,t)^2 \approx \mu(x)^2(1-2t/\tau_E)$ for $t \ll \tau_E$, with the stochastic part of the change (of order $\sqrt{t/\tau_E}$) negligible, and hence

$$r(t) \approx R(h)e^{bt} \tag{171}$$

with $R \sim \exp(-[m+h]^2/2)$ and $b \approx m^2/\tau_E \ll 1$. The first beneficial mutation will typically occur at a time τ_U at which $\int_0^{\tau_U} r(t)dt \sim 1$ so that $\tau_U \approx \log(1+b/R)/b$. For not too large $-\mu(x)$, specifically when $h < H$ where $R(H) \approx b$, we have simply $\tau_U \approx 1/R(h)$ and the time dependence of the landscape does not matter: the next mutation is very likely to occur before the environment changes by enough to make a difference. But for anomalously large $-\mu(x)$, specifically for $h(x) > H$, a beneficial mutation is likely to occur only after the environment has started to change enough to matter although still still well before it is decorrelated: here, the waiting time is proportional to how much $-\mu(x,t)$ has to decrease for the mutation to occur. It is likely after a waiting time near

$$\tau_U \approx \log(b/R)/b \approx m(h-H)/b \tag{172}$$

(the $-h^2/2$ in $\log(R)$ can be neglected). We will see that this waiting only occurs for a very small fraction of cases, i.e., that, with h approximately Gaussian with variance W, $H \gg \sqrt{W}$. This means that the distribution of h is decaying approximately exponentially for h just above H. The average waiting time, $\bar{\tau}_U$, is dominated by the rare slightly-stuck situations with $h - H \sim W/H$, yielding

$$\bar{\tau}_U \sim \frac{mW^{3/2}}{bH^2} e^{-H^2/2W} \ . \tag{173}$$

bioRxiv preprint doi: https://doi.org/10.1101/435669; this version posted October 11, 2018. The copyright holder for this preprint (which was not certified by peer review) is the author/funder, who has granted bioRxiv a license to display the preprint in perpetuity. It is made available under aCC-BY-NC-ND 4.0 International license.

For power-law correlated landscapes, we found that the effects of the past history implied that $\bar{\tau}_U/\tau_E \sim 1/m^{2/(1-\alpha)}$ thus for consistency we must have $H \approx \sqrt{2W\kappa_H \log(m)}$ with $\kappa_H = \frac{2}{1-\alpha} - 1 + \frac{1}{2}\log(W/m) > 0$ since W scales as a non-negative power of m. Now H is given by $\exp[(m+H)^2/2] = b = m^2/\tau_E$ so the typical $\tau_U(x)$, while broadly distributed with

$$\tau_U(x)_{\text{typical}} \sim e^{m^2 \pm \mathcal{O}(m)} \tag{174}$$

is much less than τ_E by a factor of

$$e^{-mH-H^2/2} \sim e^{-m\sqrt{W}\sqrt{2\kappa_H \log(m)}} \ . \tag{175}$$

Moreover, even the rare $\tau_U(x)$ that dominate the average $\bar{\tau}_U$, are smaller

$$\frac{\tau_{\text{dominant}}}{\tau_E} \sim \frac{\sqrt{W}}{m\sqrt{\log(m)}} \ll 1 \tag{176}$$

because the standard deviation of $\mu(x)/\sigma$ is much less than its mean, i.e. $\sqrt{W} \ll m$. This means that in one landscape decorrelation time τ_E, the total number of steps taken is well approximated by $\xi_D \equiv \tau_E/\bar{\tau}_U$ with smaller variations around this. Thus the dynamics is quire smooth on time scales of τ_E and length scales, ξ_D. This makes the analysis in Appendix D.3 that assumed such smoothness is justified. But, importantly, for all but a small fraction — $\sim 1/m^{\kappa_H}$ — of the steps, the effects of the time dependence of the landscape are negligible. The dynamics is thus very heterogeneous with many relatively rapid steps as if in a static landscape, and occasional steps that "waited" for small changes in the environment. Of course, as for most quantities in these Gaussian landscapes, the small parameter is only logarithmic, in this case since $m \approx \sqrt{2\log\tau_E}$.